Methanogenic Biodegradation of Polycyclic Aromatic Hydrocarbons in Oil Sands Tailings

by

Henian Guo

A thesis submitted in partial fulfillment of the requirements for the degree of

Master of Science

in

Land Reclamation and Remediation

Department of Renewable Resources

University of Alberta

Abstract

The current hot water extraction method to recover bitumen from excavated oil sands ores after surface mining generates large volumes of fluid fine tailings that are temporarily deposited in oil sands tailings ponds. Promising techniques for tailings ponds reclamation such as end-pit lakes are facing potential challenges including the aquatic toxicity and methane emissions caused by tailing-derived hydrocarbons such as polycyclic aromatic hydrocarbons (PAHs). However, little information is available about efficient PAHs determination in tailings as well as the behavior of PAHs under methanogenic conditions in tailings. Therefore, method development for determination of PAHs and the investigation of the potential for PAH biodegradation under methanogenic conditions are the aims of this study. Conventional methods for PAHs determination in solid samples such as soils and sediments yielded poor recovery of PAHs from oil sands tailings due to the potential adsorption of PAHs onto the fine particles and organic compounds of tailings. Thus, an optimized method for PAHs determination in tailings was developed, which achieved ~94% pooled mean recovery of PAHs. The optimized method includes: (1) pre-treatment of FFT sample with DCM for 24 hours before extraction; (2) extraction of PAHs from the pre-treated FFT with DCM in a Soxhlet extractor for 24 hours; (3) purification of the extract with a silica gel chromatography column using DCM as eluent; (4) measurement on GC-MS. This method has high sensitivity and reproducibility and was used for the detection of PAHs in the bench-scale biodegradation experiments in this study. Sealed anaerobic microcosms containing tailing samples from 3 tailings ponds operated by Syncrude Canada Limited (Syncrude), Canadian Natural Resources Limited (CNRL), and Albian Sands Energy Incorporated (Albian), were set up to simulate methanogenic conditions below mudline of tailings ponds and to test if indigenous microbial community is capable to degrade PAHs.

After ~700 days incubation under methanogenic conditions, no degradation of 6 abundant PAHs (naphthalene, phenanthrene, pyrene, dibenzofuran, fluorene, and dibenzothiophene) in tailings occurred, although toluene (added as a solvent of PAHs) was degraded within ~300 days in Syncrude and Albian microcosms. However, future degradation of PAHs can be expected since the potential PAHs degraders such as *Clostridia* have high relative abundance in the indigenous microbial communities of oil sands tailings.

Acknowledgements

I would like to thank my supervisor, Dr. Tariq Siddique, and our Research Associate, Dr. Alsu Kuznetsova, who have spent endless effort in helping me build solid skills of laboratory work and improve my ability of academic thinking and writing over the past two and a half years.

I would like to express my appreciation to both current and former members of Siddique lab for their invaluable assistance to my graduate work, especially Najmeh Samadi, who had taught me the essential techniques to conduct my experiments; and Iram Afzal, who is always a good friend to help me tackle all the problems associated with graduate studies. My appreciation is also own to Maryam Firoozbakht, Samia Anjum, Dr. Navreet Suri, Dr. Abigail Adebusuyi, Dr. Irum Zahara, who are always willing to help me in need and discussing interesting research topics with me.

I would also like to acknowledge the oil sands companies (Syncrude Canada Limited, Canadian Natural Resources Limited, and Albian Sands Energy Incorporated) to provide tailing samples, and NSERC for funding and supporting this research project, as well as the Government of Alberta to award the Alberta Graduate Excellence Scholarship (AGES) to me, and the Canadian Land Reclamation Association to award the CLRA Student Award to me.

Finally, I would like to thank my families for their devoted love and support to me on my way of study and always provide me with steadfast mental support.

Table of Contents

List of Tables

Chapter 2

Chapter 3

Appendix A

Appendix B

List of Figures

Chapter 1

Chapter 2

Chapter 3

Appendix A

Appendix C

Abbreviations

AER	Alberta Energy Regulator
Albian	Albian Sands Energy Inc.
ANOVA	Analysis of Variance
ANT	Anthracene
BML	Base Mine Lake
BTEX	Benzene, toluene, ethylbenzene, and isomers of xylene
CAPP	Canadian Association of Petroleum Producers
CAR	Carbazole
CHX	Cyclohexane
CNRL	Canadian Natural Resources Limited
DBF	Dibenzofuran
DBT	Dibenzothiophene
DCM	Dichloromethane (methylene chloride)
DHHS	United States Department of Health and Human Services
EPA	United States Environmental Protection Agency
EPL	End-pit Lake
FFT	Fluid fine tailings
FLU	Fluorene
GC-FID	Gas chromatograph with flame ionization detector
GC-MS	Gas chromatography with mass spectrometry
HEX	Hexane
HMN	2,2,4,4,6,8,8-heptamethylnonane
HMW-PAHs	High molecular weight PAHs
LMW-PAHs	Low molecular weight PAHs
MFT	Mature fine tailings
MLSB	Mildred Lake Settling Basin
NAP	Naphthalene
NAs	Naphthenic acids
OSPW	Oil sands process-affected water
OSTP	Oil sands tailings ponds
PAHs	Polycyclic aromatic hydrocarbons
PHE	Phenanthrene
PYR	Pyrene
SOM	Soil organic matter
Syncrude	Syncrude Canada Ltd.
WIP	West In-pit

Chapter 1: Introduction

1.1 Oil Sands Industry in Alberta

Northeastern Alberta, Canada has one of the largest oil sands reserves in the world with ~300 billion barrels of recoverable bitumen across over 142, 200 km^2 of oil sands region, including Athabasca, Peace River, and Cold Lake (Small et al., 2015; Cossey et al., 2021). An estimated amount of 515 thousand barrels of crude oil was produced per day from the Alberta oil sands region in 2023 and an increase to ~570 thousand barrels per day will be expected in 2025 (AER, 2023). The rapid development of oil sands industry has boosted the capital investment and employment positions in Alberta (Government of Alberta, 2023) while the potential environmental impacts of industry related emissions from this region and their impacts on ecosystem health have raised concerns and intrigued numerous investigations since the mining activities began in 1967 (Smith et al., 1981; Kelly et al., 2009; Ahad et al., 2015; Wnorowski et al., 2021; Zhang, 2023).

1.2 Bitumen Extraction and Production of Tailings

Bitumen is a very sticky and heavy crude oil stored in oil sands ores that is recovered through surface mining or *in-situ* recovery (Chen and Liu, 2019). Though huge reserves of oil sands were found in Alberta, most of the reserve are deeply buried below ground and requires steam assisted gravity drainage method to release bitumen (Butler, 1994), while ~20% of oil sands in Alberta are suitable for surface mining (Hsu et al., 2015). For surface-mined oil sands, a commercially used method to separate bitumen from oil sands is the Clark hot water extraction process (Clark and Pasternack, 1932), in which caustic (with addition of NaOH) hot water is used to disintegrate the oil sands ore structure and release bitumen (Chalaturnyk et al., 2002). Extracted bitumen froth is further treated with diluent (light fraction of hydrocarbons) such as naphtha (mainly C_5-C_{10} hydrocarbons) or paraffinic solvents (mainly C_5-C_6 hydrocarbons) to reduce bitumen

viscosity and further enhance the separation of bitumen from the leftover solid particles before upgrading (Mahaffey and Dubé, 2017). Different oil sand operators use different solvents in froth treatment to improve bitumen recovery, for instance, naphtha is applied by Syncrude Canada Ltd. (Syncrude) and Canadian Natural Resources Ltd. (CNRL) whereas paraffinic solvents are employed by the Albian Sands Energy Inc. (Albian, now operated by CNRL). Large volumes of fine tailings, which is known as Fluid Fine Tailings (FFT) is generated from the extraction process (Cossey et al., 2021). The FFT is mainly composed of fine particles (e.g., clay and fine silt), a small proportion of residual hydrocarbons (e.g., bitumen, naphtha, and paraffin), oil sands process-affected water (OSPW), and it harbors diverse microbial communities (Foght et al., 2017). FFT is usually temporarily deposited into oil sands tailings ponds (OSTP) in the active tailing areas pending subsequent reclamation. After being deposited into the tailings ponds, the consolidation and dewatering of fresh FFT will occur via gravity, and after ~3-5 years, the tailing slurry can be classified as mature fine tailings (MFT) due to increased solid contents, usually 30-40 wt%, and the enriched microbial communities (Mahaffey and Dubé, 2017; Cossey et al., 2021). During the consolidation process, more OSPW is released to the surface of OSTP to gradually form an upper water layer of ~2-10m (Foght et al., 2017). The OSPW is any water that has been in contact with bitumen within the mine and during the extraction processes, such as the water trapped in the pores of oil sands ores (connate water), the water used for bitumen extraction and treatment, released water during consolidation of FFT, and dyke drainage and seepage water, etc. (Li et al., 2017; Mahaffey and Dubé, 2017).

1.3 Reclamation of Tailings Ponds

Tailings ponds are temporary storages for active tailings management, and once decommissioned (no longer receive inputs of tailings from bitumen extraction process), these

ponds have to be reclaimed and integrated into mine closure landforms (CAPP, 2021). One of the promising reclamation strategies applied by Albertan oil sands industry that have received extensive investigations during the past decades is the construction of end-pit lakes (EPL) after surface mining (CAPP, 2021). The first and currently the only full-scale demonstration of EPL in Athabasca oil sands region is the Base Mine Lake (BML) operated by Syncrude, which is located in the former West In-Pit (WIP) facility of the Base Mine at Syncrude's Mildred Lake site (Syncrude, 2022). The WIP had been receiving FFT since 1995 before being removed from Syncrude's active tailing network and commissioned as an EPL in 2012. Fresh water from Beaver Creek Reservoir and additional OSPW was pumped into the existing upper water layer of BML to elevate the water layer and prevent the wind-driven resuspension of fine particles from the bottom (CAPP, 2021). Apart from the addition of fresh water, Syncrude pumped out part of the cap water from BML to a wastewater control system and reused the water for bitumen extraction (Syncrude, 2022). The flow-through process operated by adding fresh water and recycling the cap water diluted the potential contaminants in the BML such as dissolved total metals and organics to gradually help BML provide a sustainable aquatic ecosystem in the future (Syncrude, 2022). Two of the main investigations that have been continuously carried out for the BML development are (1) evaluating its potential environmental toxicity associated with dissolved trace metals and organic substrates and (2) estimating and mitigating the methane production related to potential hydrocarbons biodegradation (Syncrude, 2022).

1.4 Potential Environmental Toxicity of Tailings Ponds

1.4.1 Potential Toxicity of Naphthenic Acids

The potential toxicity of OSPW to aquatic lives including invertebrates (White and Liber, 2020), fish (Li et al., 2017), and amphibians (Robinson et al., 2023) had been studied during the

past several years. It was reported that naphthenic acids (NAs) that are native to bitumen and can be solubilized into OSPW during the bitumen extraction process, are considered as one of the major sources of the toxicity in OSPW (Mahaffey and Dubé, 2017). NAs mainly consist of alkyl-substituted acyclic and cycloaliphatic carboxylic acids, and the concentration of NAs in OSPW samples had been historically measured between 40 mg/L and 120 mg/L (Holowenko, 2002) and recently measured between 20 mg/L and 40 mg/L in the BML (Syncrude, 2022). Past reports have shown potential toxicity of NAs to various aquatic lives including invertebrates (Bartlett et al., 2017) and fish species (Marentette et al., 2015). For instance, increased abnormalities at hatch were seen in fathead minnow embryos after exposure to OSPW-derived NAs (Marentette et al., 2015). In addition, the NAs in tailings ponds may also contaminate the surrounding water through seepage since recent reports showed that the detected NAs in groundwater samples collected around a tailings pond probably derived from OSPW (Ahad et al., 2020). However, the seepage of bitumen-derived organic compounds to the mainstream of the Athabasca River was considered to be minimal (Chen et al., 2024; Sun et al., 2017).

1.4.2 Potential Toxicity of Polycyclic Aromatic Hydrocarbons

There is growing concern that another major class of hydrocarbons in FFT (Brigmon et al., 2016) that are primally derived from residual bitumen, known as the polycyclic aromatic hydrocarbons (PAHs), may also contribute to the overall tailings pond toxicity (Li et al., 2017). PAHs are a class of hundreds of hydrophobic organic contaminants with low volatility (Balmer et al., 2019) containing two or more benzene rings in structure. The relatively simple PAHs with less than four benzene rings were classified as low molecular weight PAHs (LMW-PAHs) such as naphthalene, anthracene and phenanthrene, and the more complexed PAHs with four or more benzene rings, such as pyrene are defined as high molecular weight PAHs (HMW-PAHs) (K.

Zhang et al., 2019). Some PAHs contain heteroatoms in their structure, such as dibenzofuran and dibenzothiophene, in which two benzene rings are fused to a central furan ring or a thiophene ring, respectively. Major PAHs species detected in tailings are naphthalene (NAP), phenanthrene (PHE), pyrene (PYR), dibenzofuran (DBF), fluorene (FLU), and dibenzothiophene (DBT) (Harner et al., 2018; Galarneau et al., 2014; Selucky et al., 1977). Graphical illustration of structures of typical PAHs in tailings are shown in Figure 1-1.

For protection of aquatic life, PAH concentrations in the water environment should be within 0.00001-0.006 mg/L (Canadian Council of Ministers of the Environment, 1999). However, the concentrations of some PAHs in BML such as anthracene (ANT) (LMW-PAHs) and PYR (HMW-PAHs) were recently reported to exceed the water quality guidelines (Syncrude, 2022), which might pose potential toxicities to aquatic life. Recent reports showed that when LMW-PAHs such as NAP and PHE were introduced into the water body, they may accumulate in the organs of fish and invertebrates and are detrimental to their metabolism (Honda and Suzuki, 2020). It was also reported that tailing-derived PAHs may be toxic to the early growth stages of major wild fish species in Canada (Raine et al., 2017, 2018). In these two studies, the researchers raised walleye (Raine et al., 2017) and northern pike (Raine et al., 2018) embryos in microcosms (1L) contaminated by tailings, and showed that the decreased survival of embryos may be related to the increased concentration of PAHs in the microcosms. Therefore, further research regarding the remediation of PAHs in tailings ponds is urgently required to help the BML project achieve one of its key desired outcomes to sustainably support fish populations (Syncrude, 2022).

1.5 Methanogenic Degradation of Tailing-derived Organic Compounds and the Methane Production in Oil Sands Tailings Ponds

1.5.1 Potential Sources of Methane Production in Tailings Ponds

The Government of Canada reported that in 2021, approximately 85.3 megatonnes of carbon dioxide equivalent (Mt CO_2 eq) were emitted from oil sands industry, accounting for ~12.7% of total national emissions (Government of Canada, 2023). Recent reports showed that huge amounts of methane and carbon dioxide can be released from tailings ponds each year due to biodegradation of hydrocarbons (e.g., naphtha and residual bitumen fractions) under anaerobic (methanogenic) conditions by indigenous microbial communities in tailings ponds (You et al., 2021; Siddique and Kuznetsova, 2020). Under methanogenic conditions below the mudline of tailings ponds (Stasik et al., 2014), these petroleum hydrocarbons were first used by indigenous bacteria as carbon and electron sources and degraded into simpler products (e.g., acetate) before further degraded by archaea (e.g., Acetoclastic methanogens) into methane (Siddique and Kuznetsova, 2020). A wide range of hydrocarbons that are constituents of naphtha primarily contribute to methane emissions from OSTP, including *n*-alkanes (Mohamad Shahimin et al., 2016; Siddique et al., 2006), monoaromatics (Siddique et al., 2007), and the more recalcitrant hydrocarbons such as *iso*-alkanes (Mohamad Shahimin and Siddique, 2017; Siddique et al., 2020).

Apart from residual naphtha, other hydrocarbons that are native to bitumen such as PAHs might also contribute to methane production in tailings ponds. However, no reports about the methanogenic biodegradation of tailing-derived PAHs below mudline of OSTP are currently available. Studies in the past a few years have shown the potential biodegradability of PAHs under methanogenic conditions in other environmental matrices such as soil (Ye et al., 2019) and

sediments (K. Zhang et al., 2019), especially for LMW-PAHs such as NAP and PHE with 2- or 3 benzene rings. Through 16S rRNA gene sequencing, it was found that under methanogenic conditions in a subsurface petroleum-contaminated soil, bacterial taxa such as *Alicycliphilus* and *Arcobacter* were involved in NAP and PHE degradation, respectively, with co-dominance of archaeal taxa such as *Methanobacterium* in both NAP and PHE degradation (Ye et al., 2019). In another study, bacterial family including *Clostridiaceae* (a family of *Clostridia*) as well as archaeal family including *Methanobacteriaceae* were considered to be actively involved in methanogenic PHE biodegradation in a substrate composed of soil and sludge (Z. Zhang et al., 2019). The HMW-PAHs including PYR, however, may be more recalcitrant to biodegradation under methanogenic conditions. For instance, in a river sediment, the LMW-PAHs (NAP and PHE) were found to have higher removal efficiencies (%) than HMW-PAHs such as PYR under methanogenic conditions (K. Zhang et al., 2019), which may be because HMW-PAHs have larger octanol-water partition coefficient (K_{ow}), stronger adsorption onto sediment particles and lower solubility in aqueous solutions, which result in a lower biodegradability by microorganisms (Nzila, 2018; Lu et al., 2012).

Excitingly, it was reported that the bacteria family *Clostridiaceae* that was found to be involved in methanogenic biodegradation process of PHE and substituted-NAP (Berdugo-Clavijo et al., 2012; Z. Zhang et al., 2019), also exist abundantly in the tailings ponds (Penner and Foght, 2010). The order *Clostridiales* had been shown to be the potential degraders for *n*-alkanes and naphtha compounds in tailings under methanogenic conditions (Siddique et al., 2012). It implicated that the indigenous bacterial communities of the class *Clostridia* that involved in methanogenic biodegradation of relatively simple hydrocarbons in tailings might potentially become the degraders for PAHs.

1.5.2 Modeling Methane Emissions due to Biodegradation of Hydrocarbons in Tailing Ponds

A first-order kinetic model to predict methane emissions from tailings ponds was developed in 2008 (Siddique et al., 2008) to predict methane emissions from Syncrude Mildred Lake Settling Basin (MLSB) taking into account microbial metabolism of labile hydrocarbons such as BTEX (benzene, toluene, ethylbenzene, and xylenes) compounds and naphtha-range *n*-alkanes (Siddique et al., 2006, 2007). The estimated methane emissions from this model were slightly higher than *in-situ* measured methane flux, likely because the indigenous microbial communities received more nutrients in the experimental microcosms than the *in-situ* environment (Siddique et al., 2008). Since recalcitrant fractions of naphtha such as *iso*-alkanes and cycloalkanes did not biodegrade to produce methane in a year-long experiment (Siddique et al., 2006, 2007), this model predicted methane emissions from more labile hydrocarbons such as BTEX and *n*-alkanes. Later, a refined model was developed to estimate methane emission from biodegradation of an extended range of hydrocarbons in tailings including major fraction of *iso*-alkanes (Kong et al., 2019). Apart from additional hydrocarbons, the second-generation model also took into account more biological factors such as nitrogen limitation for methane generation and microbial growth and death rates. Compared to field measurement of methane emission, the refined model had a fairly good prediction of ~50% of emission from Syncrude and ~95% from CNRL OSTP (Kong et al., 2019). They explained that the gap between predicted and measured methane emission may be due to either inaccuracies associated with field measurements and/or biodegradation of other endogenous carbon compounds. Such compounds might be additional diluent hydrocarbons that were not identified in biodegradation studies, some bitumen hydrocarbons, native organic matter, and PAHs. To further refine the stoichiometric model, more

investigations on biodegradations of other major endogenous hydrocarbons such as PAHs in OSTP over a longer period of experimental time are required.

1.6 Experiment Rationale

The increasing concerns regarding potential toxicity of tailing-derived PAHs to the aquatic ecosystem of EPL require further studies of PAHs remediation but little is known by far about the biodegradability of PAHs under methanogenic conditions below the mudline of tailings ponds. Therefore, we conducted experiments regarding methanogenic biodegradation of PAHs in FFT. It will not only help us understand the potential biodegradability of PAHs by indigenous microbial communities in tailings but may also help us refine the current stoichiometric models for predicting methane emissions from tailings ponds if methanogenic biodegradation of PAHs occurs in tailings ponds and EPLs. Considering the high relative abundance of potential PAHs degraders (e.g., *Clostridia*) in tailings, we assume that methanogenic PAHs biodegradations can be expected in this study with concurrent methane production.

An efficient and accurate method for PAH determination is required to study biodegradation of PAHs in FFT. Though traditional techniques, such as Soxhlet extraction (EPA Method 8100, 3540C), were generally suggested for PAHs determination in solid substrates, we found that the conventional Soxhlet extraction yielded low (~50-60%) PAHs recovery from FFT. It is probably because FFT samples contain substantially high proportion of fine particles such as silt and clay minerals (Jeeravipoolvarn et al., 2009), which might adsorb PAHs onto the particle surfaces (Łyszczarz et al., 2021) and reduce their recovery. Therefore, modifications have to be conducted to adapt these methods to the FFT samples. In this study, we developed and optimized a method for efficient PAHs determination in FFT samples and used it for the biodegradation experiment.

1.7 Organization of Thesis

This thesis has two data chapters: (1) development of an efficient methodology to determine PAHs in FFT samples; and (2) investigation of methanogenic biodegradation of PAHs in FFT. In the first data chapter, the extractant, extraction apparatus, extraction time, and sample cleanup method were optimized for a reproducible PAHs extraction that guarantees reliable data generation for the following experiments. In the second data chapter, three sets of microcosms (Set A, B, and C) with a total of 78 microcosms were established to investigate biodegradation of 6 abundant tailing-derived PAHs (NAP, PHE, PYR, DBF, FLU, and DBT) in different FFTs collected from 3 tailings ponds operated by Syncrude, CNRL, and Albian.

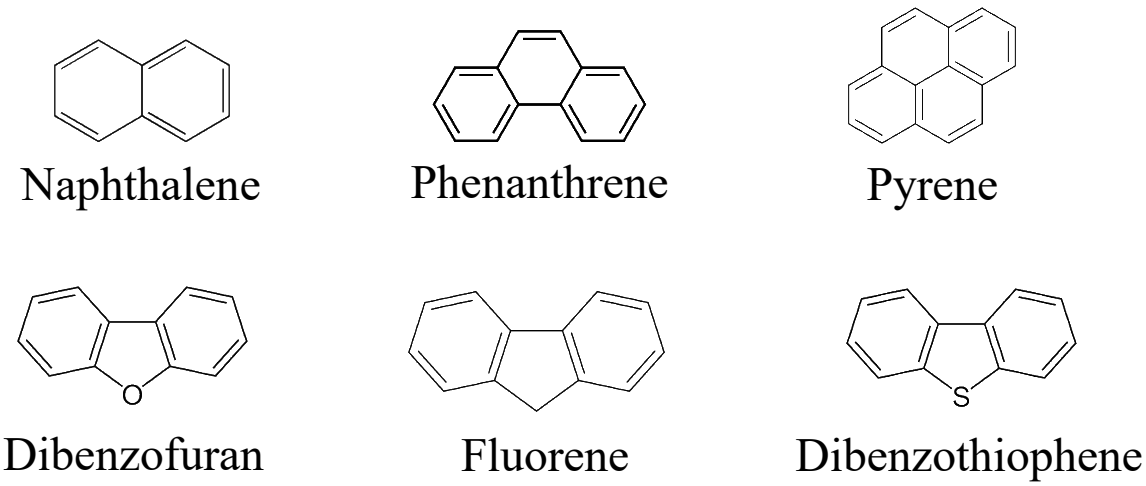

Figure 1-1 Chemical structures of typical PAHs abundant in oil sands tailings.

References

Ahad, J.M.E., Jautzy, J.J., Cumming, B.F., Das, B., Laird, K.R., Sanei, H., 2015. Sources of polycyclic aromatic hydrocarbons (PAHs) to northwestern Saskatchewan lakes east of the Athabasca oil sands. Organic Geochemistry 80, 35–45. https://doi.org/10.1016/j.orggeochem.2015.01.001

Ahad, J.M.E., Pakdel, H., Gammon, P.R., Mayer, B., Savard, M.M., Peru, K.M., Headley, J.V., 2020. Distinguishing Natural from Anthropogenic Sources of Acid Extractable Organics in Groundwater near Oil Sands Tailings Ponds. Environ. Sci. Technol. 54, 2790–2799. https://doi.org/10.1021/acs.est.9b06875

Alberta Energy Regulator, 2023. Crude Oil Production. https://www.aer.ca/providing-information/data-and-reports/statistical-reports/st98/crude-oil/production

Balmer, J.E., Hung, H., Yu, Y., Letcher, R.J., Muir, D.C.G., 2019. Sources and environmental fate of pyrogenic polycyclic aromatic hydrocarbons (PAHs) in the Arctic. Emerging Contaminants 5, 128–142. https://doi.org/10.1016/j.emcon.2019.04.002

Bartlett, A.J., Frank, R.A., Gillis, P.L., Parrott, J.L., Marentette, J.R., Brown, L.R., Hooey, T., Vanderveen, R., McInnis, R., Brunswick, P., Shang, D., Headley, J.V., Peru, K.M., Hewitt, L.M., 2017. Toxicity of naphthenic acids to invertebrates: Extracts from oil sands process-affected water versus commercial mixtures. Environmental Pollution 227, 271–279. https://doi.org/10.1016/j.envpol.2017.04.056

Berdugo-Clavijo, C., Dong, X., Soh, J., Sensen, C.W., Gieg, L.M., 2012. Methanogenic biodegradation of two-ringed polycyclic aromatic hydrocarbons. FEMS Microbiol Ecol 81, 124–133. https://doi.org/10.1111/j.1574-6941.2012.01328.x

Brigmon, R.L., Berry, C.J., Wade, A., Simpson, W., 2016. Bioprocessing-Based Approach for Bitumen/Water/Fines Separation and Hydrocarbon Recovery from Oil Sands Tailings. Soil and Sediment Contamination: An International Journal 25, 241–255. https://doi.org/10.1080/15320383.2015.1020408

Butler, R.M., 1994. Steam-Assisted Gravity Drainage: Concept, Development, Performance And Future. Journal of Canadian Petroleum Technology 33, 44–50. https://doi.org/10.2118/94-02-05

Canadian Association of Petroleum Producers (CAPP), 2021. An Introduction to Oil Sands Pit Lakes. https://www.capp.ca/wp-content/uploads/2021/05/An-Introduction-to-Oil-Sands-Pit-Lakes-392128.pdf

Canadian Council of Ministers of the Environment, 1999. Canadian Environmental Quality Guidelines. https://ccme.ca/en/res/polycyclic-aromatic-hydrocarbons-pahs-en-canadian-water-quality-guidelines-for-the-protection-of-aquatic-life.pdf

Chalaturnyk, R.J., Don Scott, J., Özüm, B., 2002. Management of Oil Sands Tailings. Petroleum Science and Technology 20, 1025–1046. https://doi.org/10.1081/LFT-120003695

Chen, Q., Liu, Q., 2019. Bitumen Coating on Oil Sands Clay Minerals: A Review. Energy Fuels 33, 5933–5943. https://doi.org/10.1021/acs.energyfuels.9b00852

Chen, Y., Wang, Y., Headley, J.V., Huang, R., 2024. Sample preparation, analytical characterization, monitoring, risk assessment and treatment of naphthenic acids in industrial wastewater and surrounding water impacted by unconventional petroleum production. Science of The Total Environment 913, 169636. https://doi.org/10.1016/j.scitotenv.2023.169636

Clark, K.A., Pasternack, D.S., 1932. Hot Water Seperation of Bitumen from Alberta Bituminous Sand. Ind. Eng. Chem. 24, 1410–1416. https://doi.org/10.1021/ie50276a016

Cossey, H.L., Batycky, A.E., Kaminsky, H., Ulrich, A.C., 2021. Geochemical Stability of Oil Sands Tailings in Mine Closure Landforms. Minerals 11, 830. https://doi.org/10.3390/min11080830

Foght, J.M., Gieg, L.M., Siddique, T., 2017. The microbiology of oil sands tailings: past, present, future. FEMS Microbiology Ecology 93. https://doi.org/10.1093/femsec/fix034

Galarneau, E., Hollebone, B.P., Yang, Z., Schuster, J., 2014. Preliminary measurement-based estimates of PAH emissions from oil sands tailings ponds. Atmospheric Environment 97, 332–335. https://doi.org/10.1016/j.atmosenv.2014.08.038

Harner, T., Rauert, C., Muir, D., Schuster, J.K., Hsu, Y.-M., Zhang, L., Marson, G., Watson, J.G., Ahad, J., Cho, S., Jariyasopit, N., Kirk, J., Korosi, J., Landis, M.S., Martin, J.W., Zhang, Y., Fernie, K., Wentworth, G.R., Wnorowski, A., Dabek, E., Charland, J.-P., Pauli, B., Wania, F., Galarneau, E., Cheng, I., Makar, P., Whaley, C., Chow, J.C., Wang, X., 2018. Air synthesis review: polycyclic aromatic compounds in the oil sands region. Environ. Rev. 26, 430–468. https://doi.org/10.1139/er-2018-0039

Holowenko, F., 2002. Characterization of naphthenic acids in oil sands wastewaters by gas chromatography-mass spectrometry. Water Research 36, 2843–2855. https://doi.org/10.1016/S0043-1354(01)00492-4

Honda, M., Suzuki, N., 2020. Toxicities of Polycyclic Aromatic Hydrocarbons for Aquatic Animals. IJERPH 17, 1363. https://doi.org/10.3390/ijerph17041363

Hsu, Y.-M., Harner, T., Li, H., Fellin, P., 2015. PAH Measurements in Air in the Athabasca Oil Sands Region. Environ. Sci. Technol. 49, 5584–5592. https://doi.org/10.1021/acs.est.5b00178

Jeeravipoolvarn, S., Scott, J.D., Chalaturnyk, R.J., 2009. 10 m standpipe tests on oil sands tailings: long-term experimental results and prediction. Can. Geotech. J. 46, 875–888. https://doi.org/10.1139/T09-033

Kelly, E.N., Short, J.W., Schindler, D.W., Hodson, P.V., Ma, M., Kwan, A.K., Fortin, B.L., 2009. Oil sands development contributes polycyclic aromatic compounds to the Athabasca River and its tributaries. Proc. Natl. Acad. Sci. U.S.A. 106, 22346–22351. https://doi.org/10.1073/pnas.0912050106

Kong, J.D., Wang, H., Siddique, T., Foght, J., Semple, K., Burkus, Z., Lewis, M.A., 2019. Second-generation stoichiometric mathematical model to predict methane emissions from oil sands tailings. Science of The Total Environment 694, 133645. https://doi.org/10.1016/j.scitotenv.2019.133645

Li, C., Fu, L., Stafford, J., Belosevic, M., Gamal El-Din, M., 2017. The toxicity of oil sands process-affected water (OSPW): A critical review. Science of The Total Environment 601–602, 1785–1802. https://doi.org/10.1016/j.scitotenv.2017.06.024

Lu, X.-Y., Li, B., Zhang, T., Fang, H.H.P., 2012. Enhanced anoxic bioremediation of PAHs-contaminated sediment. Bioresource Technology 104, 51–58. https://doi.org/10.1016/j.biortech.2011.10.011

Łyszczarz, S., Lasota, J., Szuszkiewicz, M.M., Błońska, E., 2021. Soil texture as a key driver of polycyclic aromatic hydrocarbons (PAHs) distribution in forest topsoils. Sci Rep 11, 14708. https://doi.org/10.1038/s41598-021-94299-x

Mahaffey, A., Dubé, M., 2017. Review of the composition and toxicity of oil sands process-affected water. Environ. Rev. 25, 97–114. https://doi.org/10.1139/er-2015-0060

Marentette, J.R., Frank, R.A., Bartlett, A.J., Gillis, P.L., Hewitt, L.M., Peru, K.M., Headley, J.V., Brunswick, P., Shang, D., Parrott, J.L., 2015. Toxicity of naphthenic acid fraction components extracted from fresh and aged oil sands process-affected waters, and commercial naphthenic acid mixtures, to fathead minnow (Pimephales promelas) embryos. Aquatic Toxicology 164, 108–117. https://doi.org/10.1016/j.aquatox.2015.04.024

Mohamad Shahimin, M.F., Foght, J.M., Siddique, T., 2016. Preferential methanogenic biodegradation of short-chain n-alkanes by microbial communities from two different oil sands tailings ponds. Science of The Total Environment 553, 250–257. https://doi.org/10.1016/j.scitotenv.2016.02.061

Mohamad Shahimin, M.F., Siddique, T., 2017. Sequential biodegradation of complex naphtha hydrocarbons under methanogenic conditions in two different oil sands tailings. Environmental Pollution 221, 398–406. https://doi.org/10.1016/j.envpol.2016.12.002

Nzila, A., 2018. Biodegradation of high-molecular-weight polycyclic aromatic hydrocarbons under anaerobic conditions: Overview of studies, proposed pathways and future perspectives. Environmental Pollution 239, 788–802. https://doi.org/10.1016/j.envpol.2018.04.074

Penner, T.J., Foght, J.M., 2010. Mature fine tailings from oil sands processing harbour diverse methanogenic communities. Can. J. Microbiol. 56, 459–470. https://doi.org/10.1139/W10-029

Raine, J.C., Turcotte, D., Romanowski, L., Parrott, J.L., 2018. Oil sands tailings pond sediment toxicity to early life stages of northern pike (Esox lucius). Science of The Total Environment 624, 567–575. https://doi.org/10.1016/j.scitotenv.2017.12.163

Raine, J.C., Turcotte, D., Tumber, V., Peru, K.M., Wang, Z., Yang, C., Headley, J.V., Parrott, J.L., 2017. The effect of oil sands tailings pond sediments on embryo-larval walleye (Sander vitreus). Environmental Pollution 229, 798–809. https://doi.org/10.1016/j.envpol.2017.06.038

Robinson, C.E., Elvidge, C.K., Frank, R.A., Headley, J.V., Hewitt, L.M., Little, A.G., Robinson, S.A., Trudeau, V.L., Vander Meulen, I.J., Orihel, D.M., 2023. Naphthenic acid fraction compounds reduce the reproductive success of wood frogs (Rana sylvatica) by affecting

offspring viability. Environmental Pollution 316, 120455. https://doi.org/10.1016/j.envpol.2022.120455

Selucky, M., Chu, Y., Ruo, T., Strausz, O., 1977. Chemical composition of Athabasca bitumen. Fuel 56, 369–381. https://doi.org/10.1016/0016-2361(77)90061-8

Siddique, T., Fedorak, P.M., Foght, J.M., 2006. Biodegradation of Short-Chain *n* -Alkanes in Oil Sands Tailings under Methanogenic Conditions. Environ. Sci. Technol. 40, 5459–5464. https://doi.org/10.1021/es060993m

Siddique, T., Fedorak, P.M., MacKinnon, M.D., Foght, J.M., 2007. Metabolism of BTEX and Naphtha Compounds to Methane in Oil Sands Tailings. Environ. Sci. Technol. 41, 2350–2356. https://doi.org/10.1021/es062852q

Siddique, T., Gupta, R., Fedorak, P.M., MacKinnon, M.D., Foght, J.M., 2008. A first approximation kinetic model to predict methane generation from an oil sands tailings settling basin. Chemosphere 72, 1573–1580. https://doi.org/10.1016/j.chemosphere.2008.04.036

Siddique, T., Kuznetsova, A., 2020. Linking hydrocarbon biodegradation to greenhouse gas emissions from oil sands tailings and its impact on tailings management. Can. J. Soil. Sci. 100, 537–545. https://doi.org/10.1139/cjss-2019-0125

Siddique, T., Penner, T., Klassen, J., Nesbø, C., Foght, J.M., 2012. Microbial Communities Involved in Methane Production from Hydrocarbons in Oil Sands Tailings. Environ. Sci. Technol. 46, 9802–9810. https://doi.org/10.1021/es302202c

Siddique, T., Semple, K., Li, C., Foght, J.M., 2020. Methanogenic biodegradation of iso-alkanes and cycloalkanes during long-term incubation with oil sands tailings. Environmental Pollution 258, 113768. https://doi.org/10.1016/j.envpol.2019.113768

Small, C.C., Cho, S., Hashisho, Z., Ulrich, A.C., 2015. Emissions from oil sands tailings ponds: Review of tailings pond parameters and emission estimates. Journal of Petroleum Science and Engineering 127, 490–501. https://doi.org/10.1016/j.petrol.2014.11.020

Smith, S.B., 1981. Alberta Oil Sands Environmental Research Program 1975-1980: Summary Report. S.B. Smith Environmental Consultants Limited, Calgary, AB, Canada. Accessed

Stasik, S., Loick, N., Knöller, K., Weisener, C., Wendt-Potthoff, K., 2014. Understanding biogeochemical gradients of sulfur, iron and carbon in an oil sands tailings pond. Chemical Geology 382, 44–53. https://doi.org/10.1016/j.chemgeo.2014.05.026

Sun, C., Shotyk, W., Cuss, C.W., Donner, M.W., Fennell, J., Javed, M., Noernberg, T., Poesch, M., Pelletier, R., Sinnatamby, N., Siddique, T., Martin, J.W., 2017. Characterization of Naphthenic Acids and Other Dissolved Organics in Natural Water from the Athabasca Oil Sands Region, Canada. Environ. Sci. Technol. 51, 9524–9532. https://doi.org/10.1021/acs.est.7b02082

Syncrude, 2022. 2022 Pit Lake Monitoring and Research Report (Base Mine Lake Demonstration Summary: 2012-2021).

United States Environmental Protection Agency, 1986. Method 8100. Polynuclear Aromatic Hydrocarbons.

United States Environmental Protection Agency, 1996. Method 3540 C, Revision 3. Soxhlet Extraction.

White, K.B., Liber, K., 2020. Chronic Toxicity of Surface Water from a Canadian Oil Sands End Pit Lake to the Freshwater Invertebrates Chironomus dilutus and Ceriodaphnia dubia. Arch Environ Contam Toxicol 78, 439–450. https://doi.org/10.1007/s00244-020-00720-3

Wnorowski, A., Aklilu, Y., Harner, T., Schuster, J., Charland, J.-P., 2021. Polycyclic aromatic compounds in ambient air in the surface minable area of Athabasca oil sands in Alberta (Canada). Atmospheric Environment 244, 117897. https://doi.org/10.1016/j.atmosenv.2020.117897

Ye, Q., Liang, C., Chen, X., Fang, T., Wang, Y., Wang, H., 2019. Molecular characterization of methanogenic microbial communities for degrading various types of polycyclic aromatic hydrocarbon. Journal of Environmental Sciences 86, 97–106. https://doi.org/10.1016/j.jes.2019.04.027

You, Y., Staebler, R.M., Moussa, S.G., Beck, J., Mittermeier, R.L., 2021. Methane emissions from an oil sands tailings pond: a quantitative comparison of fluxes derived by different methods. Atmos. Meas. Tech. 14, 1879–1892. https://doi.org/10.5194/amt-14-1879-2021

Zhang, K., Hu, Z., Zeng, F., Yang, X., Wang, J., Jing, R., Zhang, H., Li, Y., Zhang, Z., 2019. Biodegradation of petroleum hydrocarbons and changes in microbial community structure in sediment under nitrate-, ferric-, sulfate-reducing and methanogenic conditions. Journal of Environmental Management 249, 109425. https://doi.org/10.1016/j.jenvman.2019.109425

Zhang, Y., 2023. Sources, spatial-distributions and fluxes of PAH-contaminated dusts in the Athabasca oil sands region. Environment International.

Zhang, Z., Wang, C., He, J., Wang, H., 2019. Anaerobic phenanthrene biodegradation with four kinds of electron acceptors enriched from the same mixed inoculum and exploration of metabolic pathways. Front. Environ. Sci. Eng. 13, 80. https://doi.org/10.1007/s11783-019-1164-x

Chapter 2: Method Optimization for Higher Recovery and Efficient Determination of Polycyclic Aromatic Hydrocarbons in Fluid Fine Tailings

Graphical Abstract

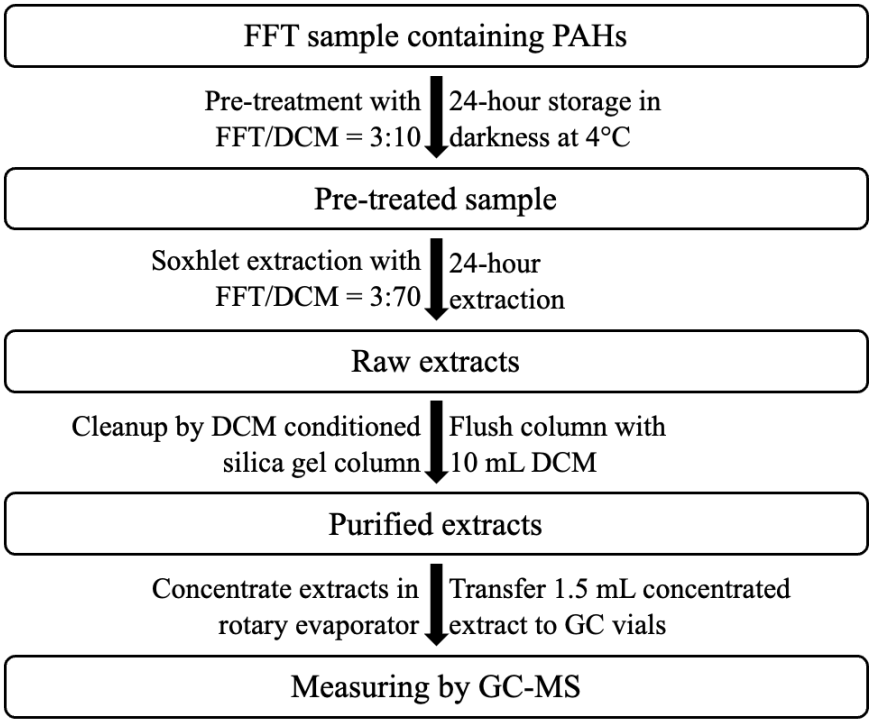

Abstract

Fluid fine tailings (FFT) generated during bitumen extraction from oil sands ores are fine textured wastes containing numerous organic compounds, including polycyclic aromatic hydrocarbons (PAHs). Growing concerns of toxicity effects of PAHs towards human and ecosystem in oil sands area warrants monitoring for environmental consequences and natural attenuation. However, we found that the generally used PAH extraction methods such as conventional Soxhlet extraction yielded low (~50-60%) recovery from FFT, which may impede efficient PAH determination. Therefore, an optimized method was developed in this study to analyze abundant PAHs in FFT [naphthalene (NAP), phenanthrene (PHE), pyrene (PYR), dibenzofuran (DBF), fluorene (FLU), and dibenzothiophene (DBT)]. The method optimization included (1) selection of a suitable solvent; (2) enhancement of PAH recovery by pre-treatment; (3) determination of extraction time; and (4) optimization of sample cleanup procedure. Results showed that (1) significantly more PAHs were recovered by dichloromethane (DCM) than hexane (HEX), cyclohexane (CHX), or their mixtures with DCM; (2) pre-treatment with DCM significantly improved PAHs recovery using either Soxhlet or mechanical shaking method; (3) 24-hour Soxhlet extraction with pre-treatment yielded the highest and the most consistent PAHs recovery; (4) DCM was an efficient eluent for sample cleanup, and consecutive cleanups with additional columns can be used to remove excessive impurities. Efficient PAH determination in FFT was achieved by applying the optimized steps since ~94% pooled mean recovery of PAHs was achieved. This method may also be used to assist PAHs analysis in other fine textured organic rich wastes such as sludge and clay sediments.

Key words: extraction method; Soxhlet; polycyclic aromatic hydrocarbons (PAHs); fluid fine tailings (FFT); fine textured organic rich wastes

2.1 Introduction

The Athabasca oil sands region in northern Alberta, Canada, has the third-largest oil reserves in the world, following Saudi Arabia and Venezuela (Small et al., 2015). The commercially used hot water extraction for bitumen recovery from excavated oil sands ore (Chalaturnyk et al., 2002; Masliyah et al., 2004) generates large volumes of Fluid Fine Tailings (FFT), which are mainly composed of oil sands process-affected water (OSPW), fine solids (<44 μm) including silt and clay minerals (Cossey et al., 2021), and a small amount of hydrocarbons such as residual naphtha (~1%, wt) and bitumen (~5%, wt) (Mahaffey and Dubé, 2017). FFT are temporarily stored in oil sands tailings ponds (OSTP) pending reclamation. One of the promising methods for the management of tailings is to reclaim FFT in mined out pits and cover with cap water to create an end-pit lake (EPL) (Government of Alberta, 2015). The first full-scale demonstration of an EPL is the Base Mine Lake operated by Syncrude Canada Ltd., which was designed to eventually become a sustainable aquatic ecosystem (Syncrude, 2022) and have sufficient water quality to be approved for reintegration with the surrounding environment (CAPP, 2021).

There are growing concerns about the potential toxicity of tailings to aquatic ecosystems of EPLs caused by organic compounds including residual hydrocarbons such as polycyclic aromatic hydrocarbons (PAHs) (Brigmon et al., 2016; Parrott et al., 2019), which are a class of semi-volatile (EPA Method 8275A) hydrocarbons with two or more benzene rings in structure that are considered to be potentially carcinogenic to humans (DHHS, 1995). Examples of abundant PAH species in tailings are naphthalene (NAP), phenanthrene (PHE), pyrene (PYR), dibenzofuran (DBF), fluorene (FLU), and dibenzothiophene (DBT) (Harner et al., 2018; Galarneau et al., 2014; Selucky et al., 1977). PAHs tend to bioaccumulate in various aquatic organisms once entering the aquatic ecosystem (CCME, 1999), and they were found to potentially decrease the

survival of embryos of major Canadian fish species such as Walleye (Raine et al., 2017) and Northern Pike (Raine et al., 2018). Therefore, further studies regarding PAHs remediation in EPL are urgently required.

An efficient and sensitive extraction method is critical to conduct PAHs related experiments, and the USEPA has suggested the use of Soxhlet extraction as a standard method to extract PAHs from general solid samples such as soils, sludges, and wastes (EPA Method 8100, 3540C). It has been shown that the Soxhlet extraction recovered >80% of several PAHs from soil samples, including NAP, PHE, FLU, and PYR (Wang et al., 2007). Apart from the Soxhlet method, mechanical shaking may also efficiently extract PAHs, and ~100% PYR was recovered from a soil sample by mechanical shaking in a previous study (Schwab et al., 1999). However, since FFT samples contain substantially high proportion of fine particles (Jeeravipoolvarn et al., 2009), traditional methods might not be effective to extract PAHs from FFT because PAHs may be adsorbed onto the particle surfaces of silt and clay minerals (Łyszczarz et al., 2021), which probably reduce their recoveries. By applying the conventional Soxhlet method (EPA Method 8100, 3540C), we only recovered ~50-60% of PAHs from FFT. Thus, in this study, we optimized traditional PAHs extraction methods for FFT samples and compared the performance of various of robust organic solvents as well as their mixtures to recover PAHs. The standard cleanup method using silica gel chromatography column (EPA Method 3630C) was also adapted to FFT samples to efficiently remove impurities (co-extracted residual bitumen compounds) from PAHs extracts before measuring by gas chromatography (GC) to prevent potential GC interferences and column damage. The results of this study will help future remediation and characterization efforts to efficiently determine PAHs in fine textured organic rich wastes such as FFT.

2.2 Materials and Methods

2.2.1 Reagents and Chemicals

The PAHs used in this study were purchased as follows: Naphthalene (N7-500; CAS#91-20-3) from Fisher Chemical; Anthracene (99%; CAS#120-12-7); Pyrene (98%; CAS#129-00-0); and Phenanthrene (97%; CAS#85-01-8) from Acros Organics; Dibenzofuran (98%; CAS#132-64-9), Dibenzothiophene (98%; CAS#132-65-0), Fluorene (98%; CAS#86-73-7) and Carbazole (≥95%; CAS# 86-74-8) from Sigma-Aldrich. Solvents were purchased as follows: 2,2,4,4,6,8,8-Heptamethylnonane (HMN) (>97.0%; H0365; CAS#4390-04-9) from Tokyo Chemical Industry Co., Ltd.; Dichloromethane (D37-4; CAS#75-09-2), hexane (HPLC grade; CAS#110-54-3), and cyclohexane (Pesticide Grade; CAS#110-82-7) were purchased from Fisher Chemical. Dry compounds for chromatography column preparation: silica gel (70-200 mesh; CAS#7631-86-9), sodium sulfate (99.0%; CAS#7757-82-6), glass wool (CAS#65997-17-3) and sand (CAS#14808-60-7) were purchased from Thermo Scientific.

2.2.2 Preparation of Microcosms for Method Optimization

FFT samples collected from Syncrude Base Mine Lake at 10.9 m below mudline in 2019 were used. Some essential physical properties of the FFT were measured and shown in Table 2-1. A 158 mL serum bottle was used to prepare spiked FFT sample in a comparable way as the microcosms used in an ongoing experiment regarding microbial degradation of PAHs (Chapter 3). Thus, 50 mL methanogenic media (Fedorak and Hrudey, 1984; Holowenko et al., 2000) was mixed with 50 mL of FFT in a serum bottle sealed with a butyl rubber stopper and an aluminum crimp top.

A stock solution for sample spiking was prepared by dissolving the powder of PAHs (weighted to the nearest 0.1 mg) in 2,2,4,4,6,8,8-Heptamethylnonane (HMN) to bring the

concentration to 50 mmol/L for each of the 6 PAHs, including naphthalene (NAP), phenanthrene (PHE), pyrene (PYR), dibenzofuran (DBF), fluorene (FLU), and dibenzothiophene (DBT). Stock solution was stored in darkness in an EPA vial tightly sealed with a PTFE-lined screw-cap. A 1000 μL and a 100 μL glass syringe were used to spike the stock solution into microcosm to bring the concentration of each PAH to 1 mmol/L in FFT-media slurry. Spiked microcosm was vigorously shaken and stored in darkness for at least 24 hours in room temperature (~21°C) before sampling for following experiments.

2.2.3 Selection of Solvents, Pre-treatment of FFT and Extraction of PAHs

The spiked samples were well mixed by hand followed by taking out samples with the syringe attached to the 18G needle and immediately extracted for PAHs. Different solvents were tested for their efficiencies to extract PAHs from FFT, including sole solvents of dichloromethane (DCM), cyclohexane (CHX), hexane (HEX), as well as mixed solvents of DCM:CHX (1:1, v/v) and DCM:HEX (1:1, v/v).

Two methods for extraction of PAHs were compared in this study, including Soxhlet extraction and mechanical shaking. In mechanical shaking, 1 mL FFT sample was placed in a tightly sealed 40 mL EPA vial before shaking at 180 rpm for 24 hours. In Soxhlet extraction, the device was set up with a 200 mL round bottom flask topped by an extraction chamber with an inside extraction thimble and capped by a condenser with continuous flow of cold water. In each extraction thimble, 2.5 g anhydrous sodium sulfate was placed at the bottom of thimble before adding 3 mL FFT sample for moisture removal. A Labconco heater was used for heating up the flasks, allowing simultaneous operation of 6 Soxhlet extractors. The joints between components of Soxhlet extractor were sealed with high vacuum grease to prevent the leak of solvent vapour.

An FFT/solvent ratio of 3:70 (v/v) was used in both methods. Different extraction times were compared in this study.

To enhance PAH recovery, a pre-treatment step was performed before extraction. The FFT sample was collected in a EPA vial with a PTFE-lined screwcap, tightly sealed, well mixed with solvent by hand and incubated with the solvent for 24 hours under 4°C in darkness to prevent photodegradation of PAHs (Marquès et al., 2016). An FFT/solvent ratio of 3:10 (v/v) was used in pre-treatment step.

2.2.4 Silica Gel Column Preparation for Cleanup of Extracted PAH Containing Solvent

The dry-packed cleanup column was prepared using a 30 cm x 2 cm clean glass burette: first plugged with glass wool at the bottom and topped with ~1 cm sand. Afterwards, 5 g activated silica gel was added to the column and topped with 3 g anhydrous sodium sulfate. The silica gel was activated by heating in the oven at 150°C for at least 24 hours before cleanup to thoroughly remove any residual moisture (water).

2.2.5 Measurement by GC-MS

A rotary evaporator (LabTech) was used to evaporate the extract. The heating bath of evaporator was set at 36°C and the rotation speed of evaporating flask was at 100 rpm. The volume of sample was brought down to 1 mL before transferring and making a total volume of 1.5 mL in a 2 mL GC vial (Thermo Scientific; Cat. number# 6ASV9-1P) sealed with screw caps (Thermo Scientific; Cat. number# 6PSC9STB1). Gas chromatograph (Thermo Fisher Scientific, Trace 1300) coupled with Mass spectrometer (Thermo Fisher Scientific ISQ) and an autosampler (TriPlus RSH, Thermo Fisher Scientific) were used for measurement of PAHs. Liquid samples were analyzed by automatically injecting 1µL of sample from 2 mL vials to the GC column. The TG-5MS capillary column (30m, 0.25mm) was used at ramping oven temperature from 30 °C to

250 °C, and at 1.2 mL/min flow rate of carrier gas (helium). External standards (0.1 mmol/L, 0.2 mmol/L, 0.5 mmol/L, 1 mmol/L, and 2 mmol/L) diluted from the stock solution were used for PAH quantification in samples.

2.2.6 Statistical Analyses

Statistical analyses were performed with R (version 4.3.2) and Origin (2023b) software. One-way ANOVA was used to test significance among different treatments regarding PAHs recoveries. Pairwise comparisons were carried out at $\alpha = 0.1$ in Tukey's Honest Significance Test. The PAHs that can be at least recovered by each tested method was calculated with estimated marginal means in R software at 90% confidence level adjusted with Bonferroni method. To apply the estimated marginal means, we used R to build an overall linear model between treatments and PAHs recoveries, in which recoveries of all replicates were pooled together. Statistical tests were performed for pooled and individual PAHs recoveries separately.

2.3 Results and Discussion

2.3.1 Selection of Solvents

To simultaneously extract various PAHs with different polarities from environmental matrices, a mixture of solvents with varying polarities such as dichloromethane (DCM), cyclohexane (CHX), and hexane (HEX) is recommended (Gbeddy et al., 2020; Lundstedt et al., 2006; Pulleyblank et al., 2020). The polarity index of DCM, CHX, and HEX is 3.1, 0.2, and 0.1, respectively, thus the mixture of DCM with CHX, or DCM with HEX may have the suitable polarity for simultaneous extraction of PAHs with different polarities (Gbeddy et al., 2020).

2.3.1.1 Comparison of DCM, CHX, and CHX/DCM (1:1, v/v)

In our study, the extraction efficiency of a solvent mixture CHX/DCM (1:1, v/v) was compared with sole solvents of CHX and DCM. For pooled PAHs analysis at 90% confidence level, it was shown that at least 76% of each PAH can be recovered by DCM (Table 2-2), which was higher than sole CHX and CHX/DCM (1:1, v/v) solvents. One-way ANOVA showed significance for pooled PAHs recoveries among the tested solvents ($p<0.1$). The mixture of CHX and DCM [CHX/DCM (1:1, v/v)] decreased the mean recovery of PAHs by 25% compared with sole DCM (Figure 2-1A). It is probably because DCM or DCM-containing solvents that have relatively higher polarities than the sole CHX are more efficient to extract PAHs that were probably bounded by the polar fractions of bitumen such as asphaltenes (Werkovits et al., 2022). Similarly, it was shown in another study that PAHs could be bounded to soil organic matters (SOM), and the dissolution of SOM-bound PAHs into solvents might enhance the recovery of PAHs (Gong et al., 2005). Regarding individual PAH analysis, DCM achieved the highest recoveries among all tested solvents (Figure 2-1B) though no significance was shown regarding NAP recovery.

2.3.1.2 Comparison of DCM and DCM/HEX (1:1, v/v)

We also tested the efficiency of DCM and DCM/HEX (1:1, v/v) to extract 8 PAHs [naphthalene (NAP), phenanthrene (PHE), pyrene (PYR), dibenzofuran (DBF), fluorene (FLU), dibenzothiophene (DBT), carbazole (CAR), and anthracene (ANT)] from FFT (Appendix A). In this experiment, DCM showed significantly higher efficiency to extract PAHs from FFT than DCM/HEX (1:1, v/v). One-way ANOVA showed a significant difference ($p<0.1$) for pooled PAHs recovery between DCM and DCM/HEX (1:1, v/v), where a mean recovery of 62% was achieved by DCM but only 19% for the mixed solvent (Figure A-2). At 90% confidence level,

only >15% PAHs can be recovered by DCM/HEX (1:1, v/v) (Table A-1). Thus, DCM was suggested to be used for PAHs extractions.

2.3.2 PAHs Extraction Optimization by Pre-treatment of FFT

Apart from solvents, extraction methods also influence analyte recovery due to their different working principles. Conducting extractions in EPA vials with a mechanical shaker was considered an effective method to extract petroleum hydrocarbons from wet soils due to complete contact between solvents and sample particles (Schwab et al., 1999). On the other hand, the standard Soxhlet method for liquid-solid extraction is renowned for its stability and high efficiency (Fabbri et al., 2013). In our study, we tested the efficiency of mechanical shaking and Soxhlet extraction to recover PAHs from FFT using DCM as the sole solvent. To maximize PAHs recoveries from FFT by mechanical shaking and Soxhlet method, a pre-treatment process was developed and applied to the two methods. Thus, four extraction processes, namely, Soxhlet method, mechanical shaking, and either method paired with DCM pre-treatment were conducted. After obtaining significance from one-way ANOVA ($p<0.1$), pairwise comparisons were applied to pooled PAHs recoveries by the four extraction processes.

Results showed that without pre-treatment, 24-hour mechanical shaking had a significantly higher recovery than Soxhlet method, which was probably because the non-agitating extraction of Soxhlet method was not as efficient for the compacted fine substrate such as FFT, in which the high proportion of fine silt and clay particles may pose great sorption to PAHs (Łyszczarz et al., 2021). On the contrary, continuous mechanical shaking enhanced the contact between DCM and tailing micropores (Schwab et al., 1999) and led to higher PAHs recoveries. After applying pre-treatment, the efficiency of Soxhlet method substantially improved from 53% to 94% (Figure 2-1C), which was probably the result of an improved DCM-tailing contact and an elongated time

(another 24 hours) for PAHs to desorb from fine particles (Łyszczarz et al., 2021). More bitumen and bitumen-bound PAHs in FFT may also be extracted by Soxhlet method after pre-treatment, which led to a higher PAHs recovery and a darker color in the resulting extracts. At 90% confidence level (Table 2-2), at least 86% PAH recoveries can be achieved by extracting pre-treated samples with Soxhlet method. In addition, PAH recoveries by mechanical shaking was also significantly improved by pre-treatment, though less stable recoveries with larger variations were shown, especially regarding individual PAHs such as PYR (Figure 2-1D). Similarly, Berset with co-authors also reported a relatively higher variation for PAHs recoveries (e.g., NAP, PHE, PYR and FLU) from mechanical shaking comparing to Soxhlet method (Berset et al., 1999). For our study, the variation for mechanical shaking may be because the effect of inhomogeneous distribution of PAHs in heterogeneous FFT was magnified when less sample was taken for extraction (1 mL in mechanical shaking compared with 3 mL in Soxhlet method). The inhomogeneous distribution of PAHs may be caused by their different adsorption activities onto various FFT fractions such as minerals and organic particles surfaces (Cossey et al., 2021; Łyszczarz et al., 2021; Shen et al., 2022). Therefore, to achieve efficient and more reproducible extractions, we used Soxhlet method with pre-treatment for all subsequent tests in this study. However, mechanical shaking with pre-treatment can be the substituted method for PAHs extraction from FFT if a Soxhlet device is not available due to its relatively simple operating procedure and high PAHs recoveries.

2.3.3 Extraction Time

Extraction time is critical to Soxhlet extraction, and 6 to 24 hours were generally recommended for Soxhlet extraction (Shu et al., 2000). The efficiencies of Soxhlet method to extract PAHs from biochar using different extraction time (18-48 hours) was previously

investigated, and 36h was considered to be the optimal time with the highest PAHs recovery (Fabbri et al., 2013). In our study, 3 Soxhlet extraction times, namely 8h, 16h, and 24h were tested. After obtaining significance from one-way ANOVA ($p<0.1$) using pooled recovery, pairwise comparisons were conducted to the three time durations at 90% confidence level (Figure 2-1E), showing 24h Soxhlet extraction had a significantly higher mean recovery of PAHs (>85%) than either 8h (>48%) or 16h (>75%) (Table 2-2). Approximately 80% PHE can be at least recovered by 24h Soxhlet extraction, which was comparable to a previous work (Fabbri et al., 2013) in which 77% PHE can be extracted after 36h Soxhlet. Regarding analysis of individual PAH (Figure 2-1F), significant recovery improvement was shown by extending duration time from 8h to 16h for each PAH, but no significance was found between 16h and 24h.

2.3.4 Preparing Cleanup Column with Different Eluents

While applying appropriate extraction is crucial for an efficient determination of PAHs, the cleanup method can jeopardize overall analysis if not properly designed and implemented. Co-extracted polar fractions from residual bitumen or endogenous organic matter were considered as impurities in our extracts and should be removed by silica gel chromatography column (Fletouris, 2007) to prevent potential GC interferences or column damage. Meanwhile, PAHs should not be retained by the column during cleanup. Low-polarity solvents such as CHX and DCM were generally recommended (EPA Method 3630C) to elute the cleanup column. To test the impurity removal efficiency of columns eluted by different eluents, we prepared two types of cleanup columns that were primed by CHX or DCM, respectively. The mobile phase of the CHX-eluted column was considered as the mixed mobile phase since ~60-70 mL DCM in the unpurified extracts was introduced into the column. Results showed the two types of columns performed similarly in removing polar impurities from extracts, with pale yellow colors in the

purified products. One-way ANOVA showed no significance between these two types of columns regarding PAHs elution (Figure 2-2 A and B), with expected PAHs recoveries at 90% confidence level shown in Table 2-3. Considering the practicability of the process, the DCM-eluted column is recommended for cleanup since only one solvent (DCM) is required in the process.

2.3.5 Column Flushing

Excessive volumes of solvents was generally required to rinse the column after sample is passed through to flush down residual analytes from the column (EPA Method 3630C). To compare PAHs recovery from the column using different volumes of the eluent, we tested 5 mL, 10 mL, and 20 mL of DCM for flushing. No significance was shown in one-way ANOVA among the three flushing volumes regarding PAHs elution while an optimal PAHs recovery may be achieved by 10 mL DCM due to its slightly higher recovery of PAHs (Figure 2-2 C and D, and Table 2-3). It is probably because the volume of DCM of the unpurified raw extract (~60-70 mL) was able to elute most of PAHs from the column so that the differences among the three volumes of flushing solvents was minimum. To reduce solvent usage while obtaining the optimal PAHs recovery, 10 mL DCM were recommended for flushing. This test, however, was specific to the size of column and the mass of packed silica gel used in this study and future tests are required toward different cleanup columns.

2.3.6 Cleanup Cycles

It must be mentioned that more than one cleanup cycle may be required to remove excessive amounts of polar impurities that probably exist in different FFT samples or other substrates. However, PAHs should not be retained by the additional columns. We used the same method to prepare an additional column to purify the extracts obtained from the first column, and one-way

ANOVA showed no significance regarding PAHs recovery from the first and the second cleanup column (Figure 2-2 E and F), and the amount of PAHs that can be at least eluted from each column at 90% confidence level were shown in Table 2-3. Although the first cleanup cycle is adequate to remove impurities from our extracts (Figure 2-3), more cleanup cycles can be applied to the extracts of other organic rich substrates without losing significant amount of PAHs.

2.3.7 Application of Optimized Method for PAHs Recoveries

One of the previous batches in extraction optimization tests (blue bars in Figure 2-1 C and D) had the combination of variables exactly same to the optimized procedure. In this batch, DCM was used to pre-treat spiked FFT samples followed by 24-hour Soxhlet extraction. Afterwards, the raw extracts were purified by DCM-eluted silica gel columns and flushed with 10 mL DCM. The purified extracts were concentrated in a rotary evaporator to decrease the volume to ~1 mL before transferring and making 1.5 mL volume in a 2 mL GC vial for subsequent measurement. More than 100% recovery (>1 mmol/L) of some PAHs in this batch (Figure 2-1D) was probably the result of their inhomogeneous distribution and different sorption potential onto the fine particles or the organic matters in FFT. Similarly, it was reported previously that >111% of FLU may be recovered from river sediments by accelerated solvent extraction (Han et al., 2019). Comparing with conventional Soxhlet method (red bars in Figure 2-1 and Figure A-2) that has relatively low recovery of PAHs (~60%), the optimized method significantly increased the mean recovery of PAHs by ~40%.

2.4 Conclusions

We optimized and developed a method for efficient determination of PAHs in FFT, in which the FFT sample should be pre-treated by DCM and extracted with Soxhlet extractor followed by

extract cleanup with silica gel columns and measured by GC-MS. DCM was effective for the whole procedure and no solvent exchange is required. Sample pre-treatment was developed to enhance the contact between fine tailing particles and solvents, allowing an extended time for the desorption of PAHs from the fine particle surfaces. The recovery of PAHs using Soxhlet method was significantly improved by pre-treatment, and the highest PAHs recoveries were shown when DCM was the sole solvent due to the potential bitumen-PAHs adsorption. Extraction time is vital for Soxhlet method, and each sample should be extracted for 24 hours to achieve optimal recovery. Similar performance of impurities removal and PAHs recovery was shown between silica gel chromatography columns that were pre-eluted by DCM or CHX. An additional 10 mL of DCM was required to flush the column, and consecutive columns can be used to remove excessive impurities that probably exist in other organic rich wastes. By applying the optimized method developed from this study, the 6 abundant PAHs in FFT [naphthalene (NAP), phenanthrene (PHE), pyrene (PYR), dibenzofuran (DBF), fluorene (FLU), and dibenzothiophene (DBT)] can be efficiently extracted using simple apparatus and easily accessible solvents, and the mean recovery of PAHs from 80% (NAP) to 103% (PHE) can be achieved. The success of this approach will help future work of PAHs determination and management in fluid fine tailings and other heavy textured organic rich wastes.

Table 2-1 Characteristics of FFT collected from Syncrude Base Mine Lake at 10.9 m below mudline.

Parameters	**Fluid Fine Tailing**
pH	7.2
Water content (wt%)	64.7%
Bitumen (wt%)	1.2%
Fine and medium sand (wt%)	10.0%
Coarse and medium silt (wt%)	10.0%
Fine silt (wt%)	37.5%
Clay (wt%)	28.5%

Table 2-2 PAHs that can be at least recovered by the applied methods at 90% confidence level (α=0.1) with n=3 and n=18 for individual and pooled PAHs, respectively. Data was shown as concentration (mmol/L) of PAHs in the final extracts measured by GC.

	NAP	PHE	PYR	DBF	FLU	DBT	PAHs†
Solvents							
CHX, sole	0.31	0.10	0.04	0.15	0.11	0.10	0.25
CHX/DCM (1:1)	0.39	0.34	0.29	0.35	0.34	0.33	0.45
DCM, sole	0.54	0.70	0.62	0.65	0.68	0.67	0.76
Methods							
Sox	0.34	0.41	0.41	0.41	0.40	0.37	0.45
Sox+Pre	0.66	0.85	0.89	0.78	0.81	0.76	0.86
Sha	0.35	0.80	0.88	0.70	0.79	0.74	0.77
Sha+Pre‡	0.55	1.07	1.15	0.98	1.09	1.08	1.04
Time							
8h	0.38	0.43	0.43	0.46	0.44	0.45	0.48
16h	0.63	0.70	0.75	0.71	0.71	0.72	0.75
24h	0.71	0.80	0.88	0.79	0.80	0.81	0.85

† Pooled recoveries for 6 PAHs.

‡ n=2 and n=17 for PYR and pooled PAHs, respectively.

Table 2-3 PAHs that can be at least eluted from applied columns at 90% confidence level (α=0.1). Data was shown as concentration (mmol/L) of PAHs in final extracts measured by GC.

	NAP	PHE	PYR	DBF	FLU	DBT	PAHs†
Mobile Phases‡							
DCM	0.56	0.77	0.86	0.72	0.82	0.79	0.77
Mixed	0.59	0.74	0.82	0.73	0.76	0.68	0.74
Flushing Volumes§							
5 mL	0.49	0.62	0.65	0.63	0.62	0.62	0.73
10 mL	0.53	0.66	0.68	0.67	0.68	0.66	0.78
20 mL	0.51	0.64	0.65	0.66	0.66	0.65	0.76
1st and 2nd Cleanup¥							
1st	0.52	0.67	0.72	0.65	0.70	0.66	0.71
2nd	0.51	0.73	0.79	0.64	0.70	0.65	0.73

† Pooled PAHs recoveries.

‡ n=3 and n=18 for individual and pooled PAHs, respectively.

§ n=2 and n=12 for individual and pooled PAHs, respectively.

¥ n=3 and n=18 for individual and pooled PAHs, respectively.

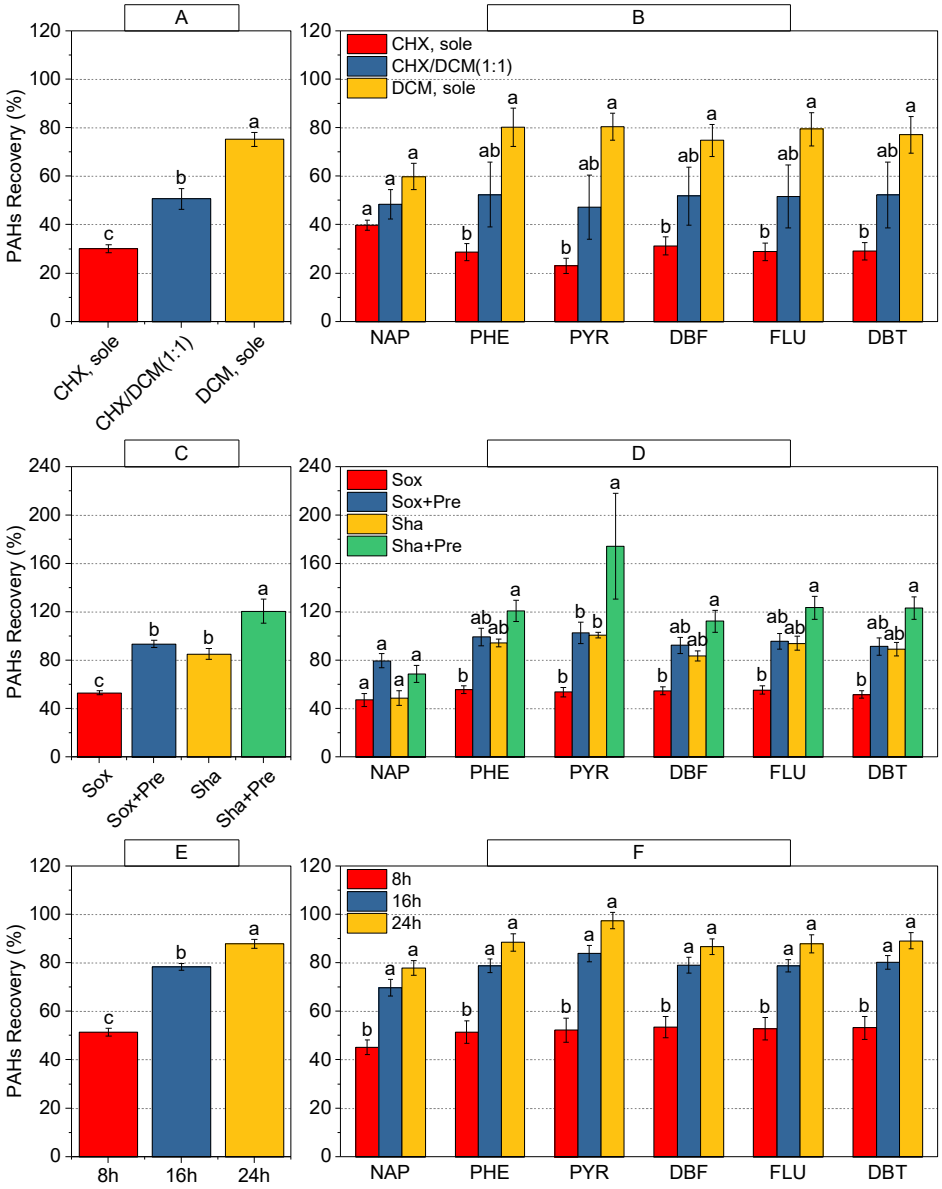

Figure 2-1 Pairwise comparisons of PAHs recoveries (%) in three optimization procedures based on Tukey's test. Significance level=0.1. Error bars of ±1 standard error with n=18 (pooled data for concentration of 6 PAHs in triplicate extraction) for pooled analysis (Panel A, C, and E) and n=3 for individual analysis (Panel B, D, and F). Letters on top of each error bar shows significance, where the column with highest pooled mean value was marked with letter a following b and/or c. No significance exists among columns share the same letter(s). **Panel A and B:** Efficiencies of using three solvents (Cyclohexane (CHX), CHX/DCM (1:1, v/v), and DCM) to extract PAHs from FFT using pooled recovery (Panel A) and individual recovery (Panel B); **Panel C and D:** Efficiencies of four methods to extract PAHs from FFT using pooled recovery (Panel C) and individual recovery (Panel D), including Soxhlet method (Sox), Soxhlet method with Pre-treatment (Sox+Pre), mechanical shaking (Sha) and mechanical shaking with Pre-treatment (Sha+Pre). **Panel E and F:** Efficiencies of three extraction duration time (8h, 16h, and 24h) in PAHs extraction from FFT using pooled recovery (Panel E) and individual recovery (Panel F).

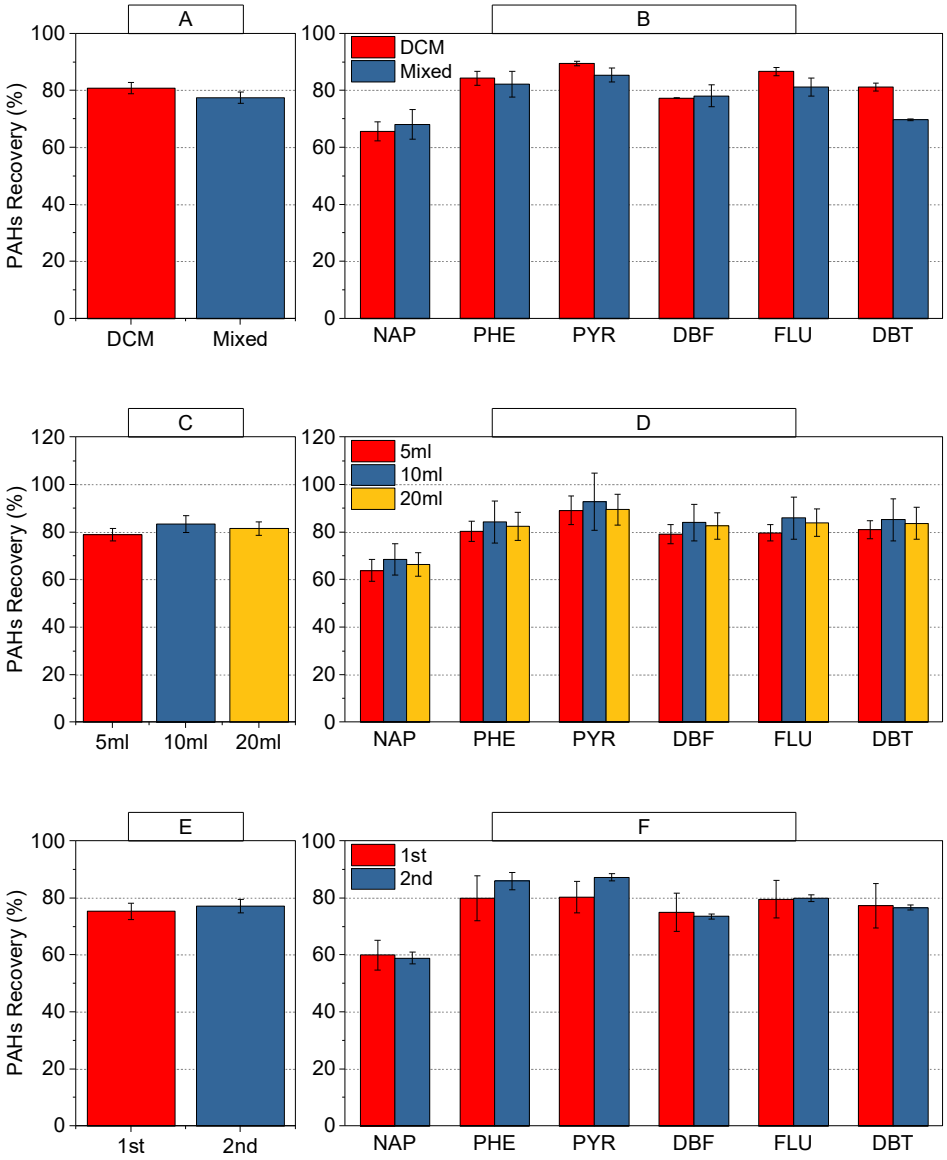

Figure 2-2 Pooled and individual analysis for PAHs recoveries (%) using population mean as column height and standard error as error bars. **Panel A and B** Pooled (Panel A, n=18) and individual (Panel B, n=3) recoveries of eluted PAHs from columns with DCM or DCM and CHX (Mixed) as the mobile phase; **Panel C and D** Pooled (Panel C, n=12) and individual (Panel D, n=2) recoveries of eluted PAHs from columns flushed with 5-, 10-, and 20 mL DCM after sample passing through; **Panel E and F** Pooled (Panel E, n=18) and individual (Panel F, n=3) recoveries of eluted PAHs from the first and the second cleanup columns.

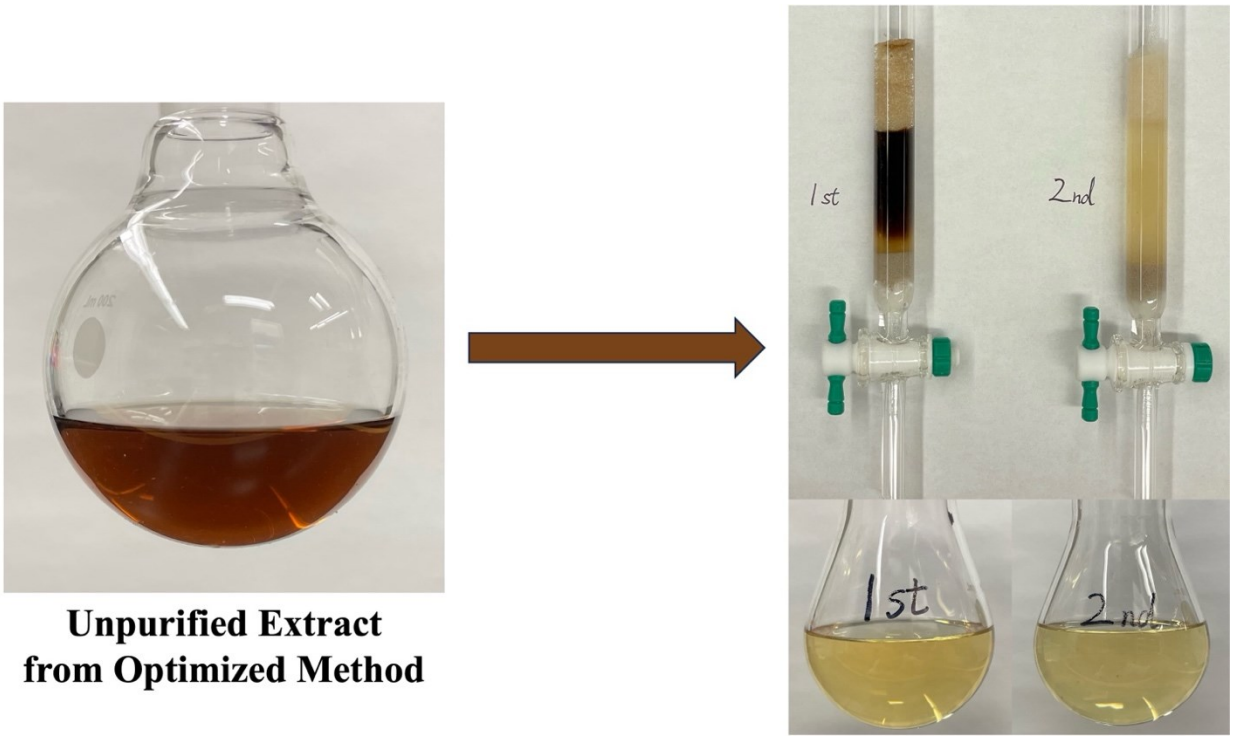

Figure 2-3 Unpurified extract (left panel) and the first and second cleanup columns with purified extracts (right panel).

References

Berset, J.D., Ejem, M., Holzer, R., Lischer, P., 1999. Comparison of different drying, extraction and detection techniques for the determination of priority polycyclic aromatic hydrocarbons in background contaminated soil samples. Analytica Chimica Acta 383, 263–275. https://doi.org/10.1016/S0003-2670(98)00817-4

Brigmon, R.L., Berry, C.J., Wade, A., Simpson, W., 2016. Bioprocessing-Based Approach for Bitumen/Water/Fines Separation and Hydrocarbon Recovery from Oil Sands Tailings. Soil and Sediment Contamination: An International Journal 25, 241–255. https://doi.org/10.1080/15320383.2015.1020408

Canadian Association of Petroleum Producers (CAPP), 2021. An Introduction to Oil Sands Pit Lakes. https://www.capp.ca/wp-content/uploads/2021/05/An-Introduction-to-Oil-Sands-Pit-Lakes-392128.pdf

Canadian Council of Ministers of the Environment, 1999. Canadian Environmental Quality Guidelines. https://ccme.ca/en/res/polycyclic-aromatic-hydrocarbons-pahs-en-canadian-water-quality-guidelines-for-the-protection-of-aquatic-life.pdf

Chalaturnyk, R.J., Don Scott, J., Özüm, B., 2002. Management of Oil Sands Tailings. Petroleum Science and Technology 20, 1025–1046. https://doi.org/10.1081/LFT-120003695

Cossey, H.L., Batycky, A.E., Kaminsky, H., Ulrich, A.C., 2021. Geochemical Stability of Oil Sands Tailings in Mine Closure Landforms. Minerals 11, 830. https://doi.org/10.3390/min11080830

Fabbri, D., Rombolà, A.G., Torri, C., Spokas, K.A., 2013. Determination of polycyclic aromatic hydrocarbons in biochar and biochar amended soil. Journal of Analytical and Applied Pyrolysis 103, 60–67. https://doi.org/10.1016/j.jaap.2012.10.003

Fedorak, P.M., Hrudey, S.E., 1984. The effects of phenol and some alkyl phenolics on batch anaerobic methanogenesis. Water Research 18, 361–367. https://doi.org/10.1016/0043-1354(84)90113-1

Fletouris, D.J., 2007. Clean-up and fractionation methods, in: Food Toxicants Analysis. Elsevier, pp. 299–348. https://doi.org/10.1016/B978-044452843-8/50011-0

Galarneau, E., Hollebone, B.P., Yang, Z., Schuster, J., 2014. Preliminary measurement-based estimates of PAH emissions from oil sands tailings ponds. Atmospheric Environment 97, 332–335. https://doi.org/10.1016/j.atmosenv.2014.08.038

Gbeddy, G., Egodawatta, P., Goonetilleke, A., Ayoko, G., Jayarathne, A., Chen, L., Russell, S., 2020. Optimized simultaneous pressurized fluid extraction and in-cell clean-up, and analysis of polycyclic aromatic hydrocarbons (PAHs), and nitro-, carbonyl-, hydroxy - PAHs in solid particles. Analytica Chimica Acta 1125, 19–28. https://doi.org/10.1016/j.aca.2020.05.021

Gong, Z., Alef, K., Wilke, B.-M., Li, P., 2005. Dissolution and removal of PAHs from a contaminated soil using sunflower oil. Chemosphere 58, 291–298. https://doi.org/10.1016/j.chemosphere.2004.07.035

Government of Alberta, 2015. Lower Athabasca Region - Tailings Management Framework for the Mineable Athabasca Oil Sands.

Han, M., Kong, J., Yuan, J., He, H., Hu, J., Yang, S., Li, S., Zhang, L., Sun, C., 2019. Method development for simultaneous analyses of polycyclic aromatic hydrocarbons and their nitro-, oxy-, hydroxy- derivatives in sediments. Talanta 205, 120128. https://doi.org/10.1016/j.talanta.2019.120128

Harner, T., Rauert, C., Muir, D., Schuster, J.K., Hsu, Y.-M., Zhang, L., Marson, G., Watson, J.G., Ahad, J., Cho, S., Jariyasopit, N., Kirk, J., Korosi, J., Landis, M.S., Martin, J.W., Zhang, Y., Fernie, K., Wentworth, G.R., Wnorowski, A., Dabek, E., Charland, J.-P., Pauli, B., Wania, F., Galarneau, E., Cheng, I., Makar, P., Whaley, C., Chow, J.C., Wang, X., 2018. Air synthesis review: polycyclic aromatic compounds in the oil sands region. Environ. Rev. 26, 430–468. https://doi.org/10.1139/er-2018-0039

Holowenko, F.M., MacKinnon, M.D., Fedorak, P.M., 2000. Methanogens and sulfate-reducing bacteria in oil sands fine tailings waste. Canadian Journal of Microbiology 46, 927–937.

Jeeravipoolvarn, S., Scott, J.D., Chalaturnyk, R.J., 2009. 10 m standpipe tests on oil sands tailings: long-term experimental results and prediction. Can. Geotech. J. 46, 875–888. https://doi.org/10.1139/T09-033

Lundstedt, S., Haglund, P., Öberg, L., 2006. Simultaneous Extraction and Fractionation of Polycyclic Aromatic Hydrocarbons and Their Oxygenated Derivatives in Soil Using

Selective Pressurized Liquid Extraction. Anal. Chem. 78, 2993–3000. https://doi.org/10.1021/ac052178f

Łyszczarz, S., Lasota, J., Szuszkiewicz, M.M., Błońska, E., 2021. Soil texture as a key driver of polycyclic aromatic hydrocarbons (PAHs) distribution in forest topsoils. Sci Rep 11, 14708. https://doi.org/10.1038/s41598-021-94299-x

Mahaffey, A., Dubé, M., 2017. Review of the composition and toxicity of oil sands process-affected water. Environ. Rev. 25, 97–114. https://doi.org/10.1139/er-2015-0060

Marquès, M., Mari, M., Audí-Miró, C., Sierra, J., Soler, A., Nadal, M., Domingo, J.L., 2016. Photodegradation of polycyclic aromatic hydrocarbons in soils under a climate change base scenario. Chemosphere 148, 495–503. https://doi.org/10.1016/j.chemosphere.2016.01.069

Masliyah, J., Zhou, Z.J., Xu, Z., Czarnecki, J., Hamza, H., 2004. Understanding Water-Based Bitumen Extraction from Athabasca Oil Sands. The Canadian Journal of Chemical Engineering 82, 628–654. https://doi.org/10.1002/cjce.5450820403

Parrott, J.L., Raine, J.C., McMaster, M.E., Hewitt, L.M., 2019. Chronic toxicity of oil sands tailings pond sediments to early life stages of fathead minnow (Pimephales promelas). Heliyon 5, e02509. https://doi.org/10.1016/j.heliyon.2019.e02509

Pulleyblank, C., Kelleher, B., Campo, P., Coulon, F., 2020. Recovery of polycyclic aromatic hydrocarbons and their oxygenated derivatives in contaminated soils using aminopropyl silica solid phase extraction. Chemosphere 258, 127314. https://doi.org/10.1016/j.chemosphere.2020.127314

Raine, J.C., Turcotte, D., Romanowski, L., Parrott, J.L., 2018. Oil sands tailings pond sediment toxicity to early life stages of northern pike (Esox lucius). Science of The Total Environment 624, 567–575. https://doi.org/10.1016/j.scitotenv.2017.12.163

Raine, J.C., Turcotte, D., Tumber, V., Peru, K.M., Wang, Z., Yang, C., Headley, J.V., Parrott, J.L., 2017. The effect of oil sands tailings pond sediments on embryo-larval walleye (Sander vitreus). Environmental Pollution 229, 798–809. https://doi.org/10.1016/j.envpol.2017.06.038

Schwab, A.P., Su, J., Wetzel, S., Pekarek, S., Banks, M.K., 1999. Extraction of Petroleum Hydrocarbons from Soil by Mechanical Shaking. Environ. Sci. Technol. 33, 1940–1945. https://doi.org/10.1021/es9809758

Selucky, M., Chu, Y., Ruo, T., Strausz, O., 1977. Chemical composition of Athabasca bitumen. Fuel 56, 369–381. https://doi.org/10.1016/0016-2361(77)90061-8

Shen, X., Dong, W., Wan, Y., Liu, Y., Yuan, Z., 2022. Function of Fe(III) in naphthalene adsorption on typical clay minerals and humic acid complexes. Journal of Environmental Chemical Engineering 10, 108271. https://doi.org/10.1016/j.jece.2022.108271

Shu, Y.Y., Lao, R.C., Chiu, C.H., Turle, R., 2000. Analysis of polycyclic aromatic hydrocarbons in sediment reference materials by microwave-assisted extraction. Chemosphere 41, 1709–1716. https://doi.org/10.1016/S0045-6535(00)00065-5

Small, C.C., Cho, S., Hashisho, Z., Ulrich, A.C., 2015. Emissions from oil sands tailings ponds: Review of tailings pond parameters and emission estimates. Journal of Petroleum Science and Engineering 127, 490–501. https://doi.org/10.1016/j.petrol.2014.11.020

Syncrude, 2022. 2022 Pit Lake Monitoring and Research Report (Base Mine Lake Demonstration Summary: 2012-2021).

United States Department of Health and Human Services, 1995. Toxicological Profile for Polycyclic Aromatic Hydrocarbons.

United States Environmental Protection Agency, 1986. Method 8100. Polynuclear aromatic hydrocarbons.

United States Environmental Protection Agency, 1996. Method 3540C, Revision 3. Soxhlet extraction.

United States Environmental Protection Agency, 1986. Method 3630C, Revision 3. Polynuclear aromatic hydrocarbons.

United States Environmental Protection Agency, 1996. Method 8275A, Revision 1. Semivolatile organic compounds (PAHs and PCBs) in soils/sludges and solid wastes using thermal extraction/gas chromatography/mass spectrometry (TE/GC/MS)

Wang, W., Meng, B., Lu, X., Liu, Y., Tao, S., 2007. Extraction of polycyclic aromatic hydrocarbons and organochlorine pesticides from soils: A comparison between Soxhlet extraction, microwave-assisted extraction and accelerated solvent extraction techniques. Analytica Chimica Acta 602, 211–222. https://doi.org/10.1016/j.aca.2007.09.023

Werkovits, S., Bacher, M., Theiner, J., Rosenau, T., Grothe, H., 2022. Multi-spectroscopic characterization of bitumen and its polarity-based fractions. Construction and Building Materials 352, 128992. https://doi.org/10.1016/j.conbuildmat.2022.128992

Chapter 3: Methanogenic Biodegradation of Polycyclic Aromatic Hydrocarbons in Fluid Fine Tailings

Abstract

Management of oil sands tailings is a component of land reclamation activities after surface mining. Bitumen extraction from oil sands ore using hot water generates huge volumes of fluid fine tailings (FFT) that are temporarily deposited in oil sands tailings ponds (OSTP) pending reclamation into parts of the closure landscape such as end-pit lakes (EPL). Methane emissions from OSTP and EPL occur because of microbial metabolism of entrained hydrocarbons in FFT that were deposited in OSTP or reclaimed in EPL, which may potentially impede Alberta's goal to reduce greenhouse gas emissions and achieve a carbon neutral economy by 2050. To support sustainable oil sands development in Alberta, it is important to predict the intensity and longevity of methane emissions from OSTP and EPL. A previously developed kinetic model predicts methane production taking into account the microbial metabolism of labile hydrocarbons such as alkanes and monoaromatics. Polycyclic aromatic hydrocarbons (PAHs) had been reported to exist in FFT, but no research has been done to assess their biodegradability under methanogenic conditions in tailings. Therefore, we investigated the biodegradation of the most abundant 6 PAHs (naphthalene [NAP], phenanthrene [PHE], pyrene [PYR], dibenzofuran [DBF], fluorene [FLU], and dibenzothiophene [DBT]) in OSTP by indigenous microbial communities under methanogenic conditions. Results show that currently the indigenous microbial communities in tailing are not able to degrade target PAHs under methanogenic conditions in ~700 days, though expected PAHs degradation may be seen in the following months due to the high relative abundance of potential PAHs degraders (e.g., *Clostridia*) in FFT. The results may not only help understand the biodegradation of recalcitrant hydrocarbons under anaerobic environments but also help improve our existing kinetic model to predict methane production and emissions from OSTPs and EPLs.

Keywords: Oil Sands Tailings Ponds Reclamation; Fluid Fine Tailings; Polycyclic Aromatic Hydrocarbons; Methanogenic Biodegradation

3.1 Introduction

The northern Alberta, Canada, including Athabasca, Peace River, and Cold Lake oil sands regions, stored an estimated 300 billion barrels of recoverable bitumen, which is one of the largest oil reserves in the world (Small et al., 2015; Cossey et al., 2021). Current techniques using hot water to extract bitumen from the oil sands after surface mining (Clark and Pasternack, 1932) generates huge amounts of tailings known as fluid fine tailings (FFT) that are temporarily deposited in to oil sands tailings ponds (OSTP) and are eventually required to be reclaimed to part of the closure landscapes such as End Pit Lakes (EPL) (CAPP, 2021). Residual bitumen and a small amount of froth treatment diluents such as naphtha are also deposited to the OSTP through FFT (Cossey et al., 2021). Reports have shown that large amounts of methane can be emitted from the OSTP each year owing to biodegradation of entrained hydrocarbons such as *n*-alkanes (Mohamad Shahimin et al., 2016; Siddique et al., 2006) and monoaromatics (Siddique et al., 2007) by indigenous microbial communities under methanogenic conditions (You et al., 2021; Siddique and Kuznetsova, 2020). For instance, the bacterial *Clostridiales* and acetoclastic methanogens (*Methanosaetaceae*) have been shown to be potentially involved in biodegradation of *n*-alkanes in tailings under methanogenic conditions (Siddique et al., 2012). Kinetic models have been developed to predict methane production from the OSTP taking into account the microbial metabolism of labile hydrocarbons such as naphtha-range *n*-alkanes (Kong et al., 2019; Siddique et al., 2008). Though the current model has fairly good predictions of methane emissions from various tailings ponds comparing with the field measured data (e.g., ~95% of measured methane emission from an OSTP operated by Canadian Natural Resources Limited) (Kong et al., 2019), the differences between predicted and measured methane requires further

studies to monitor potential degradation of other endogenous hydrocarbons in tailings ponds (Kong et al., 2019).

Polycyclic aromatic hydrocarbons (PAHs) are a class of hundreds of petroleum hydrocarbons containing two or more benzene rings that are persistent environmental pollutants existing in various of environmental matrices such as atmosphere, surface water, and soil (Galarneau et al., 2014; Hsu et al., 2015; Zavgorodnyaya et al., 2019). The delocalization of electrons within the benzene ring results in the stabilization of PAH molecule and the increased resistance to biodegradation (Hashemzadeh et al., 2024). The incorporation of heteroatoms with lone pairs of electrons such as oxygen (e.g., dibenzofuran) and sulfur (dibenzothiophene) can be involved in the π-electron delocalization (Bean, 1998) and further increase the PAH structural stability. PAHs naturally exist in bitumen and can be deposited into OSTP with tailings (Brigmon et al., 2016). No reports have shown the biodegradation of PAHs under methanogenic conditions in FFT so far, but other studies have found potential PAHs degraders in various environmental matrices. For instance, the co-dominance of bacterial taxa such as *Alicycliphilus* with archaeal taxa such as *Methanobacterium* were found to be the potential degraders for naphthalene (NAP) under methanogenic conditions in petroleum-contaminated soils (Ye et al., 2019). They reported that NAP degradation may be activated by *Alicycliphilus* through carboxylation to produce 2-naphthoic acid and further degraded by dominant methane producers such as *Methanobacterium*.

In order to investigate if endogenous PAHs in tailings can be biodegraded under methanogenic conditions, we conducted a series of experiments by setting up microcosms containing FFT samples collected from different tailings ponds. Target PAHs that are abundant in tailings (Harner et al., 2018; Galarneau et al., 2014; Selucky et al., 1977) include NAP, phenanthrene (PHE), pyrene (PYR), dibenzofuran (DBF), fluorene (FLU), dibenzothiophene

(DBT). The findings of this study may not only help understand the fate of PAHs in FFT but also help refine the current stoichiometric model to predict methane emissions from OSTP if methanogenic biodegradation of PAHs will be shown.

3.2 Methodology

3.2.1 Reagents and Chemicals

The PAHs used in this study were purchased as follows: Naphthalene (N7-500; CAS#91-20-3) from Fisher Chemical; Pyrene (98%; 180831000; CAS#129-00-0); and Phenanthrene (97%; 130090500; CAS#85-01-8) from Acros Organics; Dibenzofuran (98%; 236373-10G; CAS#132-64-9), Dibenzothiophene (98%; D32202-25G; CAS#132-65-0), Fluorene (98%; 128333-100G; CAS#86-73-7) and Carbazole (CAS# 86-74-8) from Sigma-Aldrich. Solvents were purchased as follows: 2,2,4,4,6,8,8-Heptamethylnonane (HMN) (>97.0%; H0365; CAS#4390-04-9) from Tokyo Chemical Industry Co., Ltd.; Dichloromethane (D37-4; CAS#75-09-2) was purchased from Fisher Chemical. The internal standards for monitoring toluene degradation were purchased as: 1,1,3-trimethylcyclohexane (CAS#3073-66-3) from ChemSampCo, Inc. and methylcyclohexane (99%, CAS#108-87-2) from Acros Organics. Dry compounds for chromatography column preparation: silica gel (70-200 mesh; CAS#7631-86-9), sodium sulfate (99.0%; CAS#7757-82-6), glass wool (CAS#65997-17-3) and sand (CAS#14808-60-7) were purchased from Thermo Scientific.

3.2.2 Preparation of Microcosms

FFT samples were collected from 3 different ponds: SWAN-2 Base Mine Lake (BML) operated by Syncrude Canada Ltd. (Syncrude), Horizon Tailings Pond operated by Canadian Natural Resources Limited (CNRL), and the tailings pond operated by Albian Sands Energy Inc.

(Albian). The Syncrude, CNRL and Albian FFT were received in October 2019, December 2011, and February 2014, respectively. The 158 mL serum bottles were used to contain 50 mL FFT samples with 50 mL methanogenic media (Fedorak and Hrudey, 1984; Holowenko et al., 2000) and sealed with a butyl rubber stopper with an aluminum crimp top. The headspace of each microcosm was then flushed with 20% CO_2/80% N_2 gas continuously for 5 minutes to purge out the residual air.

Methanogenic media (Appendix B) (Fedorak and Hrudey, 1984; Holowenko et al., 2000) was added to each microcosm to provide microbial communities with adequate nutrients, including macronutrients (e.g., Na^+, Ca^{2+}, Mg^{2+}, and NH_4^+), micronutrients (e.g., Zn^{2+}, Fe^{2+}, Co^{2+}, and Mn^{2+}, etc.) and vitamins (e.g., Pyridoxine, Thiamine, and Nicotinic acid, etc.), etc. Resazurin was added to the methanogenic media as an indicator for the oxidation-reduction conditions in microcosms, which shows a blue-violet color in oxidized form, a light pink color after reduction and becomes colorless after further reduction to anaerobic conditions.

There are four treatments applied to microcosms in this study, including Amended, Live Control, Sterile Control, and Unamended. The Amended microcosms were spiked with PAHs dissolved in solvent(s). Live controls were injected with solvent(s) (toluene and/or HMN) without PAHs to approximately evaluate the potential methane production from solvent degradation. Sterile controls are used to monitor potential abiotic PAHs degradations, which were prepared by autoclaving each microcosm at 121°C for 40 min and repeated twice in the following 2 consecutive days and once after a week to completely deactivate indigenous microbial communities. Unamended microcosms contain only FFT samples and methanogenic media without solvents or PAHs to show the potential methane productions from methanogenic

biodegradation of endogenous labile hydrocarbons in tailings such as residual naphtha and bitumen. The experimental layout was shown in Table 3-1.

Set A has two batches of microcosms containing FFT samples from Syncrude and CNRL tailings ponds, respectively. Triplicates of amended, live controls (contain solvents without PAHs), sterile controls, and unamended microcosms were set up for each batch. The DBF, FLU, and DBT (3 PAHs) were spiked to the amended and sterile control microcosms of Set A.

An additional 3 microcosms (Amended 4, 5, and 6) were added to Set A Syncrude batch after 417 days of incubation to verify the potential degradation of PAHs in one of the Syncrude amended microcosms of Set A (Amended 1). These 3 microcosms were injected with inoculums from the Amended 1, and the Amended 1 was re-spiked with toluene and 3 PAHs (DBF, FLU, and DBT), and was monitored with the additional 3 microcosms. An anaerobic chamber with N_2 atmosphere was used for transferring inoculum.

Set B was set up in the same way as Set A microcosms except that 6 PAHs (DBF, FLU, DBT NAP, PHE, and PYR) were used for spiking.

Set C microcosms were adopted from a previous experiment started in 2019 regarding methanogenic biodegradation of PAHs that had 3 batches of microcosms containing 3 different FFTs (Syncrude, CNRL, and Albian), respectively. Seven microcosms (triplicates for amended microcosms, duplicates for unamended microcosms, and duplicates for sterile controls) in each of 3 batches were reamended with same FFT as in the original microcosms, and with ~50 mL methanogenic media. Additional sterile controls were prepared subsequently in duplicates for each of the 3 batches of Set C because significant methane production was detected in all sterile control microcosms in the 2019 experiment after ~1000 days of incubation before Set C was established.

3.2.3 PAH Stock Solution Preparation and Microcosm Spiking

Stock solutions were prepared by dissolving PAHs powder (weighted to the nearest 0.1 mg) in organic solvents such as toluene or HMN in EPA vials tightly sealed with a PTFE-lined screwcap. Three stock solutions were prepared in this study, including: (1) mixed stock solution of 3 PAHs (FLU, DBF, and DBT), in which toluene was the solvent and the concentration of each PAH was ~1000 mmol/L; (2) mixed stock solution of 6 PAHs (NAP, PHE, PYR, DBF, FLU, and DBT), in which HMN was the solvent and the concentration of each PAH was ~50 mmol/L; and (3) the stock solution for carbazole (CAR), in which toluene was the solvent. Preparation of CAR stock solution was problematic since it is only scarcely soluble in toluene or hot toluene (90°C) and almost insoluble in HMN. Therefore, the detected CAR in spiked microcosms was close to the detection limit (Appendix C, Figure C-1) using our method and the degradation of CAR was not considered in this study. Instead, we only monitored the degradation of its solvent (toluene) in each microcosm spiked with CAR stock solution.

The 3 PAHs (DBF, FLU and DBT) stock solution and the CAR stock solution were used to spike Amended and Sterile Control microcosms in Set A whereas the 6 PAHs (NAP, PHE, PYR, DBF, FLU and DBT) stock solution and the CAR stock solution were used to spike the Amended and Sterile Control microcosms in Set B and Set C. Stock solutions were injected into each microcosm by glass syringes (50-, 100-, and 1000 µL) to bring the concentration of each PAH in each microcosm to 1 mmol/L.

For Set A Syncrude batch, ~203 µL of toluene (from the stock solution) was added to each Amended and Sterile Control microcosm, and ~105 µL of toluene (without PAHs) was added to Live Controls. For Set B and Set C, the total volume of toluene in each of Amended, Live Control, and Sterile Control microcosm was 100 µL. A total of 20 µL internal standards (1,1,3-

trimethylcyclohexane or methylcyclohexane) were injected into each microcosm as the reference material to semi-quantify the gas-phase toluene in headspace. In this study, 1,1,3-trimethylcyclohexane was used as the internal standard for the Amended, Live Control, and two of the Sterile Controls (Sterile Control 1 and 2) in Set A Syncrude batch. Methylcyclohexane was used for all other microcosms including Sterile Control 3 in Set A Syncrude batch, the Amended, Live Control, and Sterile Controls in Set A CNRL batch, Set B Syncrude and CNRL batch, and Set C Syncrude, Albian, CNRL batches.

The 0.025 g/mL Na_2S solution was added to the microcosms to reduce potential oxidants in the culture if the color of methanogenic media in the microcosm was blue-violet or pink. A total of 600 μL Na_2S was added to each of the Amended, Live Control, and Sterile Control microcosms (~0.6% v/v in each microcosm) of Set A CNRL batch, while 300 μL Na_2S (~0.3% v/v in each microcosm) was added to each microcosm of Unamended microcosms in Set A CNRL batch as well as the Amended, Live Control, and Sterile Control microcosms of Set B CNRL batch. All spiked microcosms were vigorously shaken by hand followed by storing in darkness for at least 24 hours in room temperature before the first sampling (Day 0).

3.2.4 Chemical Analysis for PAHs, Methane, and Toluene

The PAHs determination procedures optimized in Chapter 2 were applied in this study. To start sampling, each microcosm was vigorously shaken by hand to fully mix the culture slurry followed by taking out 3 mL samples by the sterile syringes attached to sterile needles (18G). Sample pre-treatment was conducted by mixing the 3 mL samples with 10 mL DCM in 40 mL EPA vials and storing in darkness under 4°C for 24 hours. The pre-treated samples were then transferred to extraction thimbles containing 2.5 g anhydrous sodium sulfate and placed inside Soxhlet extraction chambers. An additional 60 mL DCM was added to each Soxhlet device for

the subsequent 24-hour extraction. The obtained extracts were purified using DCM-eluted silica gel columns and eluted with 10 mL DCM. The purified extract was evaporated to ~1.5 mL on a rotary evaporator before measuring by the gas chromatograph (Thermo Fisher Scientific, Trace 1300) coupled with a Mass spectrometer (Thermo Fisher Scientific ISQ) and an autosampler (TriPlus RSH, Thermo Fisher Scientific). Samples for PAHs determination were taken out from the Amended and Sterile Control microcosms on Day 0, 361, and 616 for Set A Syncrude batch; Day 0 and 549 for Set A CNRL batch; Day 0 and 189 for the additional batch of Set A Syncrude; Day 0 and Day 207 for Set B Syncrude batch; Day 0 for Set B CNRL batch; Day 0 and 158 for Set C Syncrude batch; Day 0, 222, and 274 for Set C Albian batch; Day 0 and Day 335 for Set C CNRL batch. It must be mentioned that the optimized method (Chapter 2) was developed in October 2022, which was after ~300 days since the establishment of Set A and Set B, and thus the pre-treatment was not applied to the Day 0 PAHs determinations for Set A Syncrude and CNRL batch, and Day 0 PAHs determinations for Set B Syncrude and CNRL batch.

The moles of methane in the headspace of each microcosm has been monitored since the establishing day (Day 0) to show methane productions from methanogenic biodegradation of toluene and potentially PAHs. Methane was measured by taking out 0.1 mL headspace with an insulin syringe (28g, 0.5 mL) and injecting into a gas chromatograph equipped with a flame ionization detector (GC-FID; Thermo Fisher Scientific, Trace 1300) with TG-Bond Q capillary column (30m, 0.32mm). Analyses were performed at an oven temperature of 40°C using He as a carrier gas with the flow rate of 40 mL/min. Percentages of methane in the headspace were calculated using external standards and then converted to mass basis using the linear regression equation derived from the calibration curve. External standards were prepared by percentages of methane (v/v), including 0.16%, 1%, 2%, 4%, 8%, 15%, and 30% with R^2 value of the regression

equation calibrated to >0.99. External standards were measured simultaneously with samples to get the percentages of methane in headspace. Before calculating moles of methane, the moles of total headspace gas was first calculated according to the ideal gas law:

$$PV = nRT \quad (1)$$

In which the headspace pressure was measured by a pressure gauge (psi) immediately after injecting samples to GC. The pressure reading was added to atmospheric pressure, followed by unit transferring to kPa, which is the value of *P*; *V* is the headspace volume expressed in litre (L); the value of *R* is 8.3144 J/mol·K; and the room temperature of ~21°C is transferred to Kelvin and used as the temperature *T*; *n* is the moles of the gas in headspace. The moles of methane was calculated via multiplying *n* by the percentage of methane in the headspace.

Toluene concentration in the headspace of microcosms was monitored with the concurrent methane production. The gas in the headspace of microcosm was taken out by insulin syringes and injected into the GC-MS. Residual toluene in the headspace was obtained by calculating the peak ratio of toluene/internal standards from each measurement and comparing it with the ratio of Day 0 (establishing date), which was considered as 100%.

3.2.5 Stoichiometric Analyses

The theoretical maximum methane productions from the complete methanogenic biodegradation of each hydrocarbon (toluene and PAHs) in microcosms of this study were calculated according to Equation (2) derived from the modified Symons and Buswell equation (Symons and Buswell, 1933):

$$C_xH_yO_z + \left(x - \frac{y}{4} - \frac{z}{2}\right)H_2O = \left(\frac{x}{2} - \frac{y}{8} + \frac{z}{4}\right)CO_2 + \left(\frac{x}{2} + \frac{y}{8} - \frac{z}{4}\right)CH_4 \quad (2)$$

The calculation results of methane production from complete methanogenic biodegradation of toluene, NAP, PHE, PYR, DBF, FLU, and DBT (Table 3-2) were used to compare with methane in the headspace measured by GC-FID to verify potential biodegradation of PAHs.

3.2.6 Microbial Analyses

To analyze the microbial community in microcosms, the culture slurry was well-mixed before taking 1 mL sample from each microcosm by a 1 mL sterile syringe at the specific time point. Samples were stored in 2 mL Eppendorf tubes at -20°C before DNA extraction was necessary to be performed. Total genomic DNA in the sample was extracted using the Fast DNA® SPIN Kit for Soil (MP Biomedicals, USA). The extracted DNA was quantified using a Qubit 4 model fluorometer (Thermo Fisher, USA) immediately after extraction and was stored in -20°C before subsequent analyses. Extracted DNA samples were sent to the Molecular Biology Facility at the University of Alberta (MBSU). The V3-V4 variable regions of the 16S rRNA gene was amplified via PCR using universal primers 926Fi5 (5'- AAA CTY AAA KGA ATW GRC GG -3') and 1392Ri7 (5'- AC GGG CGG TGW GTR C -3'). A second round of amplification was conducted using Illumina bridge PCR-compatible primers, followed by sequencing using the Illumina MiSeq platform (Illumina, San Diego, CA,USA). The FASTA format, paired-end sequenced data obtained from Illumina was analyzed through MetaAmp Pipeline (Dong et al., 2017) to get representative operational taxonomic units (OTUs). In the first stage, MetaAmp assembles the paired-end sequenced files using “usearch-fastq_mergepairs” in USEARCH software package (Edgar, 2010). The second stage is to trim the forward and reverse primers using “trim.seqs” command in the Mothur software package (Schloss et al., 2009). The third stage is quality control, in which the MetaAmp clustered the high quality reads into the OTUs using the SILVA taxonomic database (r138.1; last updated: December 14, 2021). Finally,

MetaAmp generated the rank abundance data from the original OTU list files using Mothur. The microbial communities of each microcosm was analyzed on the establishing day (Day 0) to demonstrate the suitability of the culture to initiate methanogenic biodegradation of PAHs.

Additional samples were taken out simultaneously with subsequent PAHs determinations on Day 361 and 616 for Set A Syncrude batch; Day 549 for Set A CNRL batch; Day 189 for the additional batch of Set A Syncrude; Day 207 for Set B Syncrude batch; Day 158 for Set C Syncrude batch; Day 222 and 274 for Set C Albian batch; Day 335 for Set C CNRL batch. The additional samples were stored in darkness at -20°C. The DNA extraction and the 16S rRNA sequencing would be conducted to show the potential changes of microbial communities once PAHs degradation would be observed.

3.3 Results and Discussion

3.3.1 Set A-Methane Production, Toluene Degradation, and PAHs Monitoring

The cumulative methane production and residual toluene (%) in Set A microcosms was periodically monitored starting at Day 0.

3.3.1.1 Set A Syncrude Batch

For Syncrude microcosms in Set A, after a lag phase of ~110 days (Figure 3-1), methane production started in Live Control microcosms and increased exponentially to ~2500 μmol and plateaued afterwards, which was ~60% of theoretical maximum methane production from toluene degradation (4442 μmol, shown as the horizontal green dotted line on Figure 3-1). The methane production from Amended microcosms reached ~35%-60% of the theoretical maximum methane production (8587 μmol total for PAHs and toluene, shown as the horizontal red dotted line on Figure 3-1). Considering the concurrent depletion of toluene with methane production,

most of the methane at this stage was probably derived from methanogenic toluene degradation. The difference between measured and predicted methane may be attributed to potential toluene loss through continuous sampling and/or the microbial carbon assimilation (Mohamad Shahimin et al., 2016). Similar results were shown in another study of methanogenic biodegradation of *n*-alkanes in tailings (Mohamad Shahimin et al., 2016), in which 67%~74% of theoretical maximum methane was measured in the headspace. In addition, the methane production from toluene degradation indicated that the indigenous microbial communities are active and capable to degrade labile hydrocarbons in FFT under methanogenic conditions. No significant methane was produced in any Sterile Control or Unamended microcosms during the incubation, which indicated that neither abiotic degradation nor endogenous hydrocarbons contributed significantly to methane production.

A PAHs determination for Set A Syncrude microcosms was done on Day 361 when the moles of methane in the headspace plateaued ~200 days after depletion of toluene (Figure 3-2 left panel). In this analysis, the concentration of DBF, FLU, and DBT in the Amended 1 microcosm decreased compared to Day 0 and was close to detection limit. The methane production in Amended 1 was relatively higher than the other two replicates (Amended 2 and 3), thus we assumed that there may be co-metabolic degradation of toluene and PAHs (S. Zhang et al., 2019). Since PAHs and microbial communities were not analyzed concurrently with toluene degradation in Set A, we took inoculums from Amended 1 on Day 417 to set up an additional batch with 3 new microcosms (Amended 4, 5, and 6) by amending each microcosm with 3 PAHs (DBF, FLU, and DBT) to verify our assumption of toluene-PAHs co-metabolic biodegradation under methanogenic conditions. The Amended 1 microcosm was reamended with the 3 PAHs

(DBF, FLU, and DBT) and monitored alongside with Amended 4, 5, and 6 in the additional batch. The current results for the additional batch will be shown in section *3.3.2*.

A subsequent PAHs determination was conducted on Day 616 for the Amended 2 and 3, and Sterile Control microcosms of Set A Syncrude batch and no PAHs degradation was observed. Higher PAHs concentration was detected in Set A Syncrude Sterile Control microcosms on Day 0 (Figure 3-2 left panel), which was probably because PAHs in these microcosms were spiked before the autoclave procedure. The high temperature during autoclave process maybe increased the solubility of PAHs in the liquid phase of the culture (Richter et al., 1996) and therefore led to a higher PAHs recovery from Soxhlet extraction. During the incubation period, the dissolved PAHs due to autoclave may be gradually re-adsorbed onto fine particles such as silt and clay (Łyszczarz et al., 2021) or organic fractions such as bitumen, which resulted in a lower recovery of PAHs on Day 361 and Day 616.

3.3.1.2 Set A CNRL Batch

Comparing to Syncrude microcosms, a longer lag phase of ~400 days was required for the CNRL Amended microcosms (e.g., Amended 3) to start degrading toluene and producing methane (Figure 3-3). It may be because the CNRL FFT was collected in 2011 (~11 years prior starting the experiment) and the abundance of indigenous microbial communities may be decreased at the time this study was conducted. Besides, the solid content of the CNRL FFT is lower than Syncrude FFT, which may not be adequate to efficiently support microbial growth. Noticeable reduction of toluene in the headspace of CNRL Sterile Control microcosms was observed without concurrent methane production, which was probably because the sampling for gas and liquid analyses over the long period of incubation (~600 day) removed toluene from the headspace. Regarding PAHs monitoring, samples were taken out on Day 0 and Day 549 and no

potential degradation was shown (Figure 3-2 right panel), which was probably because the delocalization of electrons within the benzene rings stabilized the structure of PAHs and decreased their biodegradability (Hashemzadeh et al., 2024).

3.3.2 The Additional Batch of Set A Syncrude Microcosms

The additional batch for Set A has 4 microcosms, including 3 additional microcosms (Amended 4, 5, and 6) and the Amended 1 microcosm. Each of the 3 additional microcosms received 15 mL inoculum from the Amended 1 microcosm, followed by spiking all 4 microcosms with 3 PAHs (DBF, FLU, and DBT) (~1 mmol/L). The toluene degradation and concurrent methane production were shown in Figure 3-4, in which the theoretical maximum methane production from complete toluene degradation is 4230 μmol for Amended 4, 5, and 6 microcosm (shown as horizontal red dotted line), and 1903 μmol for Amended 1 microcosm (shown as horizontal blue dotted line). The difference in the amount of methane production between the new microcosms and microcosm Amended 1 was due to approximately 45 mL FFT leftover in the Amended 1 before re-amendment, resulting in a lower injection of toluene and PAHs.

The microcosms in this batch started to degrade toluene and produce methane almost immediately after setting up, with a short lag phase of <20 days, which indicated that the microbial communities in Amended 1 that potentially involved in toluene degradation were still active even after a ~200 days stationary phase, probably because they were slowly utilizing other endogenous labile hydrocarbons in tailings as carbon source. To monitor the potential co-metabolic degradation of toluene and PAHs, samples were taken from each of the 4 microcosms for PAHs determination as soon as the methane production plateaued on Day 189 in the three active microcosms (Amended 1, 5, and 6). However, no PAHs degradation in any microcosm

was found (Figure 3-5), which implied that there may be no co-metabolic biodegradation of toluene with the 3 PAHs (DBF, FLU, and DBT). The recalcitrance of PAHs to biodegradation maybe because their structure was stabilized through delocalization of electrons within benzene rings (Hashemzadeh et al., 2024). The lone pair of electrons from the incorporated heteroatoms such as oxygen (in DBF) and sulfur (in DBT) can also be involved in the π-electron delocalization to further stabilize the PAHs structure (Bean, 1998) and decrease their biodegradability.

3.3.3 Set B-Methane Production, Toluene Degradation, and PAHs Monitoring

Comparing with Set A, the Live Control microcosms of Set B Syncrude batch had a shorter lag phase of ~30 days before initiating toluene degradation (Figure 3-6). However, it took almost 90 days for two of the Amended microcosms (Amended 2 and 3) to start producing methane, and ~200 days for another Amended microcosm (Amended 1). It is probably because the HMN (~4.5 mL) spiked into Set B Amended microcosms increased the solubility of PAHs in the culture, which may be toxic to indigenous microbial communities and postponed toluene degradation. Chemical analyses on Day 207 showed that no PAHs have been degraded in Set B Amended microcosms (Figure 3-7).

For CNRL microcosms of Set B, toluene degradation only occurred in two of the Live Control microcosms (Figure 3-8), with the initial lag phase of ~100 days for Live Control 3 and ~200 days for Live Control 2, respectively. The Day 0 PAHs determination was shown in Figure 3-9. No significant methane emission was detected from any other microcosms in CNRL cultures of Set B, and monitoring will be continued.

3.3.4 Set C-Methane Production, Toluene Degradation, and PAHs Monitoring

The methane production and toluene degradation in the microcosms of Set C were measured over an incubation period of ~400 days. After a relatively short lag phase of <50 days, the Syncrude and Albian microcosms started to produce methane into the headspace, which was probably the result of the concurrent toluene degradation, as was shown in Figure 3-10 and Figure 3-11. To investigate whether there was co-metabolic biodegradation of toluene with the 6 PAHs (NAP, PHE, PYR, DBF, FLU, DBT), samples were taken out from Syncrude and Albian microcosms for the analyses of PAHs and microbial communities as soon as methane emission plateaued. Results showed that no PAHs degradation occurred in Syncrude microcosms (Figure 3-12). On the other hand, the concentration of the 6 PAHs in two of the Amended microcosms (Amended 4 and 5) of Albian batch showed a ~20-40% decrease from Day 222 to Day 274 (Figure 3-13). Since the detected PAHs concentrations in Sterile Control microcosms on Day 222 and Day 274 were similar to each other, we assumed that there was probably partial degradation of the 6 PAHs in Amended 4 and 5. Similarly, it was reported that partial degradation of PAHs (~20-30%) might occur in soil environment under methanogenic conditions (Gou et al., 2022, 2023). However, no concurrent methane production was detected in the Amended 5 microcosm, and the variation of PAHs concentration was also probably caused by the inhomogeneous distribution of PAHs in FFT due to their potential adsorption onto clay minerals and/or other organic particle surfaces in tailings (Cossey et al., 2021; Łyszczarz et al., 2021; Shen et al., 2022). Therefore, further investigations such as identifying potential metabolites have to be conducted to support our assumptions of PAHs degradation.

The CNRL microcosms in Set C took ~150 days to initiate toluene degradation, and concurrent methane production was shown in Figure 3-14. The PAHs determination on Day 335 showed that there may be no degradation occurred in Set C CNRL microcosms (Figure 3-15).

3.3.5 Microbial Analyses

Indigenous microbial communities (Day 0) of Syncrude, CNRL and Albian FFT samples in this study were analyzed via sequencing partial (V3-V4) 16S rRNA genes. The microbial communities with high relative abundance in FFTs on Day 0 are bacterial genus (Table 3-3) including *Anaerolineaceae* and *Thiobacillus*, and archaeal genus (Table 3-4) including *Methanosaeta* and *Methanoregula*, which is probably because they are potentially involved in the degradation of endogenous hydrocarbons such as naphtha compounds (Mohamad Shahimin et al., 2021, 2016) or residual bitumen in tailings ponds, and gradually develop and dominate the microbial communities (Mahaffey and Dubé, 2017; Siddique et al., 2008). The co-dominance of bacterial taxa *Desulfosporosinus* (a genus of the family *Desulfitobacteriaceae*) and archaeal taxa *Methanosaeta* (a genus of the family *Methanosaetaceae*) in the Albian FFT samples (Day 0) might be actively involved in toluene degradation, as suggested in previous reports (Fowler et al., 2012; Sun et al., 2014). The microbial analyses of Albian microcosms on Day 274 (Table 3-5 and Table 3-6) showed the predominance (~90%) of *Desulfitobacteriaceae* and *Methanosaetaceae* in the Amended 4 microcosm, which indicated that *Desulfitobacteriaceae* (a family of the class *Clostridia*) maybe the key player in methanogenic toluene degradation in syntrophic association with *Methanosaetaceae*.

Regarding potential PAHs degraders in our microcosms, it was reported that the bacterial class *Clostridia* (the class of *Desulfobacteriaceae*) in our microcosms may be involved in the degradation of 3-ring PAHs such as PHE (Berdugo-Clavijo et al., 2012; Z. Zhang et al., 2019).

Thus, we assume that the indigenous microbial communities of all FFT samples (Syncrude, CNRL, and Albian) were suitable to conduct experiments of methanogenic biodegradation of PAHs. Though no confirmed PAHs degradation was observed in the current stage, expected PAHs degradation may occur after the indigenous bacterial groups acclimatized to the PAHs-enriched environment in microcosms.

3.4 Conclusions

Three sets of experiments containing a total of 78 bottles were established to investigate potential biodegradation of abundant PAHs in oil sands tailings under methanogenic conditions using FFT samples from three different tailings ponds operated by Syncrude, CNRL, and Albian, respectively. The indigenous microbial communities of the three tailings are active and have degraded toluene under methanogenic conditions within ~300 days in Syncrude and Albian microcosms and have started to degrade toluene in CNRL microcosms after ~200 days of incubation. The PAHs determinations indicated that there is currently no confirmed degradation in any of the microcosms of our study after ~700 days of incubation. However, future PAHs degradation can be expected because the potential PAHs degraders such as *Clostridia* are abundant genus of the indigenous microbial communities in all three FFTs including Syncrude, CNRL, and Albian. Once PAHs degradation with concurrent methane production is observed (a second exponential growth of methane concentration), microbial analyses should be immediately conducted to analyze bacterial and archaeal communities that may be actively involved in the methanogenic metabolism of PAHs. The methane production patterns from methanogenic biodegradation of PAHs may also help refine our current stoichiometric models (Kong et al., 2019) to predict methane emissions from oil sands tailings ponds.

Table 3-1 Experimental layout for Sets A, B and C. All treatments were established in 158-mL microcosms. The DBF, FLU, DBT (3 PAHs) dissolved in toluene were added in the Amended and Sterile Control microcosms of Set A; NAP, PHE, PYR, DBF, FLU, DBT (6 PAHs) dissolved in HMN were added in the Amended and Sterile Control microcosms of Set B and Set C. The Live Control microcosms contain only the solvents for dissolving PAHs. No PAHs or solvents were added in the Unamended microcosms.

Set	Batch	Microcosms	Microcosm # (Replicates)	Treatments
Set A	Syncrude	Amended	1, 2 and 3	3 PAHs + toluene
		Live Control	1, 2 and 3	Toluene
		Sterile Control	1, 2 and 3	3 PAHs + toluene
		Unamended	1, 2 and 3	No PAHs, no toluene
		Additional Amended	1, 4, 5 and 6	3 PAHs + toluene
	CNRL	Amended	1, 2 and 3	3 PAHs + toluene
		Live Control	1, 2 and 3	Toluene
		Sterile Control	1, 2 and 3	3 PAHs + toluene
		Unamended	1, 2 and 3	No PAHs, no toluene
Set B	Syncrude	Amended	1, 2 and 3	6 PAHs + toluene + HMN
		Live Control	1, 2 and 3	Toluene + HMN
		Sterile Control	1, 2 and 3	6 PAHs + toluene + HMN
		Unamended	1, 2 and 3	No PAHs, no toluene, no HMN
	CNRL	Amended	1, 2 and 3	6 PAHs + toluene + HMN
		Live Control	1, 2 and 3	Toluene + HMN
		Sterile Control	1, 2 and 3	6 PAHs + toluene + HMN
		Unamended	1, 2 and 3	No PAHs, no toluene, no HMN
Set C	Syncrude	Amended	1, 2, 3, 4 and 5	6 PAHs + toluene + HMN
		Sterile Control	1 and 2	6 PAHs + toluene + HMN
		Unamended	1 and 2	No PAHs, no toluene, no HMN
	CNRL	Amended	1, 2, 3, 4 and 5	6 PAHs + toluene + HMN
		Sterile Control	1 and 2	6 PAHs + toluene + HMN
		Unamended	1 and 2	No PAHs, no toluene, no HMN
	Albian	Amended	1, 2, 3, 4 and 5	6 PAHs + toluene + HMN
		Sterile Control	1 and 2	6 PAHs + toluene + HMN
		Unamended	1 and 2	No PAHs, no toluene, no HMN

Table 3-2 Theoretical methane production (mmol) from complete biodegradation of 1 mmol of each hydrocarbon under methanogenic conditions calculated using the Equation (2).

Hydrocarbons	**Methane (mmol)**
Toluene	4.50
Naphthalene	6.00
Phenanthrene	8.25
Pyrene	9.25
Dibenzofuran	6.75
Fluorene	7.75
Dibenzothiophene	6.75

Table 3-3 Relative abundance of bacterial 16S rRNA gene sequences in Syncrude, CNRL, and Albian FFT on Day 0. Numbers represent the percentage of total bacterial reads.

Bacteria			
OTUs	**Syncrude Day 0**	**CNRL Day 0**	**Albian Day 0**
Anaerolineae; Anaerolineales			
Anaerolineaceae; Uncultured	19.9	13.3	4.6
Anaerolineaceae; *Leptolinea*	5.9	2.8	13.6
Anaerolineaceae; Uncultured	7.3	0.0	0.6
Clostridia; Clostridiales			
Desulfitobacteriaceae; *Desulfosporosinus*	1.5	1.7	10.9
Gammaproteobacteria; Burkholderiales			
Comamonadaceae; *Aquabacterium*	0.0	0.0	11.5
Comamonadaceae; Uncultured	1.0	4.4	0.7
Comamonadaceae; *Rhodoferax*	1.6	0.0	8.2
Hydrogenophilaceae; *Thiobacillus*	3.1	0.7	2.4
Gammaproteobacteria; Acidithiobacillales			
Acidithiobacillaceae; *KCM-B-112*	1.8	37.4	1.6
Latescibacteria; Latescibacterales			
Latescibacteraceae; Uncultured	3.3	0.0	0.0
Cloacimonadia; Cloacimonadales			
SHA-4; Uncultured	3.3	0.0	0.0
Desulfuromonadia			
Uncultured	0.3	3.2	0.7
Gammaproteobacteria; Immundisolibacterales			
Immundisolibacteraceae; *Immundisolibacter*	0.6	6.8	0.5
Holophagae; Subgroup_7			
Uncultured	0.0	4.8	0.0
Coriobacteriia; OPB41			
Uncultured	1.3	0.1	4.2
Others *	49.2	24.7	40.4

***** The sum of all taxa individually abundant at <3% of the total bacterial reads.

Table 3-4 Relative abundance of archaeal 16S rRNA gene sequences in Syncrude, CNRL, and Albian FFT on Day 0. Numbers represent the percentage of total archaeal reads.

Archaea			
OTUs	**Syncrude Day 0**	**CNRL Day 0**	**Albian Day 0**
Methanobacteria; Methanobacteriales			
Methanobacteriaceae; *Methanobacterium*	0.1	19.4	0.1
Thermococci; Methanofastidiosales			
Methanofastidiosaceae; *Candidatus_Methanofastidiosum*	2.9	0.3	5.4
Methanomicrobia; Methanomicrobiales			
Methanoregulaceae; *Methanolinea*	13.2	0.0	0.9
Methanoregulaceae; *Methanoregula*	32.3	9.0	34.8
Methanosarcinia; Methanosarciniales			
Methanosaetaceae; *Methanosaeta*	47.3	71.2	54.8
Methanosarcinaceae; *Methanomethylovorans*	0.5	0.0	3.4
Others *	3.6	0.1	0.7

***** The sum of all taxa individually abundant at <3% of the total archaeal reads.

Table 3-5 Relative abundance of bacterial 16S rRNA gene sequences in Albian FFT on Day 0 and Day 274. Numbers represent the percentage of total bacterial reads.

Bacteria				
OTUs	**Unamended Day 0**	**Unamended Day 274**	**Amended Day 0**	**Amended Day 274**
Anaerolineae; Anaerolineales				
Anaerolineaceae; Uncultured	4.9	3.0	4.6	0.3
Anaerolineaceae; *Leptolinea*	16.2	8.4	13.6	1.0
Anaerolineaceae; *Pelolinea*	3.6	1.6	0.9	0.1
Clostridia; Clostridiales				
Desulfitobacteriaceae; *Desulfosporosinus*	2.4	1.3	10.9	89.8
Peptococcaceae; *Pelotomaculum*	3.3	1.0	2.0	0.0
Desulfotomaculia; Desulfotomaculales				
Desulfurisporaceae; *SCADC1-2-3*	7.2	0.7	0.1	0.0
Gammaproteobacteria; Acidithiobacillales				
Acidithiobacillaceae; *KCM-B-112*	2.4	31.4	1.6	0.0
Gammaproteobacteria; Burkholderiales				
Comamonadaceae; *Aquabacterium*	0.4	0.8	11.5	0.2
Comamonadaceae; *Rhodoferax*	8.5	14.9	8.2	0.4
Comamonadaceae; Uncultured	1.0	3.0	0.7	0.0
Uncultured	4.0	2.8	2.8	0.2
Coriobacteriia; OPB41				
Uncultured	3.9	3.3	4.2	0.5
Thermodesulfovibrionia				
Uncultured	3.0	2.0	1.2	0.1
Others *	39.1	25.7	37.8	7.2

***** The sum of all taxa individually abundant at <3% of the total bacterial reads.

Table 3-6 Relative abundance of archaeal 16S rRNA gene sequences in Albian FFT on Day 0 and Day 274. Numbers represent the percentage of total archaeal reads.

Archaea				
OTUs	**Unamended Day 0**	**Unamended Day 274**	**Amended Day 0**	**Amended Day 274**
Thermococci; Methanofastidiosales				
Methanofastidiosaceae; *Candidatus_Methanofastidiosum*	1.3	1.3	5.4	0.1
Methanomicrobia; Methanomicrobiales				
Methanoregulaceae; *Methanolinea*	2.3	1.7	0.9	4.4
Methanoregulaceae; *Methanoregula*	22.4	18.6	34.8	53.6
Methanosarcinia; Methanosarciniales				
Methanosaetaceae; *Methanosaeta*	72.7	74.5	54.8	41.1
Methanosarcinaceae; *Methanomethylovorans*	0.6	0.7	3.4	0.0
Others *	0.7	3.3	0.8	0.8

* The sum of all taxa individually abundant at <3% of the total archaeal reads.

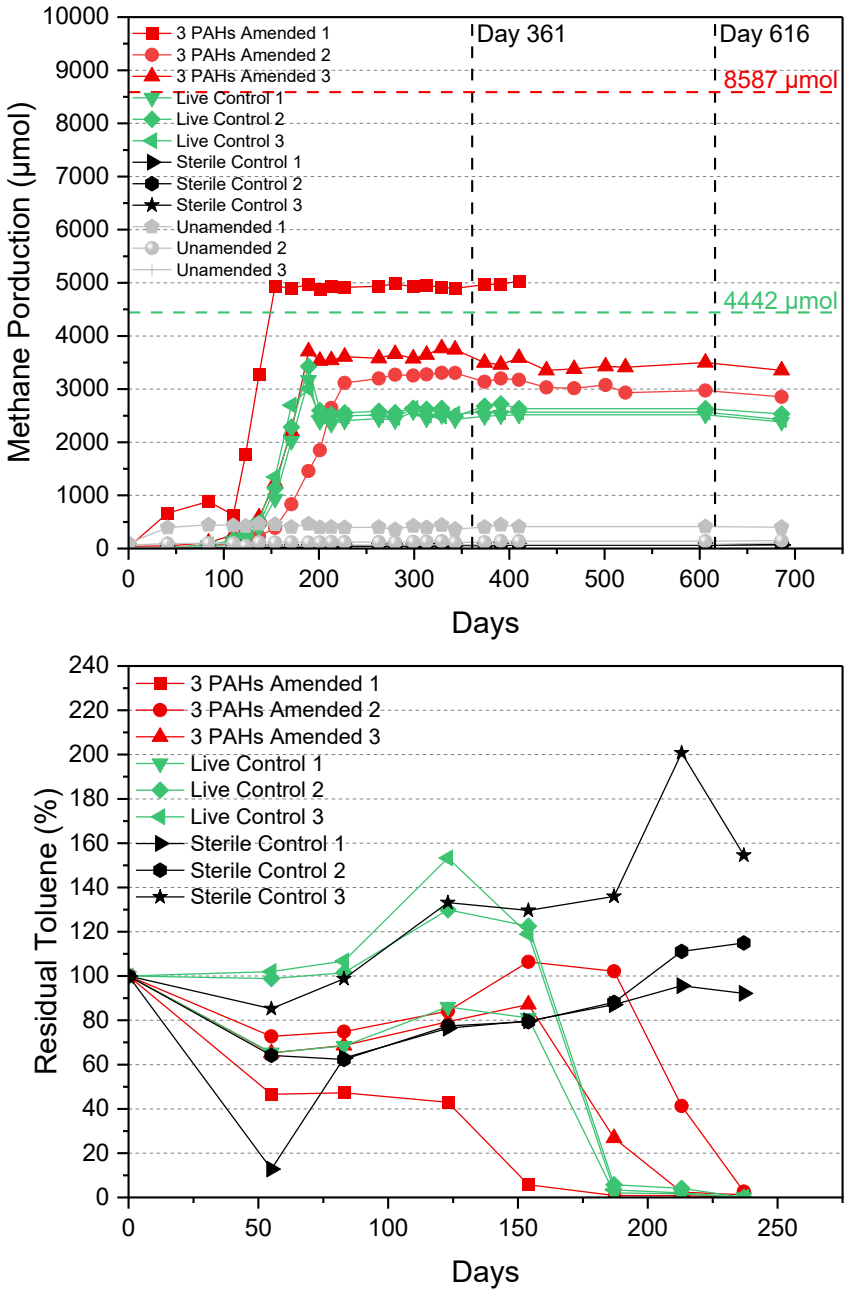

Figure 3-1 Methane production (top panel) and toluene degradation (bottom panel) in Set A Syncrude microcosms. **Top panel:** Methane concentration in the headspace measured by GC-FID. The horizontal green dotted line indicates theoretical maximum of methane production from complete toluene degradation in the Live Control microcosms. The horizontal red dotted line indicates theoretical maximum of methane production from complete toluene degradation in the Amended microcosms. The vertical black dotted lines indicate the day on which the samples were taken for PAHs determination and microbial analysis. **Bottom panel:** Residual toluene (%) in the headspace of microcosms was obtained by calculating the peak ratio of toluene/internal standards after measuring by GC-MS and comparing it to the Day 0 ratio, which was considered as 100%.

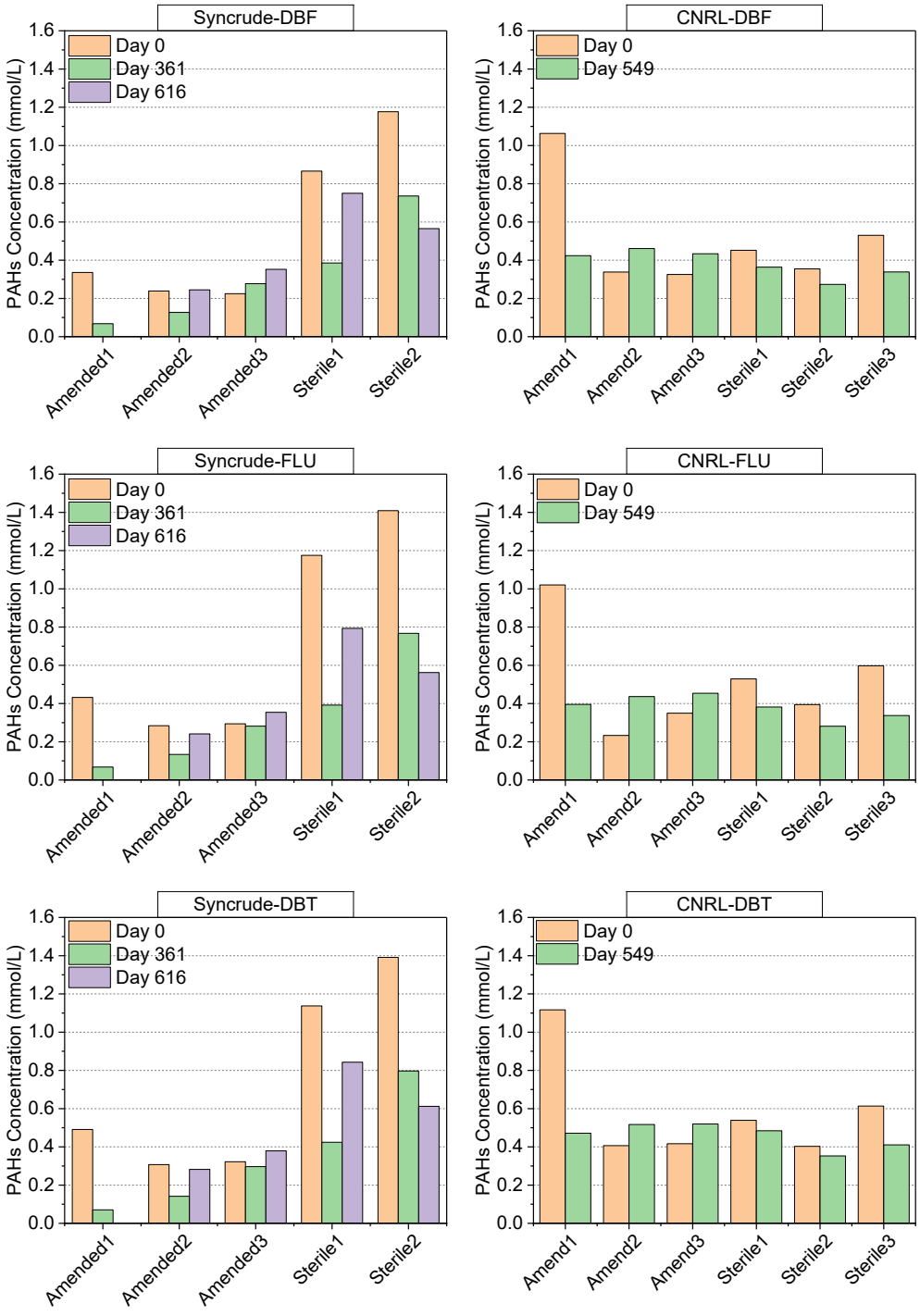

Figure 3-2 PAHs concentration in Set A Syncrude (left panels) and CNRL (right panels) microcosms. **Left panel:** PAHs in Syncrude Amended and Sterile Control microcosms detected by Soxhlet method without pre-treatment (on Day 0) and by Soxhlet method with pre-treatment on Days 361 and 616. **Right panel:** PAHs in CNRL Amended and Sterile Control microcosms detected by Soxhlet method without pre-treatment on Day 0 and by Soxhlet method with pre-treatment on Day 549.

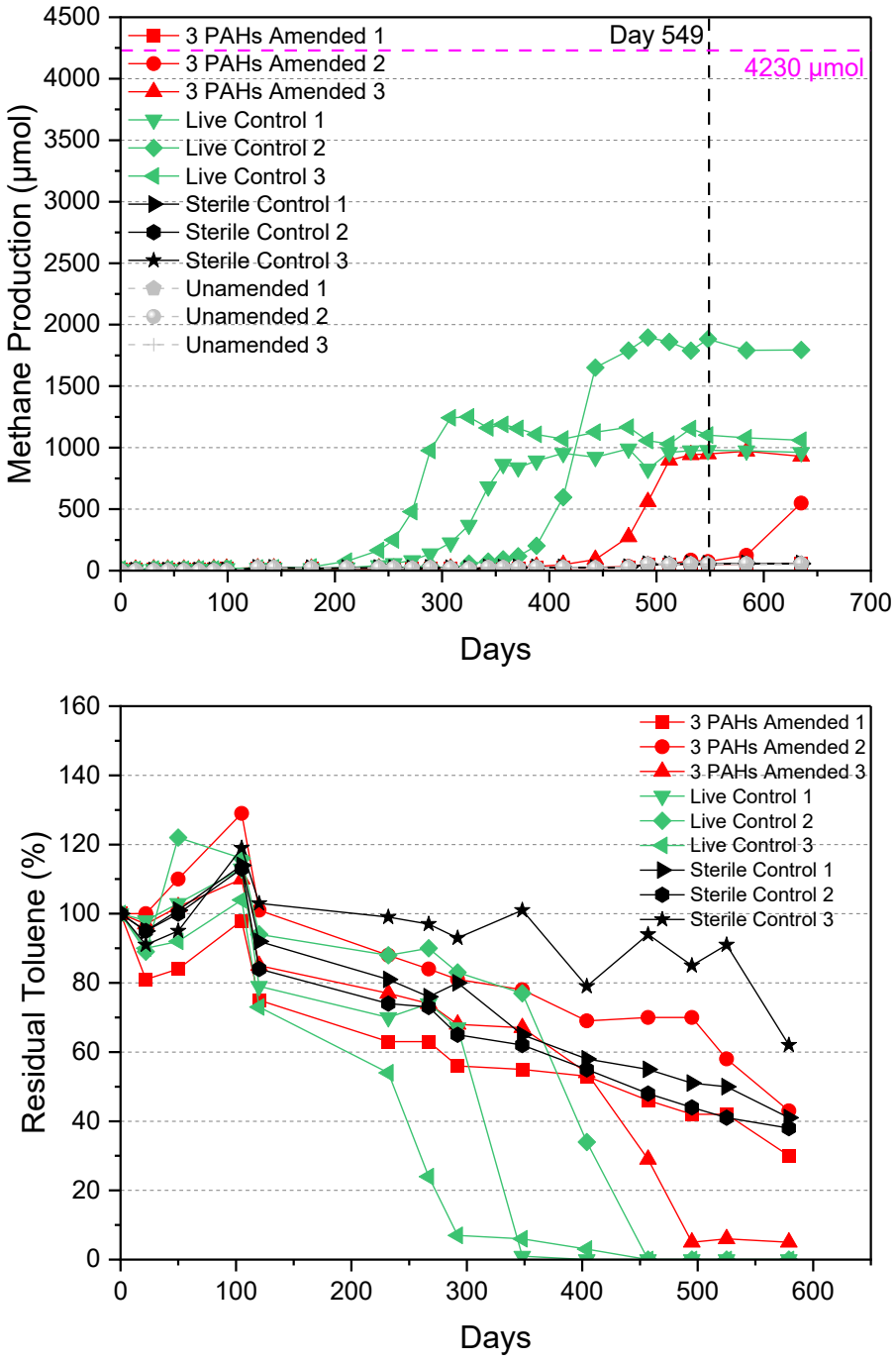

Figure 3-3 Methane production (top panel) and toluene degradation (bottom panel) in Set A CNRL microcosms. **Top panel:** Methane concentration in the headspace measured by GC-FID. The horizontal pink dotted line indicates theoretical maximum of methane production from complete toluene degradation in the Amended and the Live Control microcosms. The vertical black dotted line indicates the day on which the samples were taken for PAHs determination and microbial analysis. **Bottom panel:** Residual toluene (%) in the headspace of microcosms was obtained by calculating the peak ratio of toluene/internal standards after measuring by GC-MS and comparing it to the Day 0 ratio, which was considered as 100%.

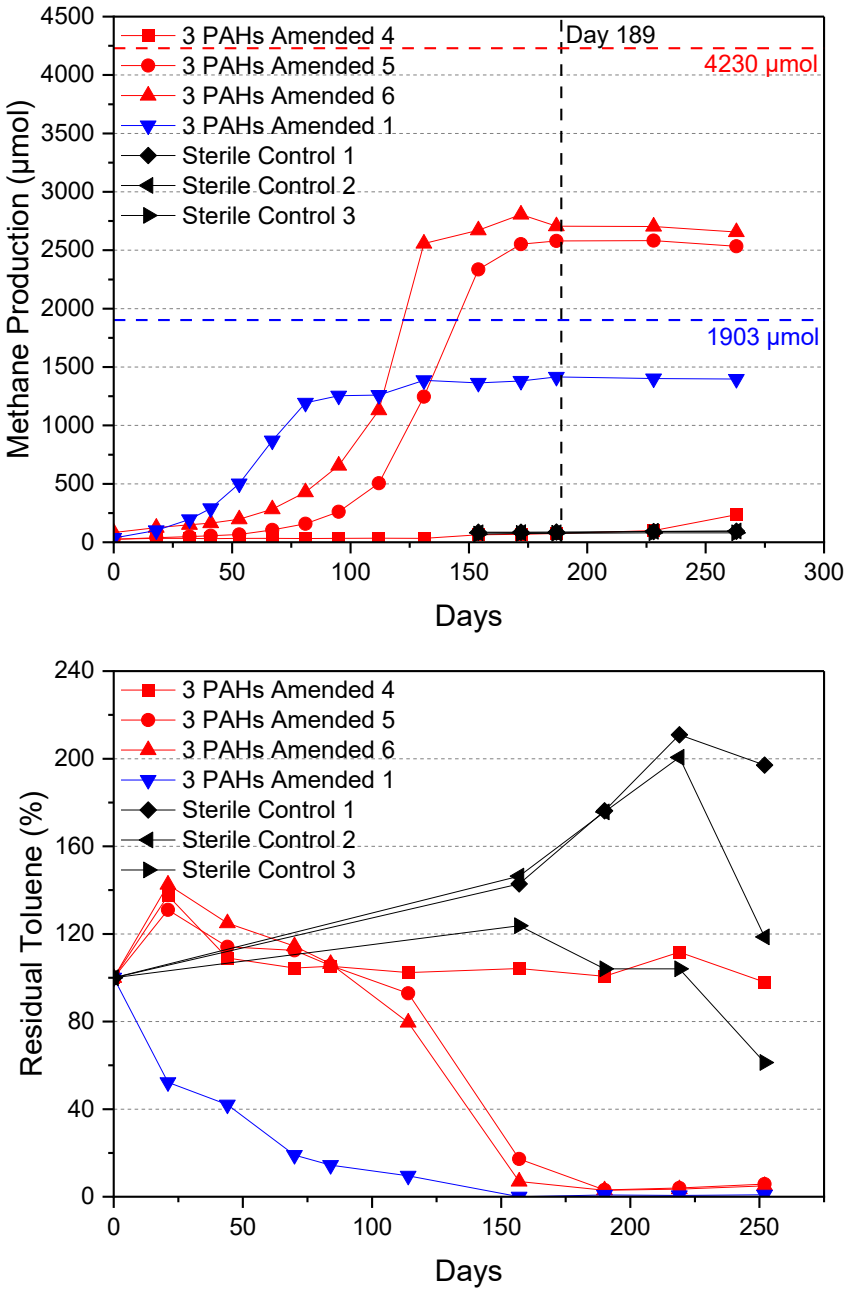

Figure 3-4 Methane production (top panel) and toluene degradation (bottom panel) in the additional batch of Set A Syncrude microcosms. **Top panel:** Methane concentration in the headspace measured by GC-FID. The horizontal pink dotted line indicates theoretical maximum of methane production from complete toluene degradation in the Amended microcosms. The vertical black dotted line indicates the day on which the samples were taken for PAHs determination and microbial analysis. **Bottom panel:** Residual toluene (%) in the headspace of microcosms was obtained by calculating the peak ratio of toluene/internal standards after measuring by GC-MS and comparing it to the Day 0 ratio, which was considered as 100%.

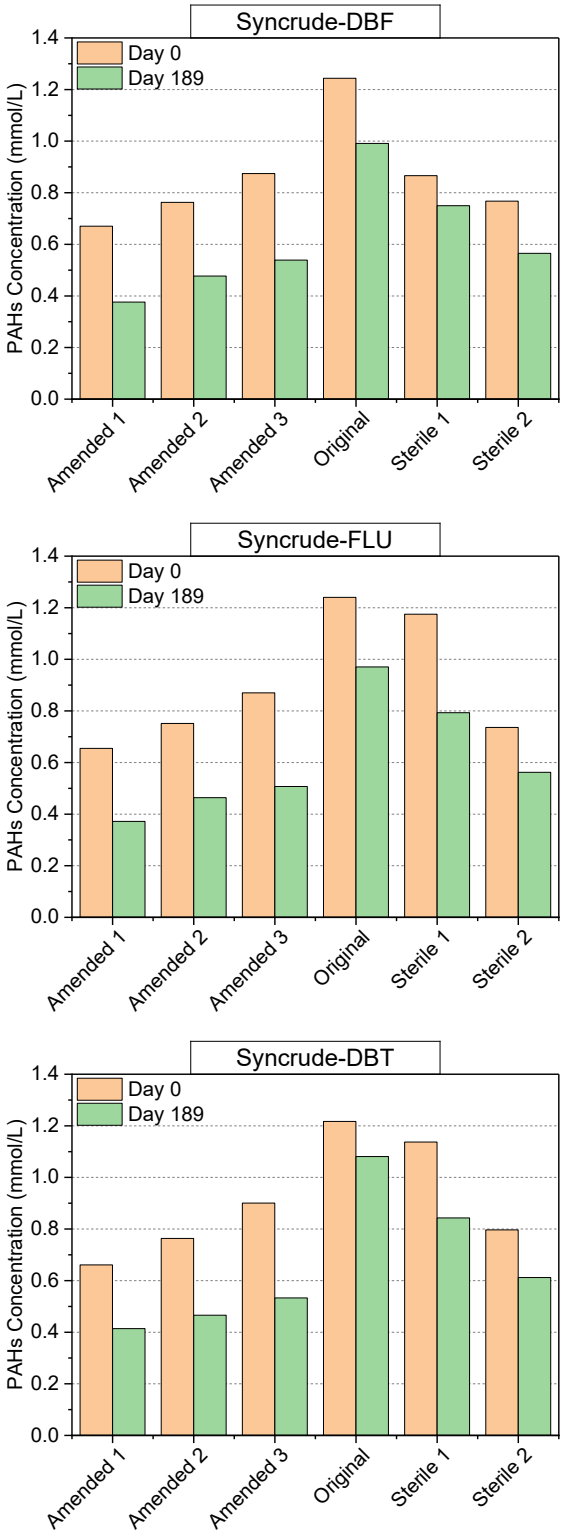

Figure 3-5 PAHs concentration in the additional batch of Set A Syncrude microcosms. PAHs in the Amended and Sterile Control microcosms were detected on Day 0 and Day 189 using Soxhlet method with pre-treatment.

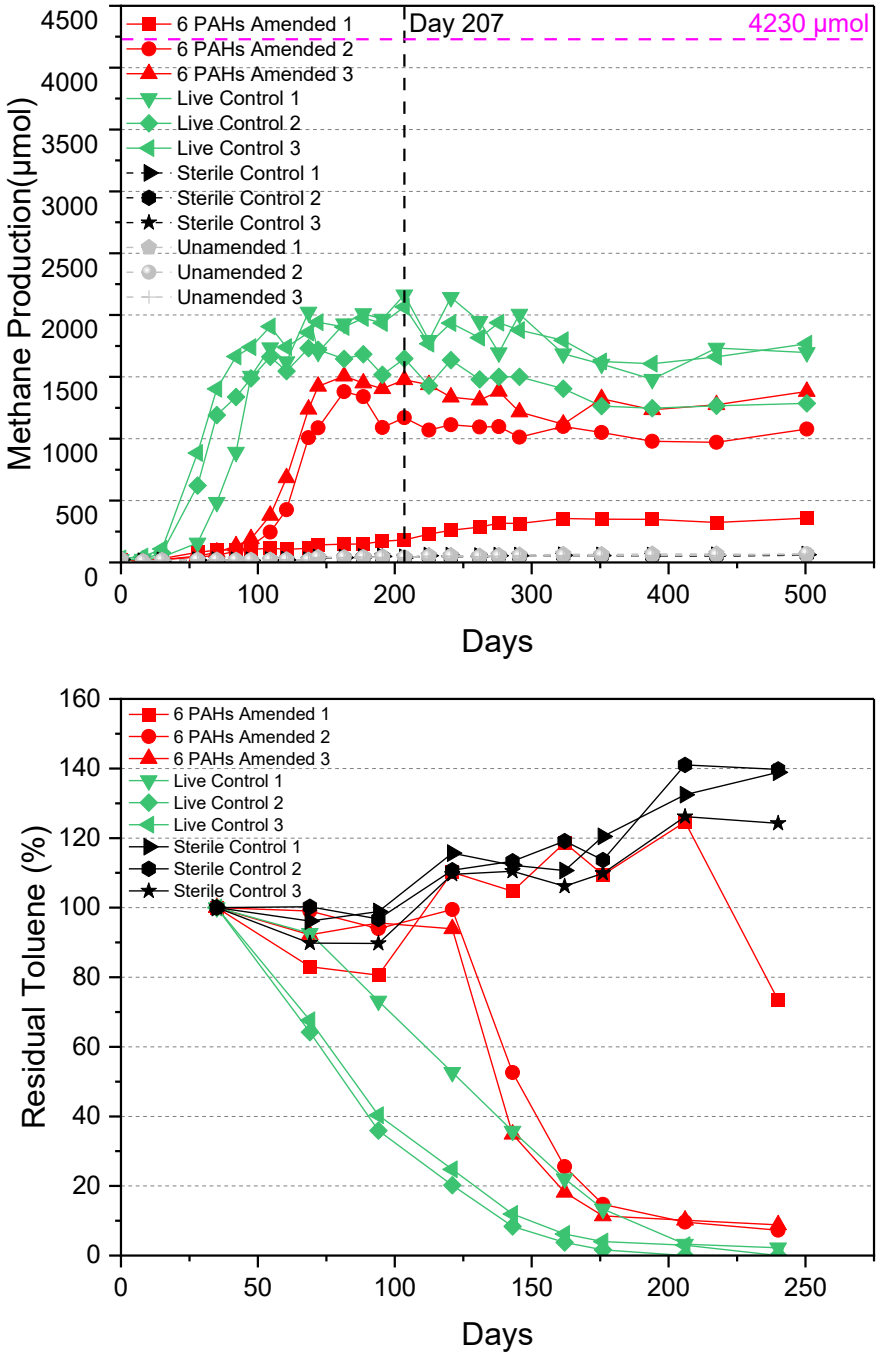

Figure 3-6 Methane production (top panel) and toluene degradation (bottom panel) in Set B Syncrude microcosms. **Top panel:** Methane concentration in the headspace measured by GC-FID. The horizontal pink dotted line indicates theoretical maximum of methane production from complete toluene degradation in the Amended and Live Control microcosms. The vertical black dotted line indicates the day on which the samples were taken for PAHs determination and microbial analysis. **Bottom panel:** Residual toluene (%) in the headspace of microcosms was obtained by calculating the peak ratio of toluene/internal standards after measuring by GC-MS and comparing it to the Day 0 ratio, which was considered as 100%.

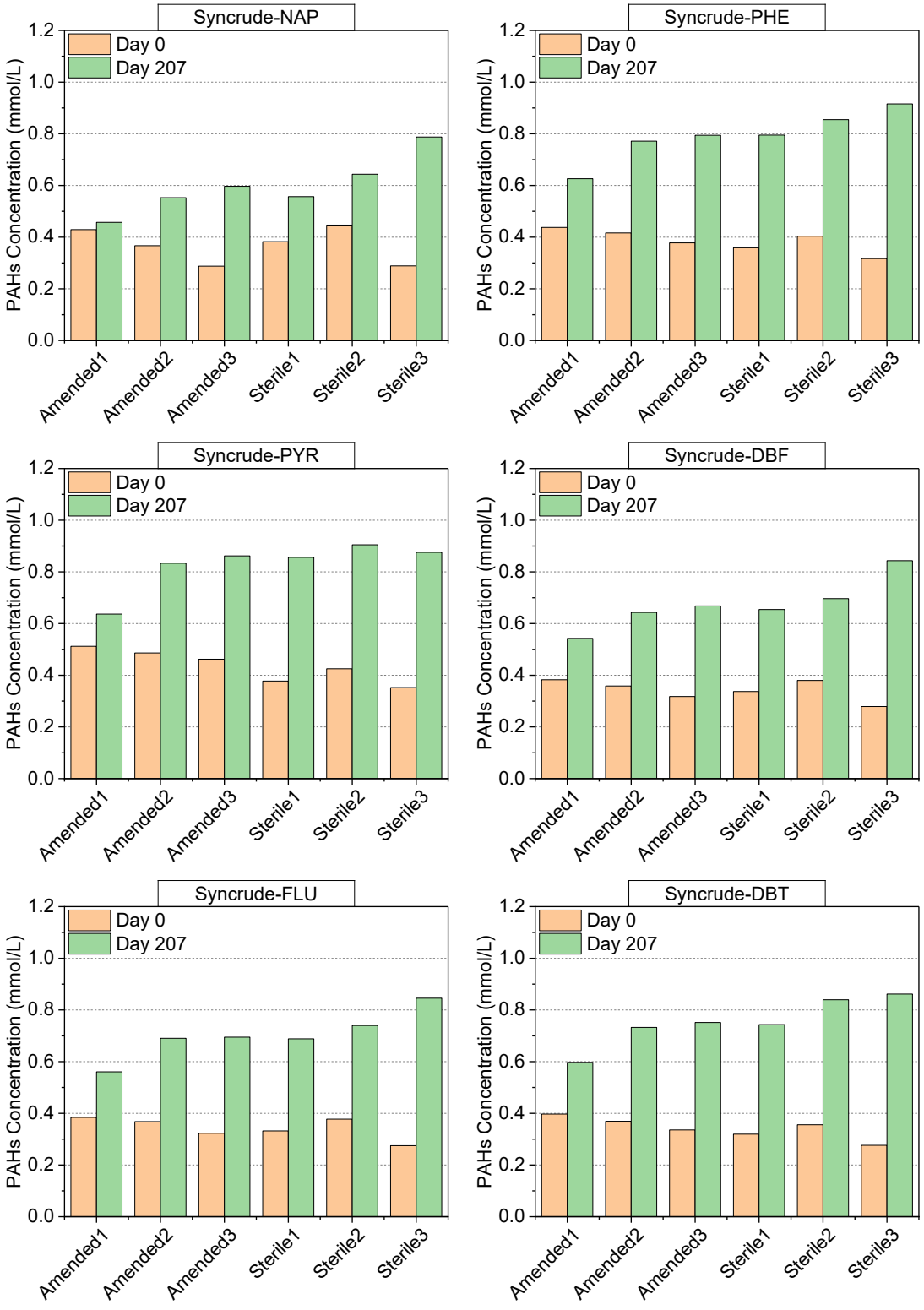

Figure 3-7 PAHs concentration in Set B Syncrude microcosms. PAHs in Amended and Sterile Control microcosms were detected by Soxhlet method without pre-treatment on Day 0 and Soxhlet method with pre-treatment on Day 207.

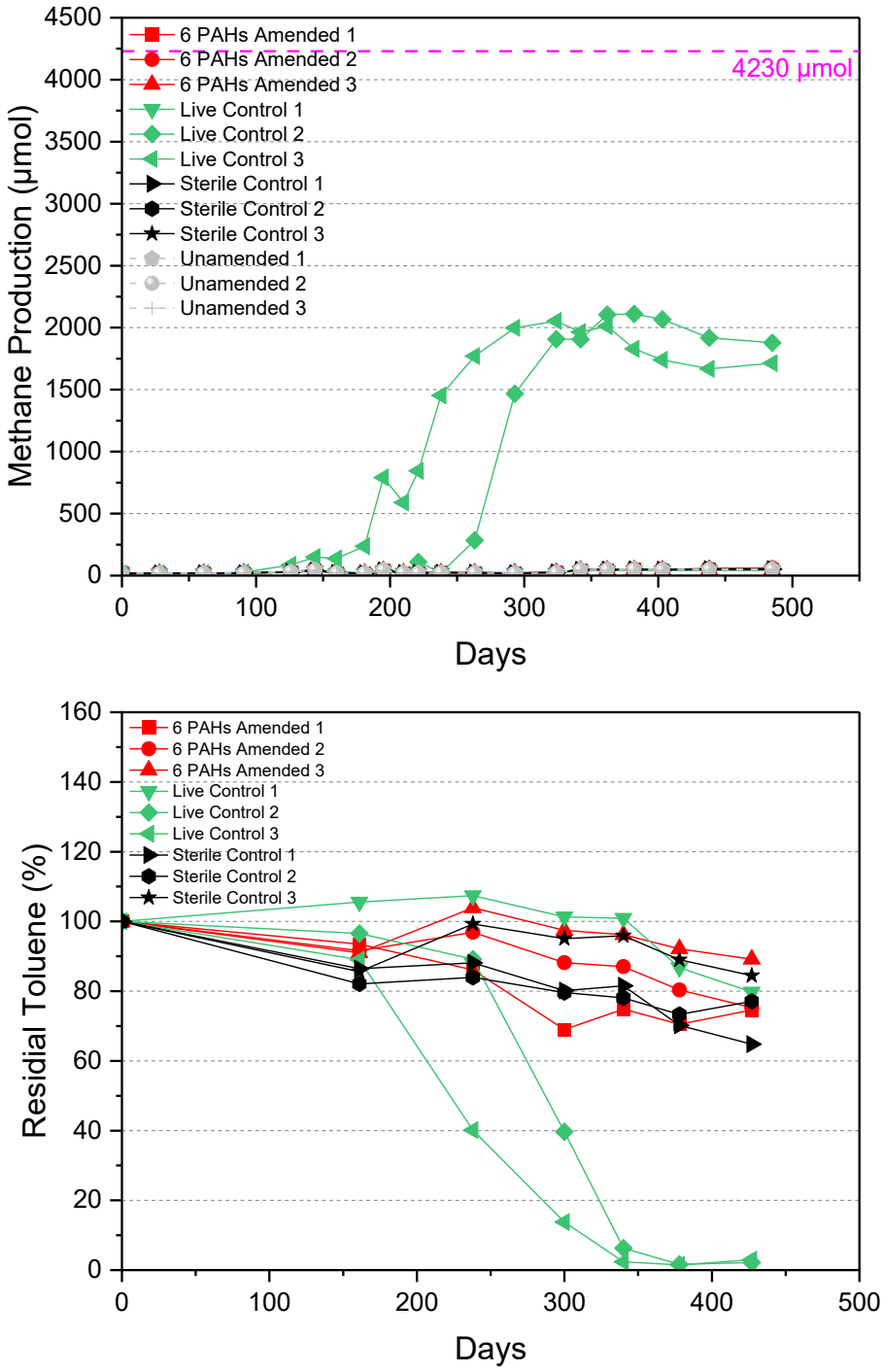

Figure 3-8 Methane production (top panel) and toluene degradation (bottom panel) in Set B CNRL microcosms. **Top panel:** Methane concentration in the headspace measured by GC-FID. The horizontal pink dotted line indicates theoretical maximum of methane production from complete toluene degradation in the Amended and Live Control microcosms. **Bottom panel:** Residual toluene (%) in the headspace of microcosms was obtained by calculating the peak ratio of toluene/internal standards after measuring by GC-MS and comparing it to the Day 0 ratio, which was considered as 100%.

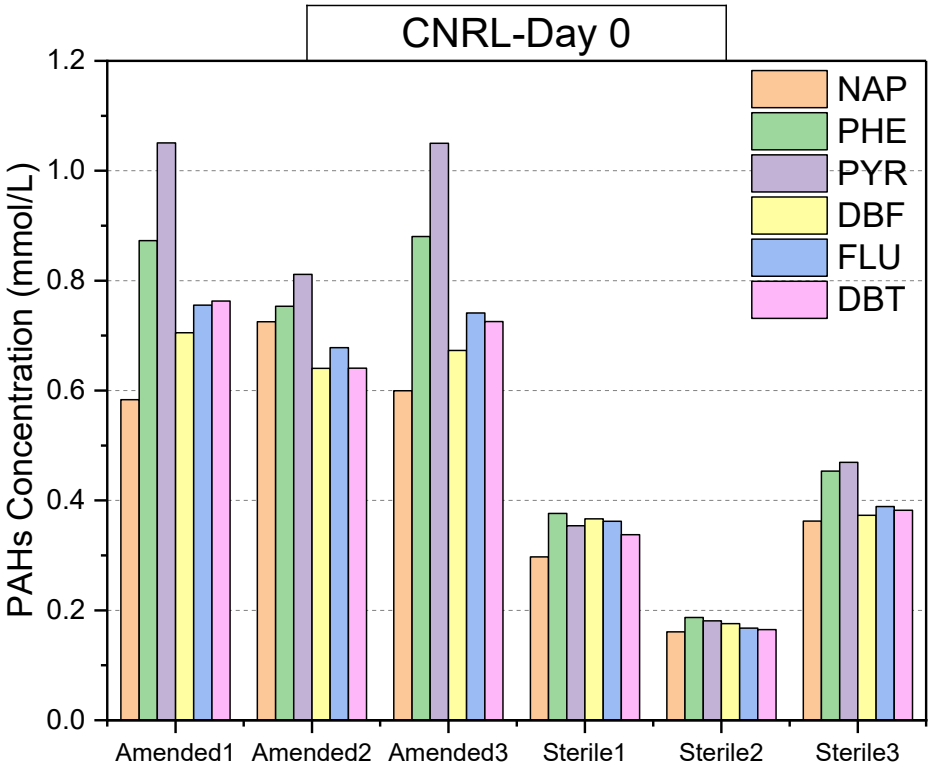

Figure 3-9 PAHs concentration in Set B CNRL microcosms. PAHs in Amended and Sterile Control microcosms were detected on Day 0 using Soxhlet method with pre-treatment.

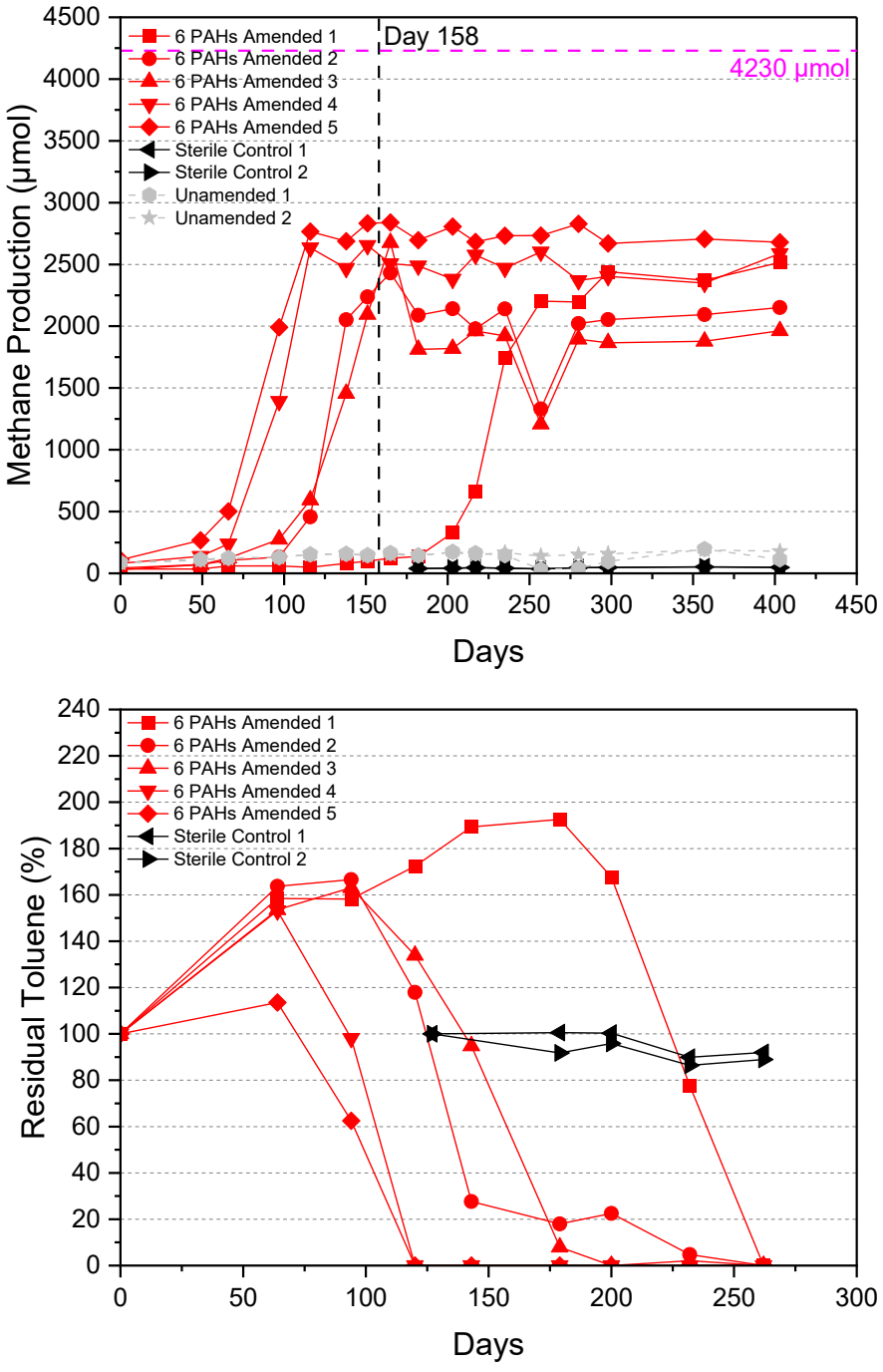

Figure 3-10 Methane production (top panel) and toluene degradation (bottom panel) in Set C Syncrude microcosms. **Top panel:** Methane concentration in the headspace measured by GC-FID. The horizontal pink dotted line indicates theoretical maximum of methane production from complete toluene degradation in the Amended microcosms. The vertical black dotted line indicates the day on which the samples were taken for PAHs determination and microbial analysis. **Bottom panel:** Residual toluene (%) in the headspace of microcosms was obtained by calculating the peak ratio of toluene/internal standards after measuring by GC-MS and comparing it to the Day 0 ratio, which was considered as 100%.

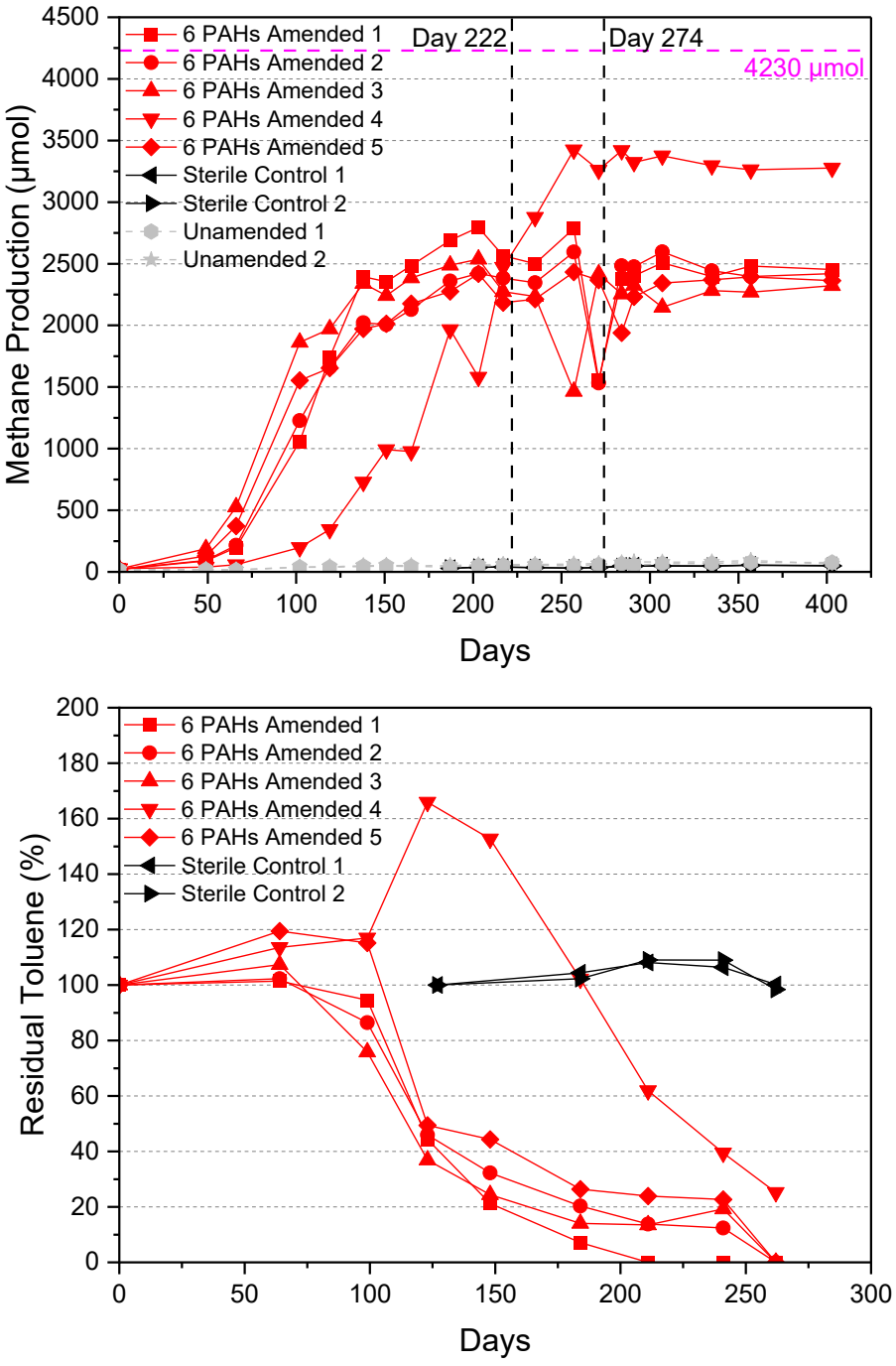

Figure 3-11 Methane production (top panel) and toluene degradation (bottom panel) in Set C Albian microcosms. **Top panel:** Methane concentration in the headspace measured by GC-FID. The horizontal pink dotted line indicates theoretical maximum of methane production from complete toluene degradation in the Amended microcosms. The vertical black dotted lines indicate the day on which the samples were taken for PAHs determination and microbial analysis. **Bottom panel:** Residual toluene (%) in the headspace of microcosms was obtained by calculating the peak ratio of toluene/internal standards after measuring by GC-MS and comparing it to the Day 0 ratio, which was considered as 100%.

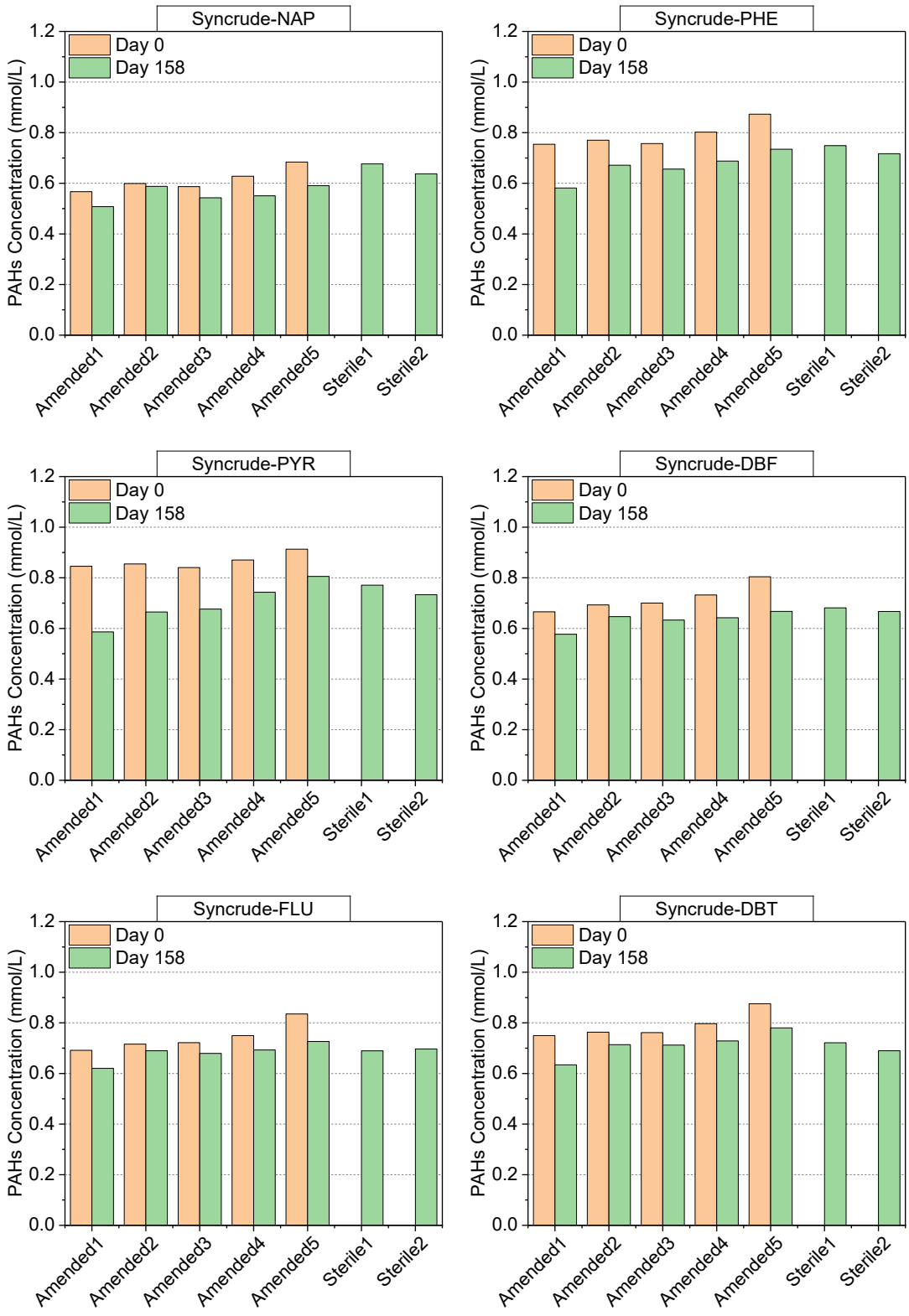

Figure 3-12 PAHs concentration in Set C Syncrude microcosms. PAHs in Amended and Sterile Control microcosms were detected by Soxhlet method with pre-treatment on Day 0 and Day 158.

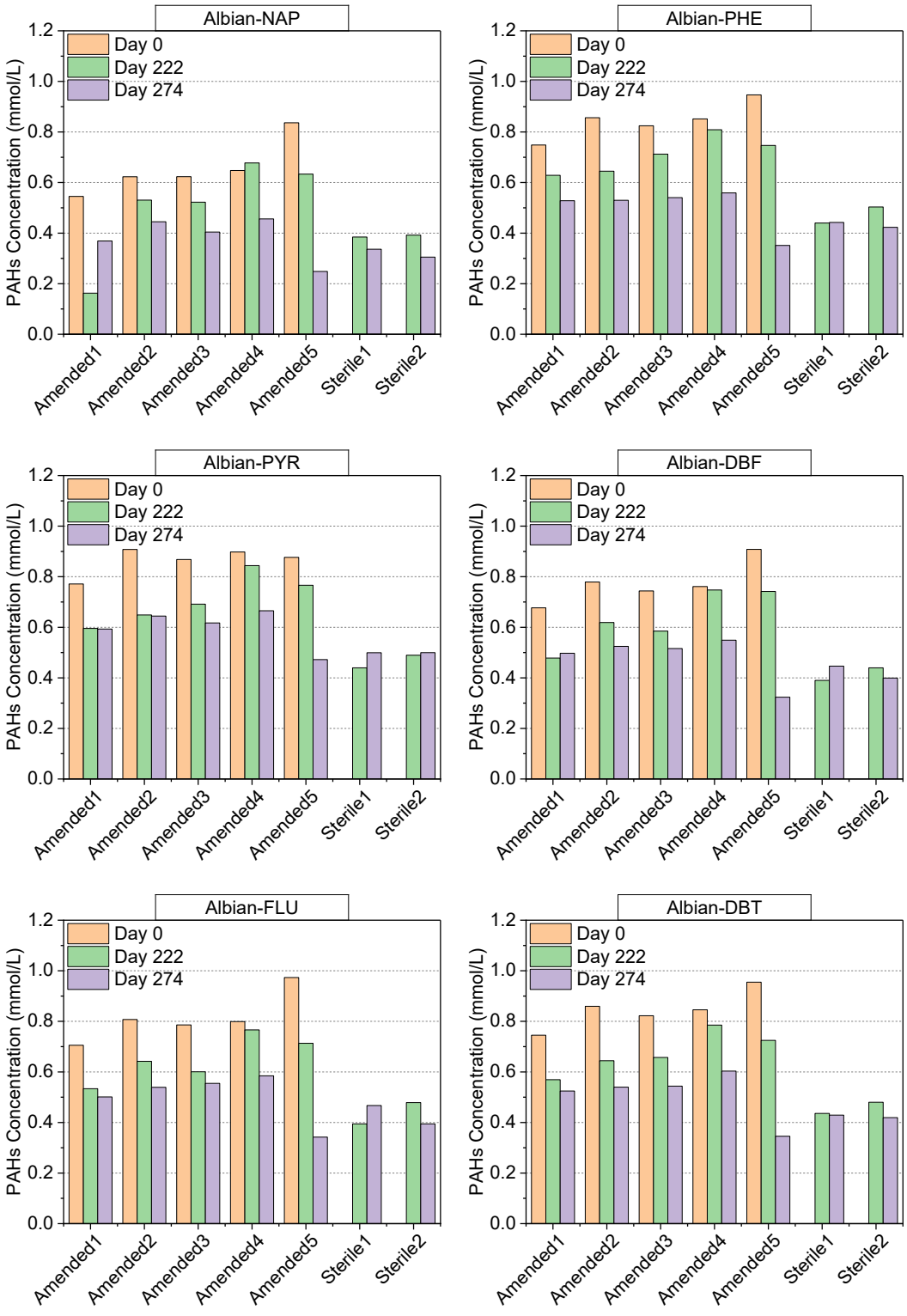

Figure 3-13 PAHs concentration in Set C Albian microcosms. PAHs in Amended and Sterile Control microcosms were detected by Soxhlet method with pre-treatment on Day 0, Day 222, and Day 274.

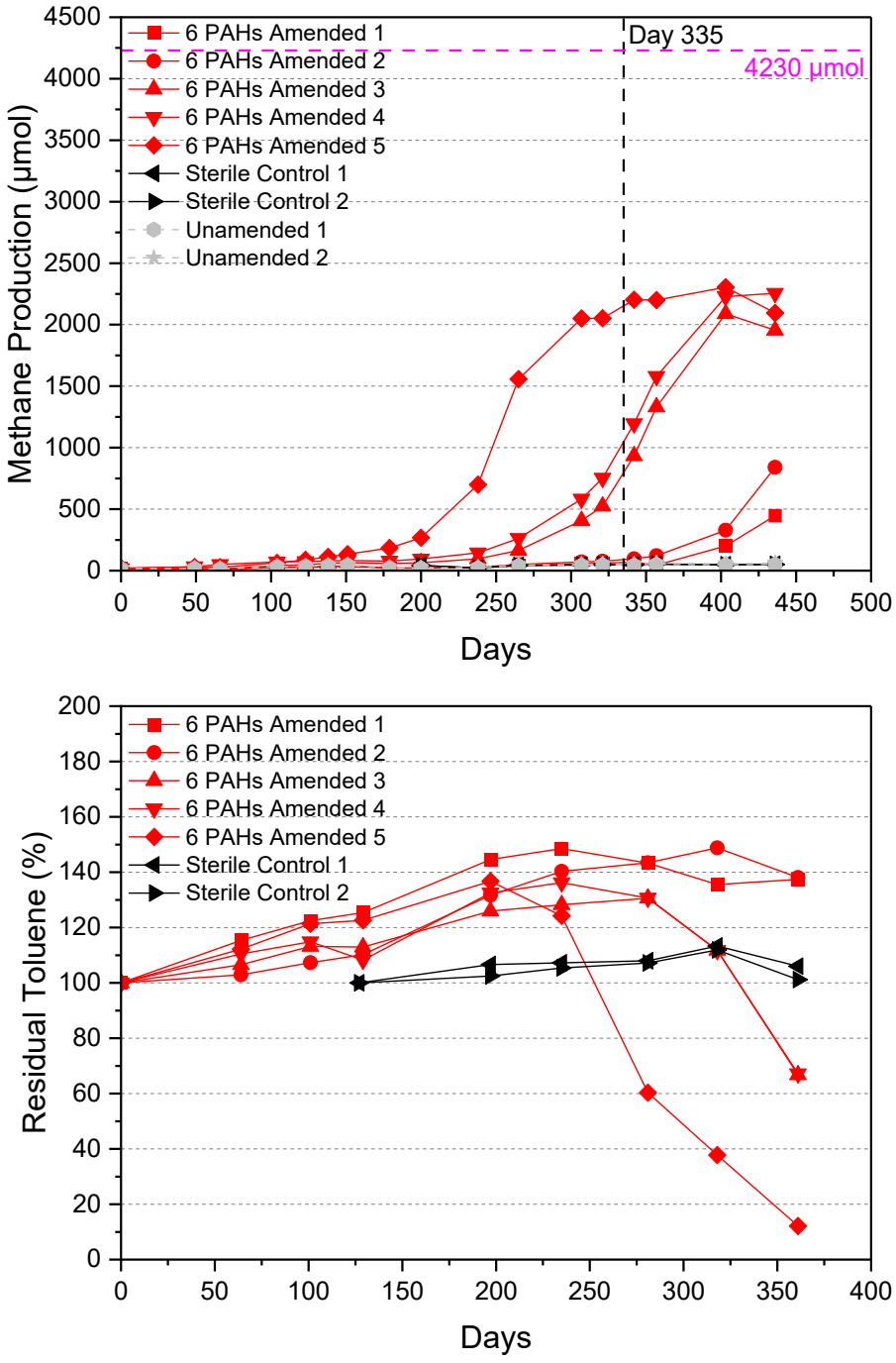

Figure 3-14 Methane production (top panel) and toluene degradation (bottom panel) in Set C CNRL microcosms. **Top panel:** Methane concentration in the headspace measured by GC-FID. The horizontal pink dotted line indicates theoretical maximum of methane production from complete toluene degradation in the Amended microcosms. The vertical black dotted line indicates the day on which the samples were taken for PAHs determination and microbial analysis. **Bottom panel:** Residual toluene (%) in the headspace of microcosms was obtained by calculating the peak ratio of toluene/internal standards after measuring by GC-MS and comparing it to the Day 0 ratio, which was considered as 100%.

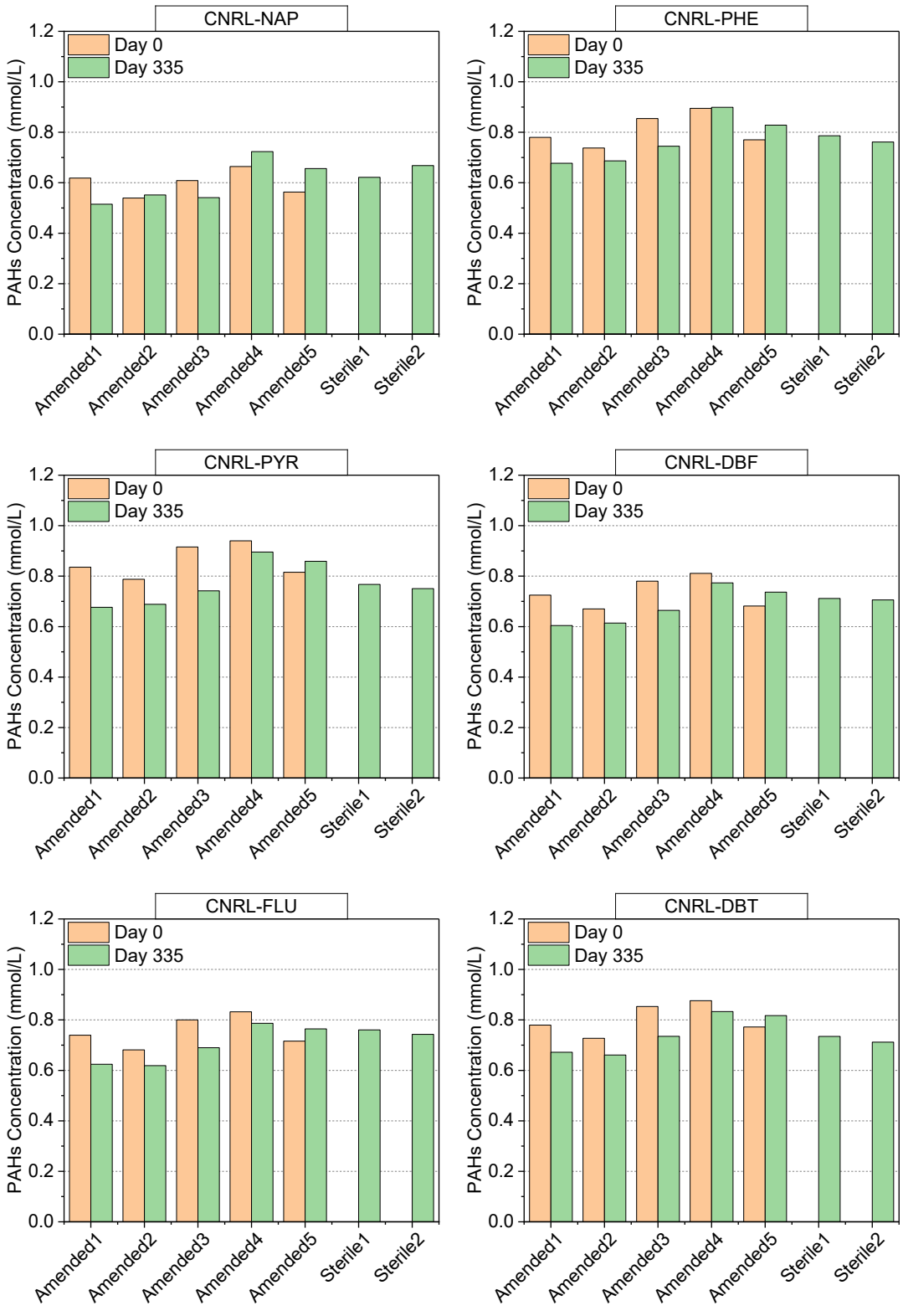

Figure 3-15 PAHs concentration in Set C CNRL microcosms. PAHs in Amended and Sterile Control microcosms were detected by Soxhlet method with pre-treatment on Day 0 and Day 335.

References

Bean, G.P., 1998. Application of Natural Bond Orbital Analysis and Natural Resonance Theory to Delocalization and Aromaticity in Five-Membered Heteroaromatic Compounds. J. Org. Chem. 63, 2497–2506. https://doi.org/10.1021/jo971725x

Berdugo-Clavijo, C., Dong, X., Soh, J., Sensen, C.W., Gieg, L.M., 2012. Methanogenic biodegradation of two-ringed polycyclic aromatic hydrocarbons. FEMS Microbiol Ecol 81, 124–133. https://doi.org/10.1111/j.1574-6941.2012.01328.x

Brigmon, R.L., Berry, C.J., Wade, A., Simpson, W., 2016. Bioprocessing-Based Approach for Bitumen/Water/Fines Separation and Hydrocarbon Recovery from Oil Sands Tailings. Soil and Sediment Contamination: An International Journal 25, 241–255. https://doi.org/10.1080/15320383.2015.1020408

Canadian Association of Petroleum Producers (CAPP), 2021. An Introduction to Oil Sands Pit Lakes. oil

Clark, K.A., Pasternack, D.S., 1932. Hot Water Seperation of Bitumen from Alberta Bituminous Sand. Ind. Eng. Chem. 24, 1410–1416. https://doi.org/10.1021/ie50276a016

Cossey, H.L., Batycky, A.E., Kaminsky, H., Ulrich, A.C., 2021. Geochemical Stability of Oil Sands Tailings in Mine Closure Landforms. Minerals 11, 830. https://doi.org/10.3390/min11080830

Dong, X., Kleiner, M., Sharp, C.E., Thorson, E., Li, C., Liu, D., Strous, M., 2017. Fast and Simple Analysis of MiSeq Amplicon Sequencing Data with MetaAmp. Front. Microbiol. 8, 1461. https://doi.org/10.3389/fmicb.2017.01461

Edgar, R. C. (2010). Search and clustering orders of magnitude faster than BLAST. Bioinformatics 26, 2460–2461. doi: 10.1093/bioinformatics/btq461

Fedorak, P.M., Hrudey, S.E., 1984. The effects of phenol and some alkyl phenolics on batch anaerobic methanogenesis. Water Research 18, 361–367. https://doi.org/10.1016/0043-1354(84)90113-1

Fowler, S.J., Dong, X., Sensen, C.W., Suflita, J.M., Gieg, L.M., 2012. Methanogenic toluene metabolism: community structure and intermediates. Environmental Microbiology 14, 754–764. https://doi.org/10.1111/j.1462-2920.2011.02631.x

Galarneau, E., Hollebone, B.P., Yang, Z., Schuster, J., 2014. Preliminary measurement-based estimates of PAH emissions from oil sands tailings ponds. Atmospheric Environment 97, 332–335. https://doi.org/10.1016/j.atmosenv.2014.08.038

Gou, Y., Song, Y., Yang, S., Yang, Y., Cheng, Y., Wu, X., Wei, W., Wang, H., 2023. Low-temperature thermal-enhanced anoxic biodegradation of polycyclic aromatic hydrocarbons in aged subsurface soil. Chemical Engineering Journal 454, 140143. https://doi.org/10.1016/j.cej.2022.140143

Gou, Y., Song, Y., Yang, S., Yang, Y., Cheng, Yanan, Li, J., Zhang, T., Cheng, Yanjun, Wang, H., 2022. Polycyclic aromatic hydrocarbon removal from subsurface soil mediated by bacteria and archaea under methanogenic conditions: Performance and mechanisms. Environmental Pollution 313, 120023. https://doi.org/10.1016/j.envpol.2022.120023

Harner, T., Rauert, C., Muir, D., Schuster, J.K., Hsu, Y.-M., Zhang, L., Marson, G., Watson, J.G., Ahad, J., Cho, S., Jariyasopit, N., Kirk, J., Korosi, J., Landis, M.S., Martin, J.W., Zhang, Y., Fernie, K., Wentworth, G.R., Wnorowski, A., Dabek, E., Charland, J.-P., Pauli, B., Wania, F., Galarneau, E., Cheng, I., Makar, P., Whaley, C., Chow, J.C., Wang, X., 2018. Air synthesis review: polycyclic aromatic compounds in the oil sands region. Environ. Rev. 26, 430–468. https://doi.org/10.1139/er-2018-0039

Hashemzadeh, F., Khoshmardan, M.E., Sanaei, D., Ghalhari, M.R., Sharifan, H., Inglezakis, V.J., Arcibar-Orozco, J.A., Shaikh, W.A., Khan, E., Biswas, J.K., 2024. Adsorptive removal of anthracene from water by biochar derived amphiphilic carbon dots decorated with chitosan. Chemosphere 352, 141248. https://doi.org/10.1016/j.chemosphere.2024.141248

Holowenko, F.M., MacKinnon, M.D., Fedorak, P.M., 2000. Methanogens and sulfate-reducing bacteria in oil sands fine tailings waste. Canadian Journal of Microbiology 46, 927–937.

Hsu, Y.-M., Harner, T., Li, H., Fellin, P., 2015. PAH Measurements in Air in the Athabasca Oil Sands Region. Environ. Sci. Technol. 49, 5584–5592. https://doi.org/10.1021/acs.est.5b00178

Kong, J.D., Wang, H., Siddique, T., Foght, J., Semple, K., Burkus, Z., Lewis, M.A., 2019. Second-generation stoichiometric mathematical model to predict methane emissions from oil sands tailings. Science of The Total Environment 694, 133645. https://doi.org/10.1016/j.scitotenv.2019.133645

Łyszczarz, S., Lasota, J., Szuszkiewicz, M.M., Błońska, E., 2021. Soil texture as a key driver of polycyclic aromatic hydrocarbons (PAHs) distribution in forest topsoils. Sci Rep 11, 14708. https://doi.org/10.1038/s41598-021-94299-x

Mahaffey, A., Dubé, M., 2017. Review of the composition and toxicity of oil sands process-affected water. Environ. Rev. 25, 97–114. https://doi.org/10.1139/er-2015-0060

Mohamad Shahimin, M.F., Foght, J.M., Siddique, T., 2021. Methanogenic Biodegradation of iso-Alkanes by Indigenous Microbes from Two Different Oil Sands Tailings Ponds. Microorganisms 9, 1569. https://doi.org/10.3390/microorganisms9081569

Mohamad Shahimin, M.F., Foght, J.M., Siddique, T., 2016. Preferential methanogenic biodegradation of short-chain n-alkanes by microbial communities from two different oil sands tailings ponds. Science of The Total Environment 553, 250–257. https://doi.org/10.1016/j.scitotenv.2016.02.061

Richter, B.E., Jones, B.A., Ezzell, J.L., Porter, N.L., Avdalovic, N., Pohl, C., 1996. Accelerated Solvent Extraction: A Technique for Sample Preparation. Anal. Chem. 68, 1033–1039. https://doi.org/10.1021/ac9508199

Schloss, P.D., Westcott, S.L., Ryabin, T., Hall, J.R., Hartmann, M., Hollister, E.B., Lesniewski, R.A., Oakley, B.B., Parks, D.H., Robinson, C.J., Sahl, J.W., Stres, B., Thallinger, G.G., Horn, D.J.V., Weber, C.F., 2009. Introducing mothur: Open-Source, Platform-Independent, Community-Supported Software for Describing and Comparing Microbial Communities. Appl. Environ. Microbiol. 75.

Selucky, M., Chu, Y., Ruo, T., Strausz, O., 1977. Chemical composition of Athabasca bitumen. Fuel 56, 369–381. https://doi.org/10.1016/0016-2361(77)90061-8

Shen, X., Dong, W., Wan, Y., Liu, Y., Yuan, Z., 2022. Function of Fe(III) in naphthalene adsorption on typical clay minerals and humic acid complexes. Journal of Environmental Chemical Engineering 10, 108271. https://doi.org/10.1016/j.jece.2022.108271

Siddique, T., Fedorak, P.M., Foght, J.M., 2006. Biodegradation of Short-Chain *n* -Alkanes in Oil Sands Tailings under Methanogenic Conditions. Environ. Sci. Technol. 40, 5459–5464. https://doi.org/10.1021/es060993m

Siddique, T., Fedorak, P.M., MacKinnon, M.D., Foght, J.M., 2007. Metabolism of BTEX and Naphtha Compounds to Methane in Oil Sands Tailings. Environ. Sci. Technol. 41, 2350–2356. https://doi.org/10.1021/es062852q

Siddique, T., Gupta, R., Fedorak, P.M., MacKinnon, M.D., Foght, J.M., 2008. A first approximation kinetic model to predict methane generation from an oil sands tailings settling basin. Chemosphere 72, 1573–1580. https://doi.org/10.1016/j.chemosphere.2008.04.036

Siddique, T., Kuznetsova, A., 2020. Linking hydrocarbon biodegradation to greenhouse gas emissions from oil sands tailings and its impact on tailings management. Can. J. Soil. Sci. 100, 537–545. https://doi.org/10.1139/cjss-2019-0125

Siddique, T., Penner, T., Klassen, J., Nesbø, C., Foght, J.M., 2012. Microbial Communities Involved in Methane Production from Hydrocarbons in Oil Sands Tailings. Environ. Sci. Technol. 46, 9802–9810. https://doi.org/10.1021/es302202c

Small, C.C., Cho, S., Hashisho, Z., Ulrich, A.C., 2015. Emissions from oil sands tailings ponds: Review of tailings pond parameters and emission estimates. Journal of Petroleum Science and Engineering 127, 490–501. https://doi.org/10.1016/j.petrol.2014.11.020

Sun, W., Sun, X., Cupples, A.M., 2014. Identification of Desulfosporosinus as toluene-assimilating microorganisms from a methanogenic consortium. International Biodeterioration & Biodegradation 88, 13–19. https://doi.org/10.1016/j.ibiod.2013.11.014

Symons, G.E., Buswell, A.M., 1933. The Methane Fermentation of Carbohydrates [1,2]. J. Am. Chem. Soc. 55, 2028–2036. https://doi.org/10.1021/ja01332a039

Ye, Q., Liang, C., Chen, X., Fang, T., Wang, Y., Wang, H., 2019. Molecular characterization of methanogenic microbial communities for degrading various types of polycyclic aromatic hydrocarbon. Journal of Environmental Sciences 86, 97–106. https://doi.org/10.1016/j.jes.2019.04.027

You, Y., Staebler, R.M., Moussa, S.G., Beck, J., Mittermeier, R.L., 2021. Methane emissions from an oil sands tailings pond: a quantitative comparison of fluxes derived by different methods. Atmos. Meas. Tech. 14, 1879–1892. https://doi.org/10.5194/amt-14-1879-2021

Zavgorodnyaya, Y.A., Chikidova, A.L., Biryukov, M.V., Demin, V.V., 2019. Polycyclic aromatic hydrocarbons in atmospheric particulate depositions and urban soils of Moscow, Russia. J Soils Sediments 19, 3155–3165. https://doi.org/10.1007/s11368-018-2067-3

Zhang, S., Hu, Z., Wang, H., 2019. Metagenomic analysis exhibited the co-metabolism of polycyclic aromatic hydrocarbons by bacterial community from estuarine sediment. Environment International 129, 308–319. https://doi.org/10.1016/j.envint.2019.05.028

Zhang, Z., Wang, C., He, J., Wang, H., 2019. Anaerobic phenanthrene biodegradation with four kinds of electron acceptors enriched from the same mixed inoculum and exploration of metabolic pathways. Front. Environ. Sci. Eng. 13, 80. https://doi.org/10.1007/s11783-019-1164-x

Chapter 4: Conclusions and Perspectives for Future Work

In the first experiment of this work (Chapter 2), we optimized a method for efficient PAHs determinations in FFT samples because the standard method recommended by EPA to extract PAHs from solid substrates including soils and sediments yielded poor recoveries (~50-60%) of PAHs from the FFT samples. After method optimization, we were able to achieve ~94% pooled mean recovery and >80% individual recovery for the 6 target PAHs from FFT, including naphthalene (NAP), phenanthrene (PHE), pyrene (PYR), dibenzofuran (DBF), fluorene (FLU), and dibenzothiophene (DBT). The essential steps of the optimized method are (1) pre-treatment of FFT sample with DCM for 24 hours before extraction; (2) extraction of PAHs from the pre-treated FFT with DCM in a Soxhlet extractor for 24 hours; (3) purification of the extract with a silica gel chromatography column using DCM as eluent; (4) measurement on GC-MS. This method is able to yield reproducible results for PAHs determination, thus was applied to the bench-scale PAHs biodegradation experiments of this study (Chapter 3). This method can not only assist PAHs analyses and management in tailings but may also help PAHs determination in other environmental substrates that have similar texture to FFT (e.g., contain high proportion of fine particles and organic compounds). Future work could address the sensitivity and reproducibility of this method to extract a broader range of PAHs species from FFT or other heavy textured organic rich wastes.

In the bench-scale experiment of this work regarding PAHs degradation, we established 78 microcosms to investigate the potential biodegradation of the 6 abundant PAHs (NAP, PHE, PYR, DBF, FLU, and DBT) in the tailing samples collected from 3 different ponds operated by Syncrude, CNRL, and Albian. Current results showed that the toluene used for dissolving and spiking PAHs has been completely degraded in the Amended (spiked with PAHs and toluene) and Live Control (spiked with toluene only) microcosms in the Syncrude and Albian batch and is

currently being degraded in the Amended and Live Control microcosms in the CNRL batch. Although there is no PAHs degradation detected in any of the 3 batches after an incubation period of ~700 days, the indigenous microbial communities in the microcosms are active and may degrade PAHs in the following months since the potential PAHs degraders such as *Clostridia* have high relative abundance in the microbial communities of FFT samples in this study. If methanogenic biodegradation of PAHs in our microcosms occurred with concurrent methane production, it will help refine the current stoichiometric model to predict methane emissions from different tailings ponds. Future work might also address the potential metabolic pathways of PAHs degradation. The findings will help people understand the PAHs behavior under methanogenic conditions below mudline of the tailings ponds.

Bibliography

Ahad, J.M.E., Jautzy, J.J., Cumming, B.F., Das, B., Laird, K.R., Sanei, H., 2015. Sources of polycyclic aromatic hydrocarbons (PAHs) to northwestern Saskatchewan lakes east of the Athabasca oil sands. Organic Geochemistry 80, 35–45. https://doi.org/10.1016/j.orggeochem.2015.01.001

Ahad, J.M.E., Pakdel, H., Gammon, P.R., Mayer, B., Savard, M.M., Peru, K.M., Headley, J.V., 2020. Distinguishing Natural from Anthropogenic Sources of Acid Extractable Organics in Groundwater near Oil Sands Tailings Ponds. Environ. Sci. Technol. 54, 2790–2799. https://doi.org/10.1021/acs.est.9b06875

Alberta Energy Regulator, 2023. Crude Oil Production. https://www.aer.ca/providing-information/data-and-reports/statistical-reports/st98/crude-oil/production

Balmer, J.E., Hung, H., Yu, Y., Letcher, R.J., Muir, D.C.G., 2019. Sources and environmental fate of pyrogenic polycyclic aromatic hydrocarbons (PAHs) in the Arctic. Emerging Contaminants 5, 128–142. https://doi.org/10.1016/j.emcon.2019.04.002

Bartlett, A.J., Frank, R.A., Gillis, P.L., Parrott, J.L., Marentette, J.R., Brown, L.R., Hooey, T., Vanderveen, R., McInnis, R., Brunswick, P., Shang, D., Headley, J.V., Peru, K.M., Hewitt, L.M., 2017. Toxicity of naphthenic acids to invertebrates: Extracts from oil sands process-affected water versus commercial mixtures. Environmental Pollution 227, 271–279. https://doi.org/10.1016/j.envpol.2017.04.056

Bean, G.P., 1998. Application of Natural Bond Orbital Analysis and Natural Resonance Theory to Delocalization and Aromaticity in Five-Membered Heteroaromatic Compounds. J. Org. Chem. 63, 2497–2506. https://doi.org/10.1021/jo971725x

Berdugo-Clavijo, C., Dong, X., Soh, J., Sensen, C.W., Gieg, L.M., 2012. Methanogenic biodegradation of two-ringed polycyclic aromatic hydrocarbons. FEMS Microbiol Ecol 81, 124–133. https://doi.org/10.1111/j.1574-6941.2012.01328.x

Berset, J.D., Ejem, M., Holzer, R., Lischer, P., 1999. Comparison of different drying, extraction and detection techniques for the determination of priority polycyclic aromatic hydrocarbons in background contaminated soil samples. Analytica Chimica Acta 383, 263–275. https://doi.org/10.1016/S0003-2670(98)00817-4

Brigmon, R.L., Berry, C.J., Wade, A., Simpson, W., 2016. Bioprocessing-Based Approach for Bitumen/Water/Fines Separation and Hydrocarbon Recovery from Oil Sands Tailings.

Soil and Sediment Contamination: An International Journal 25, 241–255. https://doi.org/10.1080/15320383.2015.1020408

Butler, R.M., 1994. Steam-Assisted Gravity Drainage: Concept, Development, Performance And Future. Journal of Canadian Petroleum Technology 33, 44–50. https://doi.org/10.2118/94-02-05

Canadian Association of Petroleum Producers (CAPP), 2021. An Introduction to Oil Sands Pit Lakes. https://www.capp.ca/wp-content/uploads/2021/05/An-Introduction-to-Oil-Sands-Pit-Lakes-392128.pdf

Canadian Council of Ministers of the Environment, 1999. Canadian Environmental Quality Guidelines. https://ccme.ca/en/res/polycyclic-aromatic-hydrocarbons-pahs-en-canadian-water-quality-guidelines-for-the-protection-of-aquatic-life.pdf

Chalaturnyk, R.J., Don Scott, J., Özüm, B., 2002. Management of Oil Sands Tailings. Petroleum Science and Technology 20, 1025–1046. https://doi.org/10.1081/LFT-120003695

Chen, Q., Liu, Q., 2019. Bitumen Coating on Oil Sands Clay Minerals: A Review. Energy Fuels 33, 5933–5943. https://doi.org/10.1021/acs.energyfuels.9b00852

Chen, Y., Wang, Y., Headley, J.V., Huang, R., 2024. Sample preparation, analytical characterization, monitoring, risk assessment and treatment of naphthenic acids in industrial wastewater and surrounding water impacted by unconventional petroleum production. Science of The Total Environment 913, 169636. https://doi.org/10.1016/j.scitotenv.2023.169636

Clark, K.A., Pasternack, D.S., 1932. Hot Water Seperation of Bitumen from Alberta Bituminous Sand. Ind. Eng. Chem. 24, 1410–1416. https://doi.org/10.1021/ie50276a016

Cossey, H.L., Batycky, A.E., Kaminsky, H., Ulrich, A.C., 2021. Geochemical Stability of Oil Sands Tailings in Mine Closure Landforms. Minerals 11, 830. https://doi.org/10.3390/min11080830

Dong, X., Kleiner, M., Sharp, C.E., Thorson, E., Li, C., Liu, D., Strous, M., 2017. Fast and Simple Analysis of MiSeq Amplicon Sequencing Data with MetaAmp. Front. Microbiol. 8, 1461. https://doi.org/10.3389/fmicb.2017.01461

Edgar, R. C. (2010). Search and clustering orders of magnitude faster than BLAST. Bioinformatics 26, 2460–2461. doi: 10.1093/bioinformatics/btq461

Fabbri, D., Rombolà, A.G., Torri, C., Spokas, K.A., 2013. Determination of polycyclic aromatic hydrocarbons in biochar and biochar amended soil. Journal of Analytical and Applied Pyrolysis 103, 60–67. https://doi.org/10.1016/j.jaap.2012.10.003

Fedorak, P.M., Hrudey, S.E., 1984. The effects of phenol and some alkyl phenolics on batch anaerobic methanogenesis. Water Research 18, 361–367. https://doi.org/10.1016/0043-1354(84)90113-1

Fletouris, D.J., 2007. Clean-up and fractionation methods, in: Food Toxicants Analysis. Elsevier, pp. 299–348. https://doi.org/10.1016/B978-044452843-8/50011-0

Foght, J.M., Gieg, L.M., Siddique, T., 2017. The microbiology of oil sands tailings: past, present, future. FEMS Microbiology Ecology 93. https://doi.org/10.1093/femsec/fix034

Fowler, S.J., Dong, X., Sensen, C.W., Suflita, J.M., Gieg, L.M., 2012. Methanogenic toluene metabolism: community structure and intermediates. Environmental Microbiology 14, 754–764. https://doi.org/10.1111/j.1462-2920.2011.02631.x

Galarneau, E., Hollebone, B.P., Yang, Z., Schuster, J., 2014. Preliminary measurement-based estimates of PAH emissions from oil sands tailings ponds. Atmospheric Environment 97, 332–335. https://doi.org/10.1016/j.atmosenv.2014.08.038

Gbeddy, G., Egodawatta, P., Goonetilleke, A., Ayoko, G., Jayarathne, A., Chen, L., Russell, S., 2020. Optimized simultaneous pressurized fluid extraction and in-cell clean-up, and analysis of polycyclic aromatic hydrocarbons (PAHs), and nitro-, carbonyl-, hydroxy - PAHs in solid particles. Analytica Chimica Acta 1125, 19–28. https://doi.org/10.1016/j.aca.2020.05.021

Gong, Z., Alef, K., Wilke, B.-M., Li, P., 2005. Dissolution and removal of PAHs from a contaminated soil using sunflower oil. Chemosphere 58, 291–298. https://doi.org/10.1016/j.chemosphere.2004.07.035

Gou, Y., Song, Y., Yang, S., Yang, Y., Cheng, Y., Wu, X., Wei, W., Wang, H., 2023. Low-temperature thermal-enhanced anoxic biodegradation of polycyclic aromatic hydrocarbons in aged subsurface soil. Chemical Engineering Journal 454, 140143. https://doi.org/10.1016/j.cej.2022.140143

Gou, Y., Song, Y., Yang, S., Yang, Y., Cheng, Yanan, Li, J., Zhang, T., Cheng, Yanjun, Wang, H., 2022. Polycyclic aromatic hydrocarbon removal from subsurface soil mediated by

bacteria and archaea under methanogenic conditions: Performance and mechanisms. Environmental Pollution 313, 120023. https://doi.org/10.1016/j.envpol.2022.120023

Government of Alberta, 2015. Lower Athabasca Region - Tailings Management Framework for the Mineable Athabasca Oil Sands.

Han, M., Kong, J., Yuan, J., He, H., Hu, J., Yang, S., Li, S., Zhang, L., Sun, C., 2019. Method development for simultaneous analyses of polycyclic aromatic hydrocarbons and their nitro-, oxy-, hydroxy- derivatives in sediments. Talanta 205, 120128. https://doi.org/10.1016/j.talanta.2019.120128

Harner, T., Rauert, C., Muir, D., Schuster, J.K., Hsu, Y.-M., Zhang, L., Marson, G., Watson, J.G., Ahad, J., Cho, S., Jariyasopit, N., Kirk, J., Korosi, J., Landis, M.S., Martin, J.W., Zhang, Y., Fernie, K., Wentworth, G.R., Wnorowski, A., Dabek, E., Charland, J.-P., Pauli, B., Wania, F., Galarneau, E., Cheng, I., Makar, P., Whaley, C., Chow, J.C., Wang, X., 2018. Air synthesis review: polycyclic aromatic compounds in the oil sands region. Environ. Rev. 26, 430–468. https://doi.org/10.1139/er-2018-0039

Hashemzadeh, F., Khoshmardan, M.E., Sanaei, D., Ghalhari, M.R., Sharifan, H., Inglezakis, V.J., Arcibar-Orozco, J.A., Shaikh, W.A., Khan, E., Biswas, J.K., 2024. Adsorptive removal of anthracene from water by biochar derived amphiphilic carbon dots decorated with chitosan. Chemosphere 352, 141248. https://doi.org/10.1016/j.chemosphere.2024.141248

Holowenko, F., 2002. Characterization of naphthenic acids in oil sands wastewaters by gas chromatography-mass spectrometry. Water Research 36, 2843–2855. https://doi.org/10.1016/S0043-1354(01)00492-4

Holowenko, F.M., MacKinnon, M.D., Fedorak, P.M., 2000. Methanogens and sulfate-reducing bacteria in oil sands fine tailings waste. Canadian Journal of Microbiology 46, 927–937.

Honda, M., Suzuki, N., 2020. Toxicities of Polycyclic Aromatic Hydrocarbons for Aquatic Animals. IJERPH 17, 1363. https://doi.org/10.3390/ijerph17041363

Hsu, Y.-M., Harner, T., Li, H., Fellin, P., 2015. PAH Measurements in Air in the Athabasca Oil Sands Region. Environ. Sci. Technol. 49, 5584–5592. https://doi.org/10.1021/acs.est.5b00178

Jeeravipoolvarn, S., Scott, J.D., Chalaturnyk, R.J., 2009. 10 m standpipe tests on oil sands tailings: long-term experimental results and prediction. Can. Geotech. J. 46, 875–888. https://doi.org/10.1139/T09-033

Kelly, E.N., Short, J.W., Schindler, D.W., Hodson, P.V., Ma, M., Kwan, A.K., Fortin, B.L., 2009. Oil sands development contributes polycyclic aromatic compounds to the Athabasca River and its tributaries. Proc. Natl. Acad. Sci. U.S.A. 106, 22346–22351. https://doi.org/10.1073/pnas.0912050106

Kong, J.D., Wang, H., Siddique, T., Foght, J., Semple, K., Burkus, Z., Lewis, M.A., 2019. Second-generation stoichiometric mathematical model to predict methane emissions from oil sands tailings. Science of The Total Environment 694, 133645. https://doi.org/10.1016/j.scitotenv.2019.133645

Li, C., Fu, L., Stafford, J., Belosevic, M., Gamal El-Din, M., 2017. The toxicity of oil sands process-affected water (OSPW): A critical review. Science of The Total Environment 601–602, 1785–1802. https://doi.org/10.1016/j.scitotenv.2017.06.024

Lu, X.-Y., Li, B., Zhang, T., Fang, H.H.P., 2012. Enhanced anoxic bioremediation of PAHs-contaminated sediment. Bioresource Technology 104, 51–58. https://doi.org/10.1016/j.biortech.2011.10.011

Lundstedt, S., Haglund, P., Öberg, L., 2006. Simultaneous Extraction and Fractionation of Polycyclic Aromatic Hydrocarbons and Their Oxygenated Derivatives in Soil Using Selective Pressurized Liquid Extraction. Anal. Chem. 78, 2993–3000. https://doi.org/10.1021/ac052178f

Łyszczarz, S., Lasota, J., Szuszkiewicz, M.M., Błońska, E., 2021. Soil texture as a key driver of polycyclic aromatic hydrocarbons (PAHs) distribution in forest topsoils. Sci Rep 11, 14708. https://doi.org/10.1038/s41598-021-94299-x

Mahaffey, A., Dubé, M., 2017. Review of the composition and toxicity of oil sands process-affected water. Environ. Rev. 25, 97–114. https://doi.org/10.1139/er-2015-0060

Marentette, J.R., Frank, R.A., Bartlett, A.J., Gillis, P.L., Hewitt, L.M., Peru, K.M., Headley, J.V., Brunswick, P., Shang, D., Parrott, J.L., 2015. Toxicity of naphthenic acid fraction components extracted from fresh and aged oil sands process-affected waters, and commercial naphthenic acid mixtures, to fathead minnow (Pimephales promelas)

embryos. Aquatic Toxicology 164, 108–117. https://doi.org/10.1016/j.aquatox.2015.04.024

Marquès, M., Mari, M., Audí-Miró, C., Sierra, J., Soler, A., Nadal, M., Domingo, J.L., 2016. Photodegradation of polycyclic aromatic hydrocarbons in soils under a climate change base scenario. Chemosphere 148, 495–503. https://doi.org/10.1016/j.chemosphere.2016.01.069

Masliyah, J., Zhou, Z.J., Xu, Z., Czarnecki, J., Hamza, H., 2004. Understanding Water-Based Bitumen Extraction from Athabasca Oil Sands. The Canadian Journal of Chemical Engineering 82, 628–654. https://doi.org/10.1002/cjce.5450820403

Mohamad Shahimin, M.F., Foght, J.M., Siddique, T., 2021. Methanogenic Biodegradation of iso-Alkanes by Indigenous Microbes from Two Different Oil Sands Tailings Ponds. Microorganisms 9, 1569. https://doi.org/10.3390/microorganisms9081569

Mohamad Shahimin, M.F., Foght, J.M., Siddique, T., 2016. Preferential methanogenic biodegradation of short-chain n-alkanes by microbial communities from two different oil sands tailings ponds. Science of The Total Environment 553, 250–257. https://doi.org/10.1016/j.scitotenv.2016.02.061

Mohamad Shahimin, M.F., Siddique, T., 2017. Sequential biodegradation of complex naphtha hydrocarbons under methanogenic conditions in two different oil sands tailings. Environmental Pollution 221, 398–406. https://doi.org/10.1016/j.envpol.2016.12.002

Nzila, A., 2018. Biodegradation of high-molecular-weight polycyclic aromatic hydrocarbons under anaerobic conditions: Overview of studies, proposed pathways and future perspectives. Environmental Pollution 239, 788–802. https://doi.org/10.1016/j.envpol.2018.04.074

Parrott, J.L., Raine, J.C., McMaster, M.E., Hewitt, L.M., 2019. Chronic toxicity of oil sands tailings pond sediments to early life stages of fathead minnow (Pimephales promelas). Heliyon 5, e02509. https://doi.org/10.1016/j.heliyon.2019.e02509

Penner, T.J., Foght, J.M., 2010. Mature fine tailings from oil sands processing harbour diverse methanogenic communities. Can. J. Microbiol. 56, 459–470. https://doi.org/10.1139/W10-029

Pulleyblank, C., Kelleher, B., Campo, P., Coulon, F., 2020. Recovery of polycyclic aromatic hydrocarbons and their oxygenated derivatives in contaminated soils using aminopropyl

silica solid phase extraction. Chemosphere 258, 127314. https://doi.org/10.1016/j.chemosphere.2020.127314

Raine, J.C., Turcotte, D., Romanowski, L., Parrott, J.L., 2018. Oil sands tailings pond sediment toxicity to early life stages of northern pike (Esox lucius). Science of The Total Environment 624, 567–575. https://doi.org/10.1016/j.scitotenv.2017.12.163

Raine, J.C., Turcotte, D., Tumber, V., Peru, K.M., Wang, Z., Yang, C., Headley, J.V., Parrott, J.L., 2017. The effect of oil sands tailings pond sediments on embryo-larval walleye (Sander vitreus). Environmental Pollution 229, 798–809. https://doi.org/10.1016/j.envpol.2017.06.038

Richter, B.E., Jones, B.A., Ezzell, J.L., Porter, N.L., Avdalovic, N., Pohl, C., 1996. Accelerated Solvent Extraction: A Technique for Sample Preparation. Anal. Chem. 68, 1033–1039. https://doi.org/10.1021/ac9508199

Robinson, C.E., Elvidge, C.K., Frank, R.A., Headley, J.V., Hewitt, L.M., Little, A.G., Robinson, S.A., Trudeau, V.L., Vander Meulen, I.J., Orihel, D.M., 2023. Naphthenic acid fraction compounds reduce the reproductive success of wood frogs (Rana sylvatica) by affecting offspring viability. Environmental Pollution 316, 120455. https://doi.org/10.1016/j.envpol.2022.120455

Schloss, P.D., Westcott, S.L., Ryabin, T., Hall, J.R., Hartmann, M., Hollister, E.B., Lesniewski, R.A., Oakley, B.B., Parks, D.H., Robinson, C.J., Sahl, J.W., Stres, B., Thallinger, G.G., Horn, D.J.V., Weber, C.F., 2009. Introducing mothur: Open-Source, Platform-Independent, Community-Supported Software for Describing and Comparing Microbial Communities. Appl. Environ. Microbiol. 75.

Schwab, A.P., Su, J., Wetzel, S., Pekarek, S., Banks, M.K., 1999. Extraction of Petroleum Hydrocarbons from Soil by Mechanical Shaking. Environ. Sci. Technol. 33, 1940–1945. https://doi.org/10.1021/es9809758

Selucky, M., Chu, Y., Ruo, T., Strausz, O., 1977. Chemical composition of Athabasca bitumen. Fuel 56, 369–381. https://doi.org/10.1016/0016-2361(77)90061-8

Shen, X., Dong, W., Wan, Y., Liu, Y., Yuan, Z., 2022. Function of Fe(III) in naphthalene adsorption on typical clay minerals and humic acid complexes. Journal of Environmental Chemical Engineering 10, 108271. https://doi.org/10.1016/j.jece.2022.108271

Shu, Y.Y., Lao, R.C., Chiu, C.H., Turle, R., 2000. Analysis of polycyclic aromatic hydrocarbons in sediment reference materials by microwave-assisted extraction. Chemosphere 41, 1709–1716. https://doi.org/10.1016/S0045-6535(00)00065-5

Siddique, T., Fedorak, P.M., Foght, J.M., 2006. Biodegradation of Short-Chain *n* -Alkanes in Oil Sands Tailings under Methanogenic Conditions. Environ. Sci. Technol. 40, 5459–5464. https://doi.org/10.1021/es060993m

Siddique, T., Fedorak, P.M., MacKinnon, M.D., Foght, J.M., 2007. Metabolism of BTEX and Naphtha Compounds to Methane in Oil Sands Tailings. Environ. Sci. Technol. 41, 2350–2356. https://doi.org/10.1021/es062852q

Siddique, T., Gupta, R., Fedorak, P.M., MacKinnon, M.D., Foght, J.M., 2008. A first approximation kinetic model to predict methane generation from an oil sands tailings settling basin. Chemosphere 72, 1573–1580. https://doi.org/10.1016/j.chemosphere.2008.04.036

Siddique, T., Kuznetsova, A., 2020. Linking hydrocarbon biodegradation to greenhouse gas emissions from oil sands tailings and its impact on tailings management. Can. J. Soil. Sci. 100, 537–545. https://doi.org/10.1139/cjss-2019-0125

Siddique, T., Penner, T., Klassen, J., Nesbø, C., Foght, J.M., 2012. Microbial Communities Involved in Methane Production from Hydrocarbons in Oil Sands Tailings. Environ. Sci. Technol. 46, 9802–9810. https://doi.org/10.1021/es302202c

Siddique, T., Semple, K., Li, C., Foght, J.M., 2020. Methanogenic biodegradation of iso-alkanes and cycloalkanes during long-term incubation with oil sands tailings. Environmental Pollution 258, 113768. https://doi.org/10.1016/j.envpol.2019.113768

Small, C.C., Cho, S., Hashisho, Z., Ulrich, A.C., 2015. Emissions from oil sands tailings ponds: Review of tailings pond parameters and emission estimates. Journal of Petroleum Science and Engineering 127, 490–501. https://doi.org/10.1016/j.petrol.2014.11.020

Smith, S.B., 1981. Alberta Oil Sands Environmental Research Program 1975-1980: Summary Report. S.B. Smith Environmental Consultants Limited, Calgary, AB, Canada.

Stasik, S., Loick, N., Knöller, K., Weisener, C., Wendt-Potthoff, K., 2014. Understanding biogeochemical gradients of sulfur, iron and carbon in an oil sands tailings pond. Chemical Geology 382, 44–53. https://doi.org/10.1016/j.chemgeo.2014.05.026

Sun, C., Shotyk, W., Cuss, C.W., Donner, M.W., Fennell, J., Javed, M., Noernberg, T., Poesch, M., Pelletier, R., Sinnatamby, N., Siddique, T., Martin, J.W., 2017. Characterization of Naphthenic Acids and Other Dissolved Organics in Natural Water from the Athabasca Oil Sands Region, Canada. Environ. Sci. Technol. 51, 9524–9532. https://doi.org/10.1021/acs.est.7b02082

Sun, W., Sun, X., Cupples, A.M., 2014. Identification of Desulfosporosinus as toluene-assimilating microorganisms from a methanogenic consortium. International Biodeterioration & Biodegradation 88, 13–19. https://doi.org/10.1016/j.ibiod.2013.11.014

Symons, G.E., Buswell, A.M., 1933. The Methane Fermentation of Carbohydrates [1,2]. J. Am. Chem. Soc. 55, 2028–2036. https://doi.org/10.1021/ja01332a039

Syncrude, 2022. 2022 Pit Lake Monitoring and Research Report (Base Mine Lake Demonstration Summary: 2012-2021).

United States Environmental Protection Agency, 1986. Method 3630C, Revision 3. Polynuclear aromatic hydrocarbons.

United States Environmental Protection Agency, 1986. Method 8100. Polynuclear Aromatic Hydrocarbons.

United States Department of Health and Human Services, 1995. Toxicological Profile for Polycyclic Aromatic Hydrocarbons.

United States Environmental Protection Agency, 1996. Method 3540 C, Revision 3. Soxhlet Extraction.

United States Environmental Protection Agency, 1996. Method 8275A, Revision 1. Semivolatile organic compounds (PAHs and PCBs) in soils/sludges and solid wastes using thermal extraction/gas chromatography/mass spectrometry (TE/GC/MS)

Wang, W., Meng, B., Lu, X., Liu, Y., Tao, S., 2007. Extraction of polycyclic aromatic hydrocarbons and organochlorine pesticides from soils: A comparison between Soxhlet extraction, microwave-assisted extraction and accelerated solvent extraction techniques. Analytica Chimica Acta 602, 211–222. https://doi.org/10.1016/j.aca.2007.09.023

Werkovits, S., Bacher, M., Theiner, J., Rosenau, T., Grothe, H., 2022. Multi-spectroscopic characterization of bitumen and its polarity-based fractions. Construction and Building Materials 352, 128992. https://doi.org/10.1016/j.conbuildmat.2022.128992

White, K.B., Liber, K., 2020. Chronic Toxicity of Surface Water from a Canadian Oil Sands End Pit Lake to the Freshwater Invertebrates Chironomus dilutus and Ceriodaphnia dubia. Arch Environ Contam Toxicol 78, 439–450. https://doi.org/10.1007/s00244-020-00720-3

Wnorowski, A., Aklilu, Y., Harner, T., Schuster, J., Charland, J.-P., 2021. Polycyclic aromatic compounds in ambient air in the surface minable area of Athabasca oil sands in Alberta (Canada). Atmospheric Environment 244, 117897. https://doi.org/10.1016/j.atmosenv.2020.117897

Ye, Q., Liang, C., Chen, X., Fang, T., Wang, Y., Wang, H., 2019. Molecular characterization of methanogenic microbial communities for degrading various types of polycyclic aromatic hydrocarbon. Journal of Environmental Sciences 86, 97–106. https://doi.org/10.1016/j.jes.2019.04.027

You, Y., Staebler, R.M., Moussa, S.G., Beck, J., Mittermeier, R.L., 2021. Methane emissions from an oil sands tailings pond: a quantitative comparison of fluxes derived by different methods. Atmos. Meas. Tech. 14, 1879–1892. https://doi.org/10.5194/amt-14-1879-2021

Zavgorodnyaya, Y.A., Chikidova, A.L., Biryukov, M.V., Demin, V.V., 2019. Polycyclic aromatic hydrocarbons in atmospheric particulate depositions and urban soils of Moscow, Russia. J Soils Sediments 19, 3155–3165. https://doi.org/10.1007/s11368-018-2067-3

Zhang, K., Hu, Z., Zeng, F., Yang, X., Wang, J., Jing, R., Zhang, H., Li, Y., Zhang, Z., 2019. Biodegradation of petroleum hydrocarbons and changes in microbial community structure in sediment under nitrate-, ferric-, sulfate-reducing and methanogenic conditions. Journal of Environmental Management 249, 109425. https://doi.org/10.1016/j.jenvman.2019.109425

Zhang, S., Hu, Z., Wang, H., 2019. Metagenomic analysis exhibited the co-metabolism of polycyclic aromatic hydrocarbons by bacterial community from estuarine sediment. Environment International 129, 308–319. https://doi.org/10.1016/j.envint.2019.05.028

Zhang, Y., 2023. Sources, spatial-distributions and fluxes of PAH-contaminated dusts in the Athabasca oil sands region. Environment International.

Zhang, Z., Wang, C., He, J., Wang, H., 2019. Anaerobic phenanthrene biodegradation with four kinds of electron acceptors enriched from the same mixed inoculum and exploration of metabolic pathways. Front. Environ. Sci. Eng. 13, 80. https://doi.org/10.1007/s11783-019-1164-x

Appendix A: The Study of 8 PAHs Recoveries from FFT by Two Different Solvents

A stock solution of 8 PAHs, namely, naphthalene (NAP), phenanthrene (PHE), pyrene (PYR), dibenzofuran (DBF), fluorene (FLU), dibenzothiophene (DBT), carbazole (CAR), and anthracene (ANT) were prepared using toluene and was used to spike FFT sample in three microcosms (Figure A-1). Each spiked microcosm contains 50 ppm of each PAH and was kept in darkness under room temperature during the experimental period. FFT sample properties and the cleanup columns used in this test were stated in the section **2.2 Materials and Methods** of Chapter 2. The sole solvent DCM and mixed solvent DCM:HEX (1:1, v/v) were tested against their efficiencies in recovering PAHs from FFT using Soxhlet method without pre-treatment. In each extraction, 60 mL of solvent was used to extract 5 g FFT.

Table A-1 PAHs that can be at least recovered by the applied methods at 90% confidence level (α=0.1) with n=6 and n=48 for individual and pooled PAHs, respectively. Data was shown in percentage of recovery (%) comparing with the theoretical 50 ppm of each PAHs.

	NAP	PHE	PYR	DBF	FLU	DBT	CAR	ANT	PAHs†
DCM	35	54	66	44	56	52	73	58	58
HEX/DCM (1:1, v/v)	13	5	2	4	5	9	43	14	15

† Pooled recoveries for 8 PAHs.

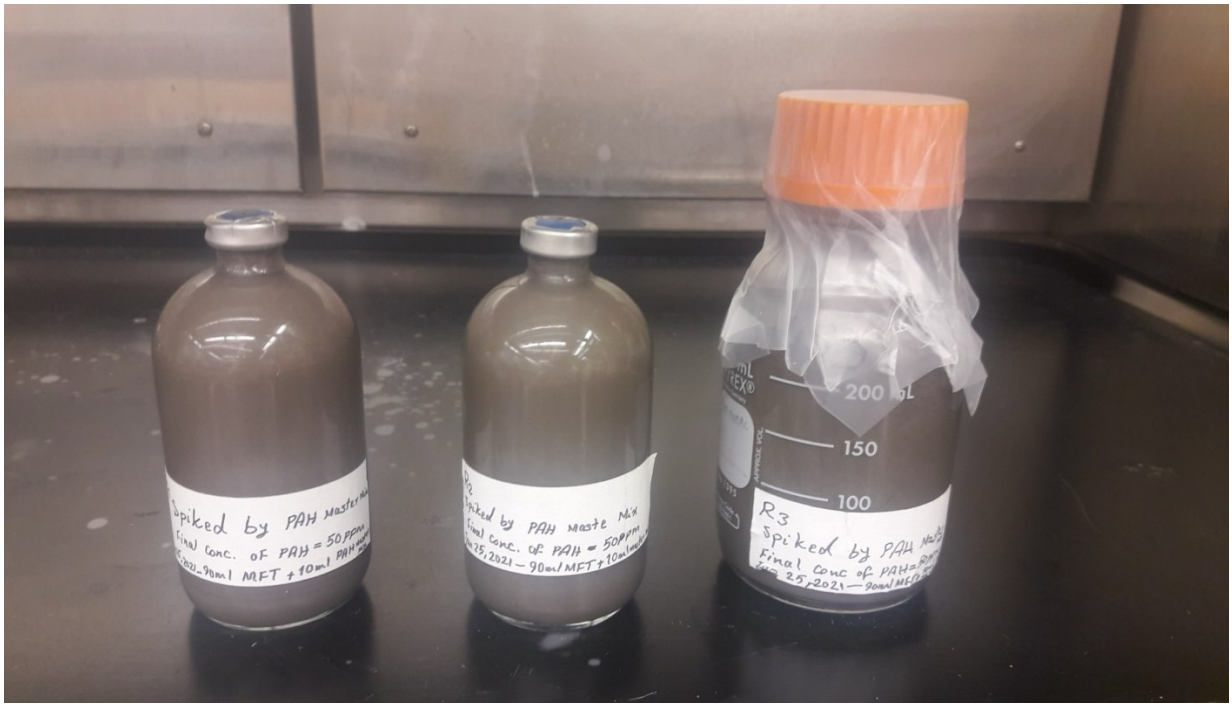

Figure A-1 Three microcosms containing FFT spiked with 8 PAHs in our preliminary experiment.

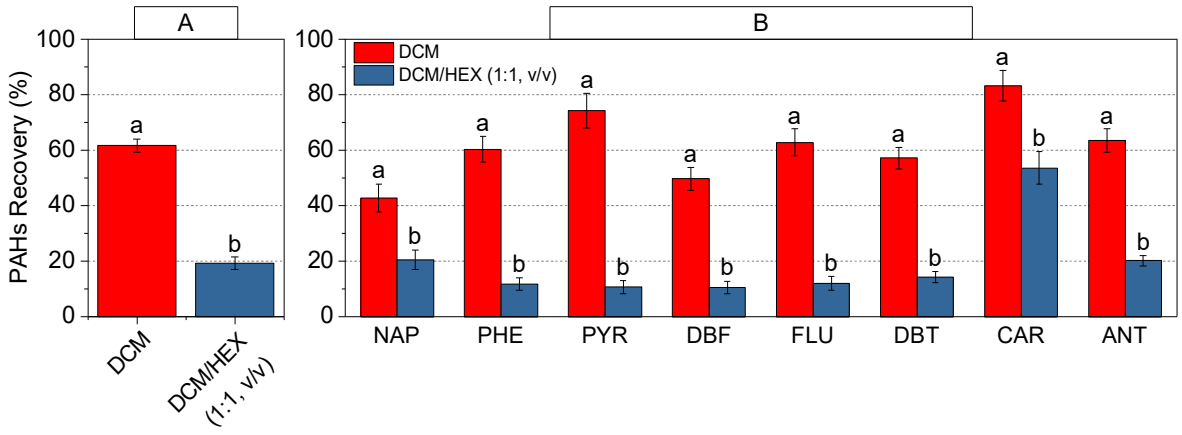

Figure A-2 Pairwise comparisons for pooled (A) and individual (B) recoveries of the 8 PAHs using DCM or DCM/HEX (1:1, v/v) as solvents.

Appendix B: Methanogenic Media Preparation

The methanogenic media used in this study was adopted and amended from (Fedorak and Hrudey, 1984; Holowenko et al., 2000). Two mineral solutions containing macronutrients (solution 1) and micronutrients (solution 2) were firstly prepared. Components of the two solutions were shown in Table B-1 and Table B-2. Deionized water was used in this process to dissolve all minerals. After preparing the two mineral solutions, 1 L deionized water was boiled in a 2 L Erlenmeyer flask to remove any dissolved oxygen while continuously purging 20% CO_2/80% N_2 gas into the water to prevent the potential dissolution of oxygen from ambient air. 14 mL solution 1, 1.4 mL solution 2,14 mL Resazurin, 14 mL phosphate solution (50 g/L KH_2PO_4), and 5.7 g $NaHCO_3$ were added to the solution. $NaHCO_3$ was used to provide terminal electron acceptor (HCO_3^-) to microbes and also served as the pH buffer in the media. After continuously stirring the solution with magnetic stirrer to fully dissolve all components, the pH of the solution was adjusted to ~7.0-7.5, preferentially ~7.2-7.3 to simulate the pH of tailings in tailings ponds. The prepared solution should be pipetted into glass serum bottles while continuously purging the headspace with 20% CO_2/80% N_2 and sealed with butyl rubber stopper and crimped with aluminum cap.

The sealed serum bottles with media should be autoclaved at 121 °C for 40 min and fully cooled down to room temperature. After cooling down, 0.15 mL filter sterilized, anaerobic vitamin B solution should be added to every 100 mL autoclaved media. To prepare vitamin B solution, mixed vitamins (Table B-3) should be dissolved in 100 mL deionized water and stored in sealed serum bottles followed by flushing the headspace with 20% CO_2/80% N_2 to remove residual air.

Table B-1 Macronutrients for methanogenic media (solution 1)

Minerals	**Concentration**
NaCl	50 g/L
$CaCl_2*2H_2O$	10 g/L
NH_4Cl	50 g/L
$MgCl_2*6H_2O$	10 g/L

Table B-2 Micronutrients for methanogenic media (solution 2)

Minerals	**Concentration**
$(NH_4)6Mo_7O_{24}*2H_2O$	10 g/L
$ZnSO_4*7H_2O$	0.1 g/L
H_3BO_3	0.3 g/L
$FeCl_2*4H_2O$	1.5 g/L
$CoCl_2*6H_2O$	10 g/L
$MnCl_2*4H_2O$	0.03g/L
$NiCl_2*6H_2O$	0.03g/L
$AlK(SO_4)_2*12H_2O$	0.1 g/L

Table B-3 Vitamin B solution for methanogenic media

Vitamins	**Concentration**
Pyridoxine	0.025 g/100 mL
Thiamine	0.005 g/100 mL
Nicotinic acid	0.01 g/100 mL
Pantothenic acid	0.0025 g/100 mL
B12 (Cyanocobalamin)	0.01 g/100 mL
p-aminobenzoic acid	0.005 g/100mL

Appendix C: Low Recovery of Carbazole from Spiked FFT Samples

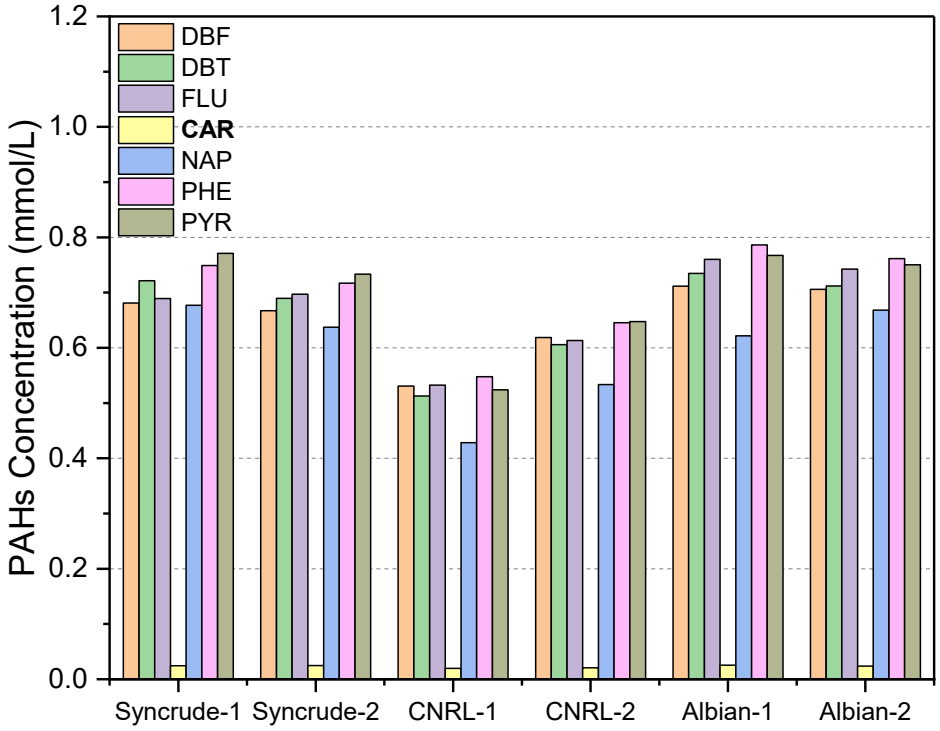

Figure C-1 The PAHs concentrations in Day 0 Sterile Control microcosms (prepared in duplicates) of Set C Syncrude, CNRL, and Albian batches. PAHs were extracted by Soxhlet method with pre-treatment. The measured carbazole (CAR) concentration in spiked microcosms was significantly lower than the other PAHs and is close to the detection limit of our method.